WADD TECHNICAL REPORT 61-133
VOLUME I

PASSIVE AERODYNAMIC ATTITUDE STABILIZATION OF NEAR EARTH SATELLITES

Volume I
LIBRATIONS DUE TO COMBINED AERODYNAMIC AND GRAVITATIONAL TORQUES

D. M. SCHRELLO

NORTH AMERICAN AVIATION, INC.
COLUMBUS, OHIO

JULY 1961

AERONAUTICAL SYSTEMS DIVISION

NOTICES

When Government drawings, specifications, or other data are used for any purpose other than in connection with a definitely related Government procurement operation, the United States Government thereby incurs no responsibility nor any obligation whatsoever; and the fact that the Government may have formulated, furnished, or in any way supplied the said drawings, specifications, or other data, is not to be regarded by implication or otherwise as in any manner licensing the holder or any other person or corporation, or conveying any rights or permission to manufacture, use, or sell any patented invention that may in any way be related thereto.

Qualified requesters may obtain copies of this report from the Armed Services Technical Information Agency, (ASTIA), Arlington Hall Station, Arlington 12, Virginia.

This report has been released to the Office of Technical Services, U. S. Department of Commerce, Washington 25, D. C., for sale to the general public.

Copies of ASD Technical Reports and Technical Notes should not be returned to the Aeronautical Systems Division unless return is required by security considerations, contractual obligations, or notice on a specific document.

WADD TECHNICAL REPORT 61-133
VOLUME I

PASSIVE AERODYNAMIC ATTITUDE STABILIZATION OF NEAR EARTH SATELLITES

Volume I
LIBRATIONS DUE TO COMBINED AERODYNAMIC AND GRAVITATIONAL TORQUES

D. M. SCHRELLO

NORTH AMERICAN AVIATION, INC.
COLUMBUS, OHIO

JULY 1961

FLIGHT DYNAMICS LABORATORY
CONTRACT Nr. AF 33(616)-7100
PROJECT Nr. 1366
TASK Nr. 13967

AERONAUTICAL SYSTEMS DIVISION
AIR FORCE SYSTEMS COMMAND
UNITED STATES AIR FORCE
WRIGHT-PATTERSON AIR FORCE BASE, OHIO

McGregor & Werner, Inc., Dayton, O.
400 - November 1961 - 10-340

FOREWORD

The research reported herein was performed by North American Aviation, Inc., Columbus, Ohio for the Hypersonic Flight Section, Flight Branch of the Flight Dynamics Laboratory, Wright Air Development Division. The work was accomplished under Air Force Contract No. AF 33(616)-7100, Project No. 1366, Task No. 13967, "A Study of Aerodynamically Oriented and Stabilized Satellites." This research was carried out by the Engineering Research and Aerothermodynamics Development Groups of the Columbus Division, North American Aviation, Inc., with Dr. D. M. Schrello, Engineering Research Group, as Project Engineer. Mr. Joseph Ondrejka, Flight Dynamics Laboratory, was WADD Project Engineer.

The results of this study are reported in a series of three volumes of which this is Volume I. The other reports in this series are:

VOLUME II: "Aerodynamic Analysis," by Paul H. Davison

VOLUME III: "Mathematical Techniques and Computer Program," by O. C. Juelich

In this report, particular credit should be given to Mr. O. C. Juelich for his contributions to the analysis described in Section 5 and to Mr. Paul H. Davison for the treatment presented in Appendix C.

ABSTRACT

The general equations governing the angular motion of a rigid satellite are investigated for the case where both gravitational and aerodynamic torques are included, and where the atmosphere is assumed to be spherically symmetric but rotating. For a non-spinning, axisymmetric satellite, these equations show the vehicle to be characterized by three dimensionless aerodynamic parameters and one inertia parameter. A Fourier series expansion of the coefficients of these equations is found to yield equations of the non-homogeneous Hill type.

The complete equations of motion are solved for the case of a circular orbit. It is shown that atmospheric rotation induces a steady-state yawing motion which prevents yaw equilibrium from being achieved for other than equatorial orbits. The effects of configuration and orbit parameters are examined in detail. It is found that gravity gradients will not generally dominate until altitudes in excess of 300-400 miles are achieved, while at lower altitudes, even small amounts of aerodynamic stability suffice to override the gravitational torques.

The stability of the pitching motion on an eccentric orbit is analyzed. It is found that an infinity of unstable regions may be encountered in which small deviations from a purely periodic motion will amplify. Computer results are presented to illustrate the catastrophic nature of these unstable regions which may appear in a situation giving the outward appearance of stability. An approximate solution for the pitching motion on an elliptical orbit is also obtained using the method of variation of parameters. The results are compared with a numerical integration of the complete governing equation.

It is generally concluded, however, that the aerodynamic and inertial design of a satellite may be accomplished so as to minimize or altogether eliminate the unstable regions. In particular, the design of the vehicle for maximum aerodynamic stability appears to have promise for achieving wholly passive attitude stabilization at low altitudes.

PUBLICATION REVIEW

This report has been reviewed and is approved.

FOR THE COMMANDER:

William C. Nielsen

WILLIAM C. NIELSEN
Colonel, USAF
Chief, Flight Dynamics Laboratory

TABLE OF CONTENTS

	Page No.
INTRODUCTION	1
DISCUSSION	
1. Equations of Motion and Coordinate Systems	3
1.1 Complete Equations of Motion	3
1.2 Effects of Orbit Perturbations	11
1.3 Introduction of Gravity Gradient Torques	13
1.4 Equations of Motion for Small Angles	14
2. External Torques on the Satellite	18
2.1 Introduction	18
2.2 Gravitational Torques	18
2.3 Aerodynamic Torques	21
2.3.1 General Considerations	21
2.3.2 Orientation of the Relative Wind Vector	22
2.3.3 Expansion of the Aerodynamic Torques	28
2.4 Other Disturbing Torques	30
2.4.1 Solar Radiation Pressure Torques	30
2.4.2 Additional Torques	34
3. Equations of Motion for Slightly Eccentric Orbits	35
3.1 Small Angle Equations for Slightly Eccentric Orbits	35
3.2 Approximate Atmospheric Density Variation	39
3.3 Order of Magnitude of Aerodynamic Terms	46
3.4 Fourier Series Expansion of Periodic Coefficients	58
4. Angular Motions on a Circular Orbit	63
4.1 Existence and Stability of Equilibrium Positions	63
4.2 Approximate Behavior of Complete System	66
4.3 Exact Results for Small Angle Pitching Motion	68
4.3.1 General	68
4.3.2 Effects of Vehicle Parameters	69
4.3.3 Effects of Orbit Parameters	70
5. Pitching Motion on an Eccentric Orbit	77
5.1 Exact Solution of the Homogeneous Pitching Equation	77
5.2 Stability of the Natural (Unforced) Motion	85
5.3 Stability of the Forced Motion	87

Page No.

5.4 Approximate Solution of Complete Pitching Equation . . 91
5.5 Numerical Results 102
5.5.1 General 102
5.5.2 Discussion of Results 104
5.5.2.1 Range of Variables 104
5.5.2.2 Effects of Aerodynamic Damping 104
5.5.2.3 Effects of Orbit Inclination 104
5.5.2.4 Effects of Initial Conditions 105
5.5.2.5 Effects of Remaining Parameters 105
5.5.2.6 Stability of the Motion 106

SUMMARY AND CONCLUSIONS 122

APPENDIX A - GRAVITATIONAL TORQUES ON A RIGID BODY 125

APPENDIX B - EXPANSION OF COEFFICIENTS IN EQUATIONS OF ANGULAR MOTION 132

APPENDIX C - EFFECTS OF AERODYNAMIC DRAG AND DAMPING ON THE MOTION OF NEAR-EARTH SATELLITES 137

BIBLIOGRAPHY 144

LIST OF FIGURES

Figure		Page No.
1.	Orientation of the Orbit Plane in Space	4
2.	Orbital Coordinate System	6
3.	Vehicle Orientation Angles	8
4.	Vehicle Body-Fixed Coordinate System	9
5.	Behavior of Gravity Gradient Torque	20
6.	Geometry of Dumbbell-Shaped Satellite	21
7.	Orientation of the Relative Wind Vector with Respect to the Vehicle	23
8.	Orientation of the Relative Wind Vector with Respect to the Orbital Coordinates	24
9.	Comparison of Solar and Aerodynamic Initial Torque Slopes	32
10.	Maximum Values of Various Torques on a Conical Satellite	33
11.	Atmospheric Rotation Parameter, d , as a Function of Perigee Altitude and Orbit Inclination	43
12.	Variation of Exponential Factor, $\varkappa_A$, with Altitude	44
13.	Atmosphere Parameter, λ , as a Function of Perigee Altitude and Orbital Eccentricity	45
14.	Aerodynamic Moment Parameter Γ for a Number of Optimum Body Shapes, $V/V_T = 1/2$.	54
15.	Aerodynamic Moment Parameter Γ for a Number of Optimum Body Shapes, $V/V_T = 3/4$.	55
16.	Aerodynamic Damping Parameter Γ_ℓ for a Number of Optimum Body Shapes, $V/V_T = 1/2$.	56
17.	Aerodynamic Damping Parameter Γ_ℓ for a Number of Optimum Body Shapes, $V/V_T = 3/4$.	57
18.	Modified Bessel Functions Versus λ	62

Figure		Page No.
19.	Stability Boundaries of the Aerodynamic Parameter σ_p^* for Circular Orbits	65
20.	Approximate Behavior of the Forced Rolling and Yawing Motions	68
21.	Combined Effects of Inertia and Static Aerodynamic Moment Parameters, M and Γ, on Circular Orbit Amplitude	72
22.	Combined Effects of Inertia and Static Aerodynamic Moment Parameters, M and Γ, on Circular Orbit Amplitude	73
23.	Typical Effect of Inertia Parameter, M, on the Angular Oscillations	74
24.	Equilibrium Displacement Angle due to Aerodynamic Damping	75
25.	Typical Effect of Orbit Inclination, ι, on the Angular Oscillations	76
26.	Behavior of the Characteristic Exponent, μ, as a Function of ξ^2	80
27.	Stability Boundaries on the $\sigma_p^* - \lambda$ Plane Based upon Mathieu's Equation	90
28.	Comparison of Approximate and Exact Pitching Motion for the Dumbbell Satellite	98
29.	Comparison of Approximate and Exact Pitching Motion for an Aerodynamically Stabilized Satellite	100
30.	Solutions for Slightly Eccentric Orbit at 400 Miles Perigee Altitude and Small Aerodynamic Stability	108
31.	Solutions for Slightly Eccentric Orbit at 400 Miles Perigee Altitude and Substantial Aerodynamic Stability	110
32.	Behavior of Pitching Motion as Orbital Eccentricity Increases	112
33.	Pitching Motion on an Eccentric Orbit at 125 Miles Perigee Altitude	119

LIST OF SYMBOLS

a	Mean distance or semi-major axis of elliptical orbit
a_E	Earth equatorial radius
$\{a_n\}$	Coefficients of Fourier series expansion in Hill's differential equation
A, B	Natural frequencies of the unforced pitching and yawing motions for a circular orbit, Section 4.2
$\{A_n\}$	Coefficients of a Fourier series expansion of $\mathcal{L}(v)$, see Eqs. (70)
$\alpha, \mathcal{B}, \mathcal{C}, \mathcal{D}$	Initial condition constants in solutions of pitching and yawing motions
$\alpha^*, \mathcal{B}^*$	Constants in variation of parameters solution, defined in Eqs. (107)
b	Ballistic coefficient, $\equiv C_D S_\pi / 2m$; also semi-minor axis of elliptical orbit
$\{b_\nu\}$	Coefficients in the series solution to Hill's differential equation
C_A	Constant in exponential approximation to atmospheric density
$\bar{c}$	Characteristic vehicle length
C_D	Dimensionless aerodynamic drag coefficient
C_ℓ, C_m, C_n	Dimensionless aerodynamic rolling, pitching and yawing moment coefficients, defined by Eq. (39)
C_{ℓ_p}	Dimensionless aerodynamic damping in roll
C_{m_α}	Dimensionless aerodynamic pitching moment coefficient slope versus α
C_{m_q}	Dimensionless aerodynamic damping in pitch
$\{C_n\}, \{D_n\}$	Coefficients of a Fourier series expansion of $\mathcal{M}(v)$, defined in Eqs. (72)
d	Atmospheric rotation parameter, $\equiv \omega_e \sin \iota / \dot{v}_p$

D	Diameter
D_n	$n \times n$ determinant, defined in Section 5.1
ϵ	A small parameter
$\vec{e}_n$	Unit vectors defining vehicle body axes, Appendix A
E	Eccentric anomaly, defined in Fig. C-1
$\vec{F}$	Force vector, Appendix A
q	Coefficient in Mathieu's equation, Eq. (97)
h	True altitude over a spherical Earth, $\equiv r - a_E$
H	Angular momentum, Appendix A
i	$\sqrt{-1}$; also a counting index
I	The unit matrix
$\bar{I}_i$	Principal moment of rotary inertia about the i^{th} body-fixed axis
$I_n(\lambda)$	Modified Bessel function of the first kind of order n and argument λ, $\equiv i^{-n} J_n(i\lambda)$
$J_n(\lambda)$	Bessel function of the first kind and order n
$\bar{J}_{ij}$	Product of rotary inertia
J	Dimensionless coefficient of the second spherical harmonic in Legendre expansion of Earth's gravitational potential
k	Unspecified function of altitude which permits the atmospheric motion to differ from purely rigid body rotation; also initial condition constant for rolling motion, Section 3.3
ℓ, l	Distance from vehicle mass center to any mass element, Appendix A; also total length of a satellite
L_i	Applied external torque component about the i^{th} body axis
L_{Ri}	$L_i - L_{g_i}$
$\mathcal{L}(\nu)$	Periodic function of ν appearing as coefficient of $\bar{\theta}$ in the equation for the generalized pitching motion
m	Mass

M	An inertia parameter, $\equiv(\bar{I}_z-\bar{I})/\bar{I}$; also total mass of a collection of particles, Appendix A
$m(\nu)$	Non-homogeneous portion of the equation for the generalized pitching motion
n	Keplerian mean motion, $\equiv 2\pi/P$; also a counting index
N	Number of particles in a rigid collection, Appendix A; also number of revolutions, Section 5.4 and Appendix C
p	Semi-latus rectum or semi-parameter of ellipse
P	Orbital period, $\equiv 2\pi a^{3/2}/\sqrt{\mu}$
p,q,k	Components of instantaneous angular velocity vector along the x,y,z body axes
P,Q,R	Aerodynamic parameters defined by Eqs. (45)
$\mathcal{P}_P,\mathcal{Q}_P,\mathcal{R}_P$	Aerodynamic parameters defined by Eqs. (48)
$\mathcal{P}_P^*,\mathcal{Q}_P^*,\mathcal{R}_P^*$	Aerodynamic parameters defined by Eqs. (57)
$\vec{Q}$	Inertial position vector, Appendix A
r	Geocentric radius, distance from the planet's center
r_E	Geocentric radius of the Earth
r_i	Components of r along principal body fixed axes
s	Vehicle spin velocity about the x-axis
S_π	Vehicle reference area
t	Time
u	Angle between the geocentric radius vector and the equator, measured in the orbit plane, defined in Fig. 2
U_1,U_2	Two independent solutions to Hill's differential equation, defined by Eqs. (90)
ν	True anomaly, defined in Fig. 2
V	Velocity of the vehicle relative to inertial space
V_R	Velocity of the vehicle relative to the planetary atmosphere
$\mathcal{V}$	Volume

W	Sea level satellite weight; also a matrix, the determinant of which is the Wronskian of the solutions $\bar{\theta}_1$ and $\bar{\theta}_2$
x_{cm}	Longitudinal coordinate of the body's mass center
x, y, z	Principal orthogonal body-fixed axes
x_o, Y_o, Z_o	Orbital coordinates, defined in Fig. 2
X, Y, Z	Inertial coordinates, defined in Fig. 1
X_p, Y_p, Z_p	Perifocal coordinates, defined in Fig. 1
α, β	Aerodynamic angle of attack and sideslip angle, defined in Fig. 7
γ, Λ	Angles between the relative velocity vector and orbital coordinates, defined in Fig. 8
γ^*	Angle between the inertial velocity vector and the local horizontal, defined in Appendix B
$\Gamma, \Gamma_\gamma, \Gamma_\Psi$	Aerodynamic parameters, defined by Eqs. (59)
δ	A constant in the variation of parameters solution, defined in Eq. (107)
$\Delta(0)$	Hill's determinant evaluated at $\mu = 0$, defined by Eq. (88)
ϵ	Orbital eccentricity, defined in Appendix B
η	Inertial pitch angle, $\equiv (\theta - u)$
θ, ψ, ϕ	Angles orienting the vehicle with respect to the orbital coordinates, defined in Fig. 3
$\bar{\theta}, \bar{\psi}, \bar{\phi}$	Transformed dependent variables, defined by Eqs. (62)
$\theta_0, \theta_1, \theta_2$	Three solutions of the complete pitching equation analogous to $\bar{\theta}_0, \bar{\theta}_1, \bar{\theta}_2$
$\bar{\theta}_0, \bar{\theta}_1, \bar{\theta}_2$	Three solutions of the complete transformed pitching equation, defined in Section 5.3
$\bar{\theta}_1^*, \bar{\theta}_2^*$	Two linearly independent real solutions to Hill's differential equation, defined by Eqs. (94)
φ	Geocentric latitude
ι	Inclination of the orbit plane to the equator, defined in Fig. 1

χ_A	Exponent of exponential approximation to atmospheric density
λ	Dimensionless atmosphere parameter, $\equiv \chi_A r_p \epsilon$
μ	Characteristic exponent; also product of Earth's mass and universal gravitational constant
ν	Counting index
ξ	A parameter related to the characteristic exponent through Eq. (89)
ρ	Atmospheric density
φ	Transformed independent variable, $\equiv \nu/2$
Φ	Gravitational potential function or potential energy per unit mass
ω	Argument of perigee, angle between the semi-major axis and the equator, measured in the orbit plane, defined in Fig. 1
ω_a	Atmospheric rotation rate, $\equiv k\,\omega_\epsilon$
ω_ϵ	Angular velocity of Earth's daily rotation
Ω	Longitude of the ascending node, defined in Fig. 1
$\vec{\Omega}$	Angular velocity vector of a moving reference frame, Appendix A

Subscripts

a	Apogee
A	Aerodynamic
g	Gravitational
i	$i^{\underline{th}}$ particle
l	Semi-latus rectum
max	Maximum value
o	Orbital coordinates or initial value of a function
p	Perigee or perigee conditions

R	Relative
S	Solar
T	Total volume enclosed by satellite

Notation

$\dot{(\,)}$	Denotes derivative with respect to time
$(\,)'$	Denotes derivative with respect to ν or ϕ
$\vec{(\,)}$	Denotes a vector quantity
$\overline{(\,)}$	Denotes the average value of the quantity
$O(\,)$	Denotes the order of magnitude of the enclosed quantity
$\vec{(\,)}\times\vec{(\,)}$	Denotes a vector product
det( )	Denotes the determinant of the enclosed matrix
grad( )	Denotes the gradient of the enclosed scalar function
Im( )	Denotes the imaginary part of a complex number
Re( )	Denotes the real part of a complex number
$\cong$	Denotes approximate equality

INTRODUCTION

The problem of achieving precise attitude stabilization of artificial satellites has, of late, received increasing attention, principally because adequate means of orientation and control are necessary prerequisites to the serious scientific and/or military use of such vehicles. The general subject may be divided into two rather distinct but interrelated areas: (1) the determination of the external torques which act on the satellite together with the passive response of the vehicle to various combinations of these torques, and (2) the synthesis of active attitude sensing and control systems which utilize these torques to achieve and hold some desired vehicle orientation.

The general framework within which this problem may be treated has been discussed by numerous authors, and reasonably comprehensive surveys of the field have been published by Roberson (Ref. 3) and Frye and Stearns (Ref. 4). Since the synthesis of attitude control systems cannot, in general, be accomplished without detailed knowledge of the vehicle's response to the applied external torques, this latter subject has received the most extensive treatment. The majority of the published work in this area has, however, been confined to examining the effect of only a single external torque and/or the assumption of a circular orbit.

For example, the effects of gravity gradient torques alone on the librations of a dumbbell-shaped satellite have been studied by Schindler (Ref. 5) and Klemperer and Baker (Ref. 6) for the circular orbit case, while Stocker and Vachino (Ref. 7) and Baker (Ref. 8) have discussed the motion on an eccentric orbit. Roberson (Refs. 9, 10) has qualitatively discussed this entire problem with considerable generality.

The influence of aerodynamic torques on a vehicle in a circular orbit has been examined by Wall (Ref. 11) and the combined effect of aerodynamic and gravitational torques has been covered briefly by DeBra (Ref. 12) and DeBra and Stearns (Ref. 13), again for the circular orbit case. Beletskiy (Ref. 14) has also considered this problem in a somewhat more general form. Along similar lines, the solar torques have been discussed by Sohn (Ref. 15), Frye and Stearns (Ref. 4) and, more recently, by Newton (Ref. 16).

Almost without exception, none of the papers have attempted to evolve rational design criteria or to provide detailed analytical results for the vehicle's angular motion when combinations of several torques act. In particular, the combined influence of aerodynamic and gravitational torques has apparently not been carefully considered in spite of the fact that these may be readily shown to be the dominant external torques for orbits below about 400 miles altitude. Although DeBra (Ref. 12) draws some preliminary conclusions about the interaction of these two torques,

---

Manuscript released by the author February 1961 for publication as a WADD Technical Report.

he has considered only the equilibrium case and has greatly oversimplified the aerodynamic treatment. Moreover, no analytical consideration of elliptic orbits has been made.

Since the satellite's external configuration determines the aerodynamic torques in a manner analogous to the way the mass distribution determines the gravitational torques, it is clear that an understanding of both of these torques, and their mutual interaction, is essential for a rational design to be made.

Accordingly, this work seeks to extend the theory of satellite attitude control by examining the detailed aerodynamic influence on the angular motion including interactions with the gravitational torques and considering a general elliptical orbit of small eccentricity. The effect of atmospheric rotation is also considered to the extent to which it affects the vehicle's angular motion. Torques due to radiation pressure, electromagnetic effects and internal moving parts are considered briefly but are concluded to be negligible over the altitude range for which aerodynamic effects are significant. The motion of the vehicle's mass center (which is only weakly coupled to the angular motion through the gravitational gradient and the drag) is assumed to be independent and specified. As shown by Moran (Ref. 29), the uncoupling thus performed introduces essentially no error into the final results for the librations, at least for small eccentricity orbits.

1. EQUATIONS OF MOTION AND COORDINATE SYSTEMS

1.1 Complete Equations of Motion

For a rigid body of constant mass possessing principal axes of inertia x, y, z the equations of angular motion about the mass center are the well-known Euler Equations of a rigid rotator:

$$\begin{aligned} L_x &= \dot{p}\bar{I}_x + qr\left(\bar{I}_z - \bar{I}_y\right) \\ L_y &= \dot{q}\bar{I}_y + pr\left(\bar{I}_x - \bar{I}_z\right) \\ L_z &= \dot{r}\bar{I}_z + pq\left(\bar{I}_y - \bar{I}_x\right) \end{aligned} \tag{1}$$

where p, q, r are components of the instantaneous angular velocity of the body (relative to an inertial reference frame) along the principal body-fixed axes and L_x, L_y, L_z are the corresponding components of the instantaneous applied external torque. The products of inertia are absent, of course, due to the choice of principal axes. The applied external torques will be examined in detail in Section 2. The motion of the body's mass center is assumed to be known and independent of the angular motions about the mass center.

The problem is to choose an orientation scheme such that the equations of motion, Eqs. (1), assume their simplest form. Since the method of orientation determines the simplicity or complexity of the angular velocity vector, judicious choice of coordinates is of considerable value. Roberson (Ref. 9) has discussed this problem qualitatively at some length. Although only three independent coordinates are required, it is desirable to introduce more than this number in order to retain a clear physical significance for each coordinate. The inertial reference frame chosen here is oriented with respect to the planet as shown in Fig. 1. The Y-axis lies along the planet's axis of rotation and points south, while X and Z lie in the equatorial plane with $-Z$ directed toward the most recent vernal equinox in the customary astronomical fashion[1].

---

[1]It is assumed here that the only significant motion of the earth which precludes its use as an inertial reference frame is its daily rotation. Thus, the inertial coordinates defined above differ from geocentric earth-fixed coordinates by a uniform rotation of the latter about their common Y-axis.

Following the astronomical convention (Ref. 17), three Euler angles are adopted to orient the instantaneous orbit and orbit plane relative to the inertial reference frame. These are the nodal longitude (or right ascension) Ω , the orbital inclination ι[1] and the argument of perigee, ω . Their general relationship is shown in Fig. 1, where it is noted that, owing to the choice of inertial coordinates, the rotations Ω , ι and ω are left-handed. The radial distance from the planet's mass center to the vehicle's mass center is denoted by r .

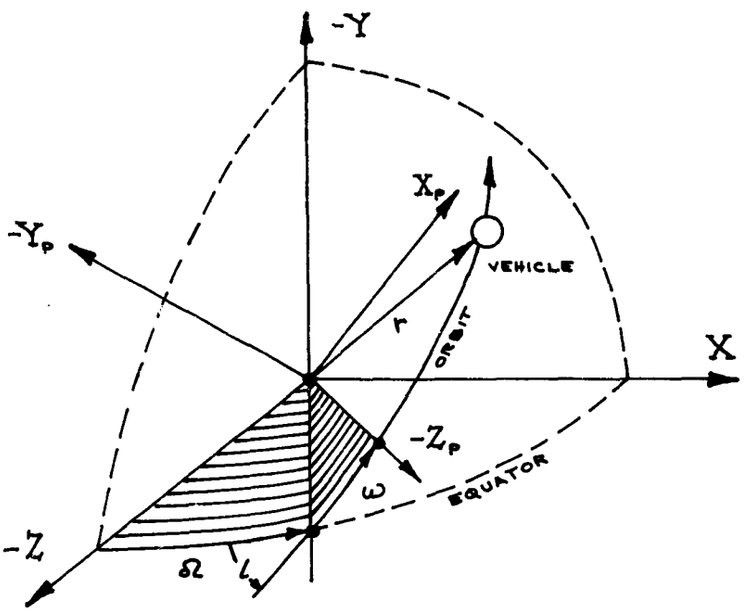

Figure 1. Orientation of the Orbit Plane in Space

The result of performing these rotations is a right-handed, orthogonal coordinate triad with origin at the primary focus of the instantaneous ellipse with $-Z_p$ pointing toward perigee and X_p pointing in the direction of vehicle motion through perigee (Fig. 1). In the absence of all perturbations, the vehicle's motion is given by the well-known Keplerian laws of motion and the angles Ω , ι and ω are constants. When perturbative influences such as those due to planetary oblateness, atmospheric drag, etc., are considered these angles change with time, having secular and/or periodic variations, but the rates are generally small (Ref. 18). These angular rates will be considered further shortly and will be shown to have only a second-order effect on the vehicle's motion.

---

[1]It is conventional to denote the orbit inclination by i ; however ι is used here to avoid later confusion.

The location of the vehicle on the orbit path is most conveniently specified by the true anomaly, ν, which is measured in the orbit plane from perigee and is positive in the direction of motion. The angles Ω, ι and $\omega + \nu \equiv u$ define a set of orbital coordinates which move with the vehicle, and are completely determined by the translational motion of the vehicle's mass center. The transformation from the inertial coordinates to the orbital coordinates is given in matrix notation by

$$\begin{bmatrix} X_o \\ Y_o \\ Z_o \end{bmatrix} = (u)(\iota)(\Omega) \begin{bmatrix} X \\ Y \\ Z \end{bmatrix} \tag{2}$$

where the matrices (Ω), (ι) and (u) are defined by

$$(\Omega) = \begin{bmatrix} c\Omega & 0 & s\Omega \\ 0 & 1 & 0 \\ -s\Omega & 0 & c\Omega \end{bmatrix}$$

$$(\iota) = \begin{bmatrix} c\iota & -s\iota & 0 \\ s\iota & c\iota & 0 \\ 0 & 0 & 1 \end{bmatrix} \tag{3}$$

$$(u) = \begin{bmatrix} cu & 0 & su \\ 0 & 1 & 0 \\ -su & 0 & cu \end{bmatrix} .$$

The abbreviations C = cosine and S = sine have been used here for brevity. The appropriate geometry is shown in Fig. 2. The Z_o axis, which is always directed inward along the radius vector, represents a sort of "down" direction, while X_o, which points in the direction of vehicle motion, indicates the "forward" direction.

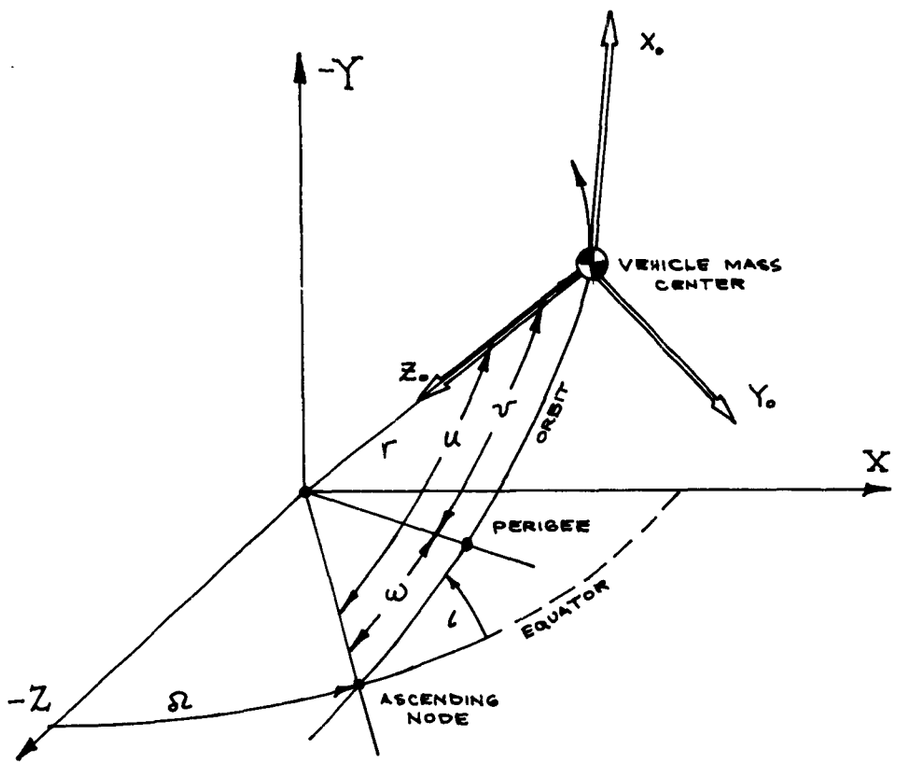

Figure 2. Orbital Coordinate System

Inasmuch as the orbital coordinates are completely defined by the motion of the vehicle's mass center, three independent angles are yet required to orient the vehicle. The choice is again dictated by the resulting simplicity of the equations of motion. Roberson (Ref. 9) and DeBra (Ref. 12) have pointed out that when gravitational torques are to be considered, the first of these three remaining angles should be formed by a rotation about Z_o, since the gravity gradient (for a spherical central body) occurs along this axis. This point is also demonstrated in Section 2.2. On the other hand, for the current work where aerodynamic torques are of interest, it is desirable to keep the first angle in the nominal pitch plane and so the first rotation should occur about Y_o.

Roberson, in his extensive treatment of this subject (Refs. 3, 9, 10) has shown that for small angles, the equations of motion uncouple such that the order in which the rotations are performed is immaterial. However, since it may be desirable to examine larger deviation angles in pitch[1], the first rotation about Y_o will be employed. The angles which shall be used here are denoted by θ, ψ, ϕ and are defined as shown in Fig. 3. Thus the transformation from the orbital coordinates to the body axes is

$$\begin{bmatrix} x \\ y \\ z \end{bmatrix} = (\phi)(\psi)(\theta) \begin{bmatrix} X_o \\ Y_o \\ Z_o \end{bmatrix} \tag{4}$$

where

$$(\theta) = \begin{bmatrix} c\theta & 0 & -s\theta \\ 0 & 1 & 0 \\ s\theta & 0 & c\theta \end{bmatrix}$$

$$(\psi) = \begin{bmatrix} c\psi & -s\psi & 0 \\ s\psi & c\psi & 0 \\ 0 & 0 & 1 \end{bmatrix} \tag{5}$$

$$(\phi) = \begin{bmatrix} 1 & 0 & 0 \\ 0 & c\phi & s\phi \\ 0 & -s\phi & c\phi \end{bmatrix} .$$

---

[1]For a non-spinning vehicle, Roberson (Ref. 3) has shown the pitching motion to be independent of the rolling and yawing motions, which are inherently coupled. This point is also discussed in Section 1.4.

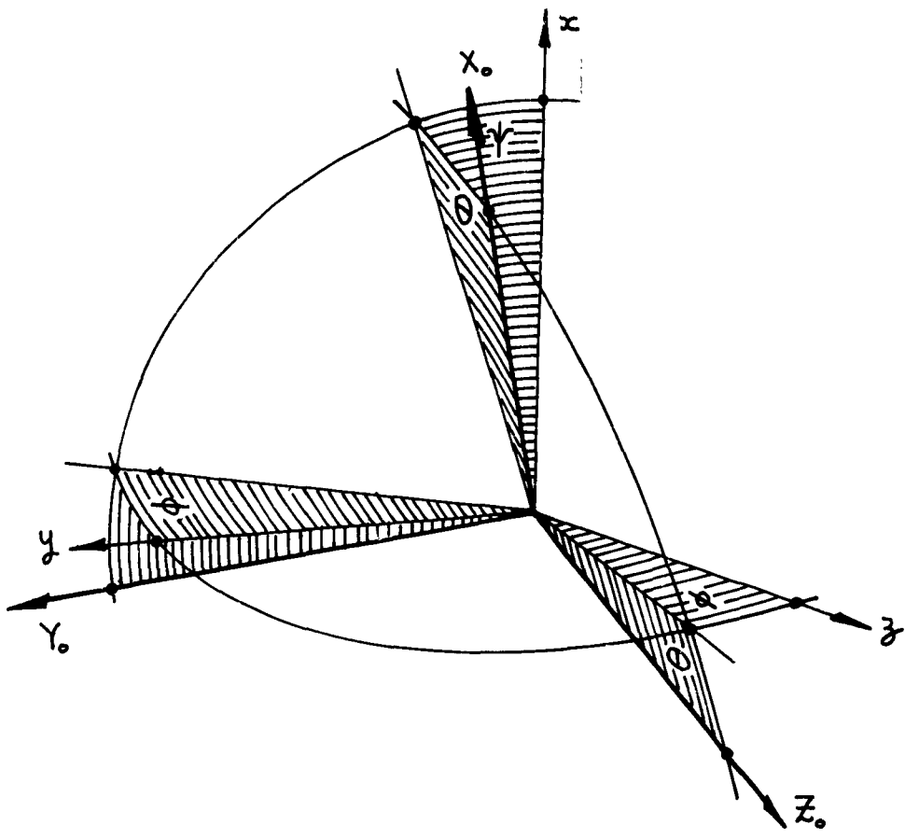

Figure 3. Vehicle Orientation Angles

The complete orientation transformation from the inertial coordinates to the principal body axes is therefore composed of six angles as follows:

$$\begin{bmatrix} x \\ y \\ z \end{bmatrix} = (\phi)(\psi)(\theta)(u)(i)(\Omega) \begin{bmatrix} X \\ Y \\ Z \end{bmatrix} . \qquad (6)$$

Here θ , ψ and ϕ are the only unknowns, since the center of mass motion is assumed to be specified. The principal body axes defined above are shown in relation to the vehicle in Fig. 4.

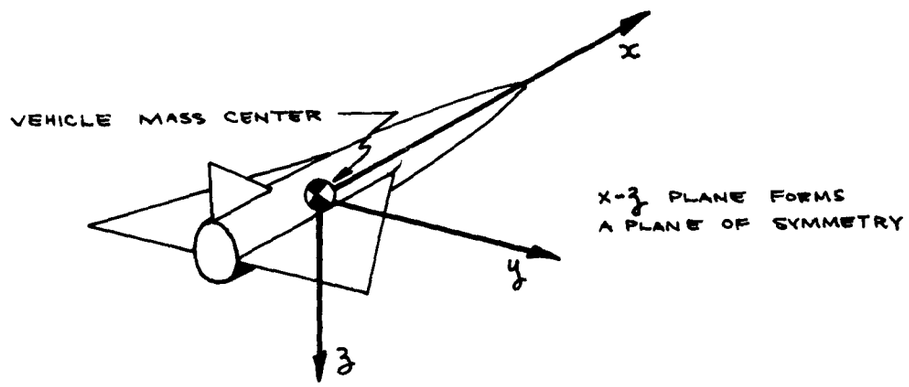

Figure 4. Vehicle Body - Fixed Coordinate System

The angular velocity components in the body axes are readily found from the transformation equation, Eq. (6), in the following general form:

$$\begin{bmatrix} p \\ q \\ r \end{bmatrix} = \begin{bmatrix} s+\dot{\phi} \\ 0 \\ 0 \end{bmatrix} - (\phi)\begin{bmatrix} 0 \\ 0 \\ \dot{\psi} \end{bmatrix} + (\phi)(\psi)\begin{bmatrix} 0 \\ \dot{\theta} \\ 0 \end{bmatrix} - (\phi)(\psi)(\theta)\begin{bmatrix} 0 \\ \dot{u} \\ 0 \end{bmatrix}$$

$$-(\phi)(\psi)(\theta)(u)\begin{bmatrix} 0 \\ 0 \\ i \end{bmatrix} - (\phi)(\psi)(\theta)(u)(i)\begin{bmatrix} 0 \\ \dot{\Omega} \\ 0 \end{bmatrix}$$

where s is a possible spin velocity about the x axis. It is noted, however, that it is convenient to define

$$\eta \equiv \theta - u \qquad (7)$$

since

$$(\theta)(u) = \begin{bmatrix} (c\theta cu + s\theta su) & o & (c\theta su - s\theta cu) \\ o & 1 & o \\ (s\theta cu - c\theta su) & o & (c\theta cu + s\theta su) \end{bmatrix}$$

$$= \begin{bmatrix} c\eta & o & -s\eta \\ o & 1 & o \\ s\eta & o & c\eta \end{bmatrix} .$$

Thus,

$$\begin{bmatrix} p \\ q \\ r \end{bmatrix} = \begin{bmatrix} s+\dot{\phi} \\ o \\ o \end{bmatrix} - (\phi)\begin{bmatrix} o \\ o \\ \dot{\psi} \end{bmatrix} + (\phi)(\psi)\begin{bmatrix} o \\ \dot{\eta} \\ o \end{bmatrix} - (\phi)(\psi)(\eta)\begin{bmatrix} o \\ o \\ i \end{bmatrix} - (\phi)(\psi)(\eta)(\iota)\begin{bmatrix} o \\ \dot{\delta\iota} \\ o \end{bmatrix} . \tag{8}$$

Expanding Eq. (8) there is obtained,

$$p = \dot{\phi} + s - \dot{\eta}\sin\psi + \dot{\iota}\sin\eta\cos\psi + \dot{\delta\iota}\left[\sin\psi\cos\iota + \cos\psi\cos\eta\sin\iota\right]$$

$$q = -\dot{\psi}\sin\phi + \dot{\eta}\cos\phi\cos\psi - \dot{\iota}\left[\cos\eta\sin\phi - \cos\phi\sin\psi\sin\eta\right] + \dot{\delta\iota}\left[\sin\phi\sin\eta\sin\iota - \cos\phi\cos\psi\cos\iota + \cos\eta\sin\iota\cos\phi\sin\psi\right] \tag{9}$$

$$r = -\dot{\psi}\cos\phi - \dot{\eta}\sin\phi\cos\psi - \dot{\iota}\left[\cos\eta\cos\phi + \sin\phi\sin\psi\sin\eta\right] + \dot{\delta\iota}\left[\cos\phi\sin\eta\sin\iota + \sin\phi\cos\psi\cos\iota - \cos\eta\sin\iota\sin\phi\sin\psi\right]$$

which are the complete angular velocity components in the body axes.

1.2 Effects of Orbit Perturbations

Before proceeding with the expansion of the various torque components, it is desirable to simplify the equations of motion somewhat, by simplifying the angular velocity components P, q, h. For order of magnitude purposes, all angular velocities may be compared with the angular velocity of the orbital coordinates, $\dot{\nu}$.

As mentioned previously, the angular velocities $\dot{\Omega}$, $\dot{i}$ and $\dot{\omega}$ arise because of perturbations from the otherwise inverse-square (Keplerian) motion. Examples are anomalies in the gravitational field (such as oblateness) and atmospheric drag. These perturbations affect not only the angles Ω, i and ω but also the orbital period, the perigee distance and other parameters which characterize motion on the Keplerian ellipse (Ref. 17). The perturbations are of two types, secular perturbations, which are monotonous functions of time, and periodic perturbations, which vary harmonically with (say) the true anomaly, ν. For motion near an oblate primary body, the gravitational potential, Φ, may be expanded as a series in spherical harmonics, the coefficients of which are functions of the radial distance r,

$$\Phi = -\frac{\mu}{r}\left\{ 1 + \frac{1}{3} J \left(\frac{a_e}{r}\right)^2 \left[1 - 3\sin^2\varphi\right] + \cdots \right\}$$

where μ is the product of the universal gravitational constant and the mass of the primary body, a_e is the mean equatorial radius of the primary body, φ the geocentric latitude measured from the equator and J is a small constant. Using the standard methods of variation of parameters (Ref. 17), Krause (Ref. 18) finds that when J is not negligible, the leading perturbation terms for $\dot{\Omega}$ and $\dot{\omega}$ are secular while $\dot{i}$ has no first order secular component, but experiences an appreciable periodic perturbation. These results may be written in the form:

$$\begin{aligned}
\dot{\Omega} &= -\frac{\dot{\nu} J}{(1-\epsilon^2)^2}\left(\frac{a_e}{a}\right)^2 \cos i \\
\dot{i} &= -\frac{\dot{\nu} J}{(1-\epsilon^2)^2}\left(\frac{a_e}{a}\right)^2 (1+\epsilon\cos\nu)\sin 2u \sin i \cos i \qquad (10) \\
\dot{\omega} &= \frac{\dot{\nu} J}{(1-\epsilon^2)^2}\left(\frac{a_e}{a}\right)^2 \left[2 - \frac{5}{2}\sin^2 i\right]
\end{aligned}$$

where ϵ is the orbital eccentricity, a the mean distance (or semi-major axis) of the elliptical orbit and n the Keplerian mean motion (or mean angular velocity of the motion). For nearly circular orbits (Ref. 18),

$$n \equiv 2\pi/P \cong \dot{v}$$

where P is the orbital period, and hence for order of magnitude purposes it is approximately true that

$$O\left(\frac{\dot{\Omega}}{\dot{v}}\right) \cong O\left(\frac{\dot{\iota}}{\dot{v}}\right) \cong O\left(\frac{\dot{\omega}}{\dot{v}}\right) \cong J .$$

For Earth, $J \cong 1.6 \times 10^{-3}$ and hence the above terms are negligibly small compared to unity. Beletskiy (Ref. 14) arrives at essentially this same result by means of substantially similar arguments.

The perturbations due to atmospheric drag are not so readily disposed of. Krause (Ref. 18) has shown that when the planetary atmosphere does not rotate, drag produces no change at all in the angles Ω and ι and so the orbit remains on a space-fixed plane. Under these circumstances ω possesses a small periodic perturbation which may be taken into account through the variable η . More recently, Sterne (Ref. 19) has considered the problem in great generality, accounting for atmospheric rotation as well as the "flattening" of the atmosphere due to planetary oblateness. In the presence of atmospheric rotation, Sterne's results for the secular perturbations of Ω , ι and ω may be written approximately (for small eccentribity orbits) as

$$\frac{\dot{\Omega}}{\dot{v}} \cong -\frac{b}{2}\left(\frac{\omega_E}{\dot{v}}\right) a\rho_\ell \, I_2(\lambda) \sin 2\omega$$

$$\frac{\dot{\iota}}{\dot{v}} \cong -\frac{b}{2}\left(\frac{\omega_E}{\dot{v}}\right) a\rho_\ell \left\{ I_0(\lambda) \sin\iota + I_2(\lambda) \sin\iota \cos 2\omega \right\}$$

$$\frac{\dot{\omega}}{\dot{v}} \cong -\frac{\dot{\Omega}}{\dot{v}} \cos\iota$$

where b is the ballistic coefficient of the body, ω_E is the Earth's angular velocity of daily rotation, ρ_ℓ the atmospheric density at the semi-latus rectum of the orbit and $I_n(\lambda)$ is the modified Bessel function of the first kind and order n of argument λ . Here λ is an atmosphere parameter which is defined in Section 3.2. It will be shown later that for Earth, $(\omega_E/\dot{v}) < O(10^{-1})$ while $a\rho_\ell < O(10^{-4})$ and since b is generally at most of order 10, then the secular contributions to $\dot{\Omega}$, $\dot{\iota}$ and $\dot{\omega}$ due to atmospheric drag on the satellite are also negligible in comparison to $\dot{v}$.

The resulting angular velocity components are found from Eqs. (9) as,

$$\begin{aligned} p &= \dot{\phi} + S - \dot{\eta}\sin\psi \\ q &= -\dot{\psi}\sin\phi + \dot{\eta}\cos\phi\cos\psi \\ r &= -\dot{\psi}\cos\phi - \dot{\eta}\sin\phi\cos\psi \end{aligned} \tag{11}$$

where the equations of the angular motion are given by Eq. (1) and are complete once the torque components L_x, L_y and L_z are specified.

1.3 Introduction of Gravity Gradient Torques

The determination of the external torques acting on the satellite will be performed in Section 2. However, it is noted that one primary torque known to act on any satellite is that due to the gravity gradient across the vehicle. Since this torque arises from the vehicle's mass distribution, it bears a close association with the body's inertia characteristics and is therefore best included in the basic equations of motion.

From Eq. (A-15), Appendix A, the gravitational torques for an inverse-square central force field may be given to a first order in the ratio ℓ/r (where ℓ is the maximum body dimension) by

$$\begin{bmatrix} L_{g_x} \\ L_{g_y} \\ L_{g_z} \end{bmatrix} = 3\frac{\mu}{r^3}\begin{bmatrix} -\frac{r_y r_z}{r^2}\left(\bar{I}_y - \bar{I}_z\right) \\ \frac{r_x r_z}{r^2}\left(\bar{I}_z - \bar{I}_x\right) \\ \frac{r_x r_y}{r^2}\left(\bar{I}_x - \bar{I}_y\right) \end{bmatrix} \tag{12}$$

where μ is the product of the earth's mass and the universal gravitational constant as before and r_x/r, r_y/r and r_z/r are direction cosines between the radius vector and the x, y, z body-fixed axes. These direction cosines may be expanded in terms of the angles θ, ψ, ϕ from Eqs. (4) and (5) as

$$\begin{aligned} \frac{r_y r_z}{r^2} &= -\frac{1}{2}\left\{\sin 2\psi\left[\sin^2\psi\sin^2\theta - \cos^2\theta\right] + \cos 2\phi\sin\psi\sin 2\theta\right\} \\ \frac{r_x r_z}{r^2} &= \frac{1}{2}\left\{\sin\phi\sin 2\psi\sin^2\theta + \cos\phi\cos\psi\sin 2\theta\right\} \\ \frac{r_x r_y}{r^2} &= \frac{1}{2}\left\{-\cos\phi\sin 2\psi\sin^2\theta + \sin\phi\cos\psi\sin 2\theta\right\} \end{aligned} \tag{13}$$

and so,

$$\begin{bmatrix} L_{g_x} \\ L_{g_y} \\ L_{g_z} \end{bmatrix} = \frac{3}{2}\frac{\mu}{r^3} \begin{bmatrix} \left[s2\phi\,(s^2\psi s^2\theta - c^2\theta) + (c^2\phi - s^2\phi)\, s\psi\, s2\theta \right](\bar{I}_y - \bar{I}_z) \\ \left[s\phi\, s2\psi\, s^2\theta + c\phi\, c\psi\, s2\theta \right](\bar{I}_z - \bar{I}_x) \\ \left[-c\phi\, s2\psi\, s^2\theta + s\phi\, c\psi\, s2\theta \right](\bar{I}_x - \bar{I}_y) \end{bmatrix} . \tag{14}$$

The complete equations of angular motion may now be obtained by substituting Eqs. (14) into Eqs. (1). Because of the aforementioned relationship between the gravitational torques and the angular inertia, it is convenient to group these terms together, viz:

$$\begin{aligned} L_{R_x} &= \dot{p}\,\bar{I}_x + \left\{ qh + \frac{3\mu}{2r^3}\left[s2\phi\,(s^2\psi s^2\theta - c^2\theta) \right.\right. \\ &\qquad \left.\left. + (c^2\phi - s^2\phi)\, s\psi\, s2\theta \right]\right\}(\bar{I}_z - \bar{I}_y) \\ L_{R_y} &= \dot{q}\,\bar{I}_y + \left\{ ph + \frac{3\mu}{2r^3}\left[s\phi\, s2\psi\, s^2\theta + c\phi\, c\psi\, s2\theta \right]\right\}(\bar{I}_x - \bar{I}_z) \\ L_{R_z} &= \dot{h}\,\bar{I}_z + \left\{ pq + \frac{3\mu}{2r^3}\left[s\phi\, c\psi\, s2\theta - c\phi\, s2\psi\, s^2\theta \right]\right\}(\bar{I}_y - \bar{I}_x) \end{aligned} \tag{15}$$

where L_{R_x}, L_{R_y}, L_{R_z} denote all other torques acting on the vehicle except those due to the gravity gradients.

Eqs. (15) constitute the complete equations of angular motion of a "small" satellite vehicle moving in the vicinity of an essentially spherical primary body. The equations are written in principal body axes, but apart from these restrictions, no other significant assumptions have been made.

1.4 Equations of Motion for Small Angles

Now suppose that ϕ and ψ are small, but θ need not be small. Then squares and products of ϕ and ψ are negligible but sines and cosines of θ must be retained. Eqs. (15) become, under these conditions,

$$\begin{aligned} L_{R_x} &= \dot{p}\,\bar{I}_x + \left\{ qh + 3\frac{\mu}{r^3}\left[\psi \sin\theta\cos\theta - \phi\cos^2\theta \right]\right\}(\bar{I}_z - \bar{I}_y) \\ L_{R_y} &= \dot{q}\,\bar{I}_y + \left\{ ph + 3\frac{\mu}{r^3}\sin\theta\cos\theta \right\}(\bar{I}_x - \bar{I}_z) \\ L_{R_z} &= \dot{h}\,\bar{I}_z + \left\{ pq + 3\frac{\mu}{r^3}\left[\phi\sin\theta\cos\theta - \psi\sin^2\theta \right]\right\}(\bar{I}_y - \bar{I}_x) \end{aligned} \tag{16}$$

where the angular velocity components from Eqs. (11) simplify to read,

$$\begin{aligned} p &\cong \dot{\phi} + s - \psi\dot{\eta} \\ q &\cong -\phi\dot{\psi} + \dot{\eta} \\ r &\cong -\dot{\psi} - \phi\dot{\eta} \ . \end{aligned} \tag{17}$$

To the same order of approximation, if the rates $\dot{\psi}$ and $\dot{\phi}$ are small so that squares and products of these terms are negligible also,

$$\begin{aligned} qr &\cong -\dot{\psi}\dot{\eta} - \phi\dot{\eta}^2 \\ pr &\cong -s(\phi\dot{\eta} + \dot{\psi}) \\ pq &\cong +(s+\dot{\phi})\dot{\eta} - \psi\dot{\eta}^2 \end{aligned}$$

and (if s = constant),

$$\begin{aligned} \dot{p} &\cong \ddot{\phi} - \dot{\psi}\dot{\eta} \\ \dot{q} &\cong \ddot{\eta} \\ \dot{r} &\cong -\ddot{\psi} - \dot{\phi}\dot{\eta} \end{aligned} \tag{18}$$

whereupon, Eqs. (16) take the form,

$$\begin{aligned} L_{R_x} &= \ddot{\phi}\bar{I}_x - \dot{\psi}\dot{\eta}(\bar{I}_z - \bar{I}_y + \bar{I}_x) - \left\{\phi\dot{\eta}^2 - 3\frac{\mu}{r^3}\left[\psi \sin\theta\cos\theta \right.\right. \\ &\qquad \left.\left. - \phi\cos^2\theta\right]\right\}(\bar{I}_z - \bar{I}_y) \\ L_{R_y} &= \ddot{\eta}\bar{I}_y - \left\{s(\phi\dot{\eta} + \dot{\psi}) - 3\frac{\mu}{r^3}\sin\theta\cos\theta\right\}(\bar{I}_x - \bar{I}_z) \\ L_{R_z} &= -\ddot{\psi}\bar{I}_z - (s+\dot{\phi})\dot{\eta}(\bar{I}_z - \bar{I}_y + \bar{I}_x) - \left\{\psi\dot{\eta}^2 - 3\frac{\mu}{r^3}\left[\phi\sin\theta\cos\theta \right.\right. \\ &\qquad \left.\left. - \psi\sin^2\theta\right]\right\}(\bar{I}_y - \bar{I}_x) \ . \end{aligned} \tag{19}$$

These equations describe the angular motion of a satellite vehicle in the presence of a non-negligible spin velocity, allowing θ to be arbitrarily large. For most applications of interest, however, θ is also small and in this case the equations become

$$L_{Rx} = \ddot{\phi}\bar{I}_x - \dot{\psi}\dot{\eta}(\bar{I}_z - \bar{I}_y + \bar{I}_x) - \phi\left\{\dot{\eta}^2 + 3\frac{\mu}{r^3}\right\}(\bar{I}_z - \bar{I}_y)$$

$$L_{Ry} = \ddot{\eta}\bar{I}_y - \left\{S(\phi\dot{\eta} + \dot{\gamma}) - 3\frac{\mu}{r^3}\theta\right\}(\bar{I}_x - \bar{I}_z) \qquad (20)$$

$$L_{Rz} = -\ddot{\psi}\bar{I}_z - (S + \dot{\phi})\dot{\eta}(\bar{I}_z - \bar{I}_y + \bar{I}_x) - \gamma\dot{\eta}^2(\bar{I}_y - \bar{I}_x) \ .$$

These equations are essentially identical to those presented by Frye and Stearns (Ref. 4) and Roberson (Ref. 9), although these authors do not consider the possibility of a spinning vehicle. When the spin, S, is zero, the second of Eqs. (20) is uncoupled from the first and third and, provided that L_{Ry} is independent of ϕ and γ, the θ variation (and hence the η variation) may be explicitly determined. The first and third of these equations then contain only the terms γ and ϕ as coupled unknowns and may be solved by iteration. Note further that since the time variation of η may be found from the second of Eqs. (20), the above system of equations is linear[1], in spite of the obvious complexity.

For simplicity, only the case of a non-spinning, symmetrical vehicle will be considered in detail here; that is, one for which the x-axis is an axis of symmetry:

$$\bar{I}_y = \bar{I}_z \equiv \bar{I}$$

and for which $S = 0$. The equations of angular motion become, in this case,

$$L_{Rx} = \left\{\ddot{\phi} - \dot{\psi}\dot{\eta}\right\}\bar{I}_x$$

$$L_{Ry} = \ddot{\eta}\bar{I} + 3\frac{\mu}{r^3}\theta(\bar{I}_x - \bar{I}) \qquad (21)$$

$$L_{Rz} = -\ddot{\psi}\bar{I} - \dot{\phi}\dot{\eta}\bar{I}_x + \gamma\dot{\eta}^2(\bar{I}_x - \bar{I}) \ .$$

It is to be noted from Eqs. (20) that for small angles, the gravitational torques have no direct effect on the yawing motion. For a body of revolution ($\bar{I}_y = \bar{I}_z = \bar{I}$) , these torques also vanish from the rolling

---

[1] L_{Rx}, L_{Ry} and L_{Rz} must also be linear.

motion equation as shown by Eqs. (21). The gravitational torques do, however, influence these motions through their coupling with the pitching motion.

Finally, it is appropriate to employ the definition of η , Eq. (7), and note that for small angular rates,

$$\dot{\eta}\,\dot{\psi} \cong -\dot{u}\,\dot{\psi}$$

$$\dot{\eta}\,\dot{\phi} \cong -\dot{u}\,\dot{\phi}$$

$$\dot{\eta}^2\psi \cong \dot{u}^2\psi \quad .$$

Hence Eqs. (21) become, after some algebraic rearrangement,

$$\ddot{\phi} = L_{Rx}/\bar{I}_x - \dot{u}\,\dot{\psi}$$

$$\ddot{\theta} + 3\frac{\kappa}{r^3}M\theta = L_{Ry}/\bar{I} + \ddot{u} \qquad (22)$$

$$\ddot{\psi} - M\dot{u}^2\psi = -L_{Rz}/\bar{I} + \dot{u}(M+1)\dot{\phi}$$

where M is an inertia parameter, defined by

$$M \equiv \frac{\bar{I}_x - \bar{I}}{\bar{I}} \quad . \qquad (23)$$

Eqs. (22) are the equations of angular motion to be considered in detail. Inasmuch as the orbital motion of the vehicle is assumed to be known, u and all of its derivatives are known and Eqs. (22) may be solved for the three unknowns ψ , θ , ϕ as functions of time. It is well to re-emphasize that the rolling and yawing motions are inherently coupled, principally because $\dot{u}$ is not negligible (see Eqs. 22); that is, because the orbital coordinates are rotating with angular velocity $\dot{u}$ relative to the inertial axes. Roberson (Ref. 3) has also made this observation previously.

Before seeking a solution to Eqs. (22), the expressions for the remaining moments acting on the vehicle must be obtained. This development is performed in the next section.

2. EXTERNAL TORQUES ON THE SATELLITE

2.1 Introduction

One can readily conceive a number of torques which may act on an orbital vehicle, among the most significant being (Refs. 3, 4): (1) gravitational torques due to gravity gradients across the vehicle, (2) aerodynamic torques due to motion through the rarefied atmosphere, (3) electromagnetic torques due to motion through a magnetic field and surface charge on the vehicle, (4) "radiation pressure" torques due to motion in a photon stream from some body such as the Sun, and (5) mechanical torques due to moving parts internal to the vehicle.

While it is generally true that most, if not all, of these torques would be insignificant at the Earth's suface, they predominate on an orbital vehicle owing to the absence of all other major influences. In the following sections, a discussion of these torques is presented.

2.2 Gravitational Torques

The influence of the gravity gradient is perhaps best evidenced by the Earth's natural satellite, the Moon, which, due to an asymmetrical mass distribution, always keeps approximately the same side pointed toward the Earth. The recent literature is rich in material on the use of these torques for satellite attitude control (Refs. 3-10), although as mentioned previously, much of the work must be classed as feasibility studies since overly restrictive assumptions (such as omission of all other disturbing torques, circular orbit, etc.) have been made. Since the Earth's gravitational field may be utilized for these purposes even at great heights, however, it is not surprising that the problem has received so much attention.

The general development of the gravity gradient torques which act on an orbiting vehicle has been performed by Roberson (Refs. 9, 10) considering the gravitational potential which corresponds to the oblate Earth, but his discussion has been unnecessarily complicated by the introduction of numerous Euler angles which are particular to the problem of satellite vehicle orientation. DeBra (Ref. 12), in essentially repeating this development for a spherical Earth, arrives at an incorrect result which, in the limit of small deviation angles, merges with the correct expressions given by Roberson. More recently, Nidey (Ref. 20) has published a concise discussion of the gravitational torques acting on a rigid body.

For completeness, the expressions for the gravitational torque components along arbitrary axes fixed in a rigid body are derived from first principles in Appendix A. Although only a simple inverse-square

attracting force field is considered, the extension to include oblateness effects or other anomalies in the force field may be readily performed. The result, as used in Section 1.3, Eq. (12), is

$$\begin{bmatrix} L_{g_x} \\ L_{g_y} \\ L_{g_z} \end{bmatrix} = 3\frac{\mu}{r^3} \begin{bmatrix} -\frac{r_y r_z}{r^2}\left(\bar{I}_y - \bar{I}_z\right) \\ \frac{r_x r_z}{r^2}\left(\bar{I}_z - \bar{I}_x\right) \\ \frac{r_x r_y}{r^2}\left(\bar{I}_x - \bar{I}_y\right) \end{bmatrix}$$

where the direction cosines between the radius vector $\vec{r}$ and the principal body axes, r_x/r, r_y/r and r_z/r are given by Eqs. (13). It may be noted that when θ, ψ, ϕ are small angles such that $\sin\psi \cong \psi$ and $\cos\psi \cong 1$ and squares and products of the small angles are negligible, Eqs. (12) and (13) combine to yield,

$$\begin{bmatrix} L_{g_x} \\ L_{g_y} \\ L_{g_z} \end{bmatrix} \cong \frac{3}{2}\frac{\mu}{r^3} \begin{bmatrix} \left(\bar{I}_y - \bar{I}_z\right)\sin 2\phi \\ \left(\bar{I}_z - \bar{I}_x\right)\sin 2\theta \\ 0 \end{bmatrix} . \qquad (24)$$

Thus, as indicated previously, there is no gravitational yawing torque for small angular deviations of the body from the orbital coordinates.

To illustrate the behavior of the gravitational torques, assume that $\phi \cong 0$ and consider the torque about the y-axis, which is normal to the orbit plane. The appropriate geometry is shown in Fig. 5. In this case, Eq. (24) becomes

$$L_{g_y} = \frac{3}{2}\frac{\mu}{r^3}\left(\bar{I}_z - \bar{I}_x\right)\sin 2\theta$$

which is shown sketched qualitatively in Fig. 5.

Because L_{g_y} depends upon $\sin 2\theta$, the gravitational torque vanishes at $\theta = 0, \pi/2, \pi, \cdots$. Accordingly, these represent possible equilibrium positions of the vehicle. Note further, however,

that only for $dL_{g_y}/d\theta < 0$ is the equilibrium stable, since in this case a small positive increase in θ yields a negative (or restoring) torque on the body. Thus, when $\bar{I}_x > \bar{I}_z$, $\theta = 0, \pi, 2\pi, \cdots$ represent positions of stable equilibrium while for $\bar{I}_z > \bar{I}_x$, $\theta = \pi/2, 3\pi/2, \cdots$ represent stable positions. The gravitational torques, therefore, imply a position of stable equilibrium only when the body's axis of least inertia points toward the force center (Refs. 3, 4).

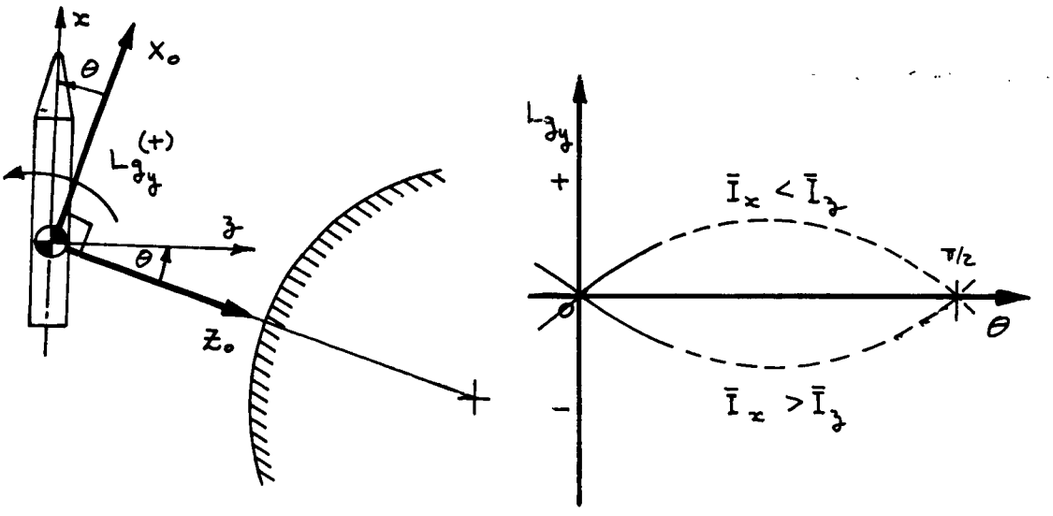

Figure 5. Behavior of Gravity Gradient Torque

The motion of a rigid, dumbbell-shaped satellite under the influence of the gravity gradient torques alone has been studied extensively in the literature; for example, Schindler (Ref. 5), Stocker and Vachino (Ref. 7), and Baker (Ref. 8). It is of interest, therefore, to note how the present analysis may be reconciled with these previous investigations.

Referring to Fig. 6 for the geometry of the dumbbell-shaped satellite, it is clear that

$$\bar{I}_x = \bar{I}_y = 2ml^2 + \frac{4}{5}m\left(\frac{D}{2}\right)^2$$

$$\bar{I}_z = \frac{4}{5}m\left(\frac{D}{2}\right)^2$$

hence for $D \ll \ell$,

$$L_{g_y} = \frac{3}{2}\frac{\mu}{r^3}\bar{I}_y\left[\frac{\bar{I}_z - \bar{I}_x}{\bar{I}_y}\right]\sin 2\theta \cong -\frac{3}{2}\frac{\mu}{r^3}\bar{I}_y \sin 2\theta \ .$$

Comparing this result with the second of Eqs. (22), it is seen that in the subsequent work, the pitching motion of a dumbbell-shaped satellite may be recovered by setting $M = 1$ and neglecting all aerodynamic influences.

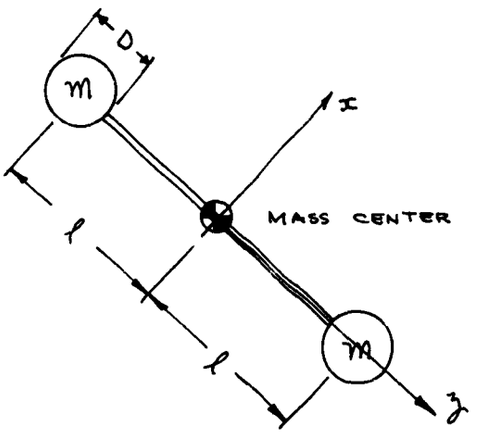

Figure 6. Geometry of Dumbbell-Shaped Satellite

2.3 Aerodynamic Torques

2.3.1 General Considerations

The open literature contains surprisingly little detailed work on the influence of the aerodynamic torques on the vehicle's motion, in spite of the fact that for Earth these torques are known to be significant over a wide range of altitudes (c.f. Refs. 4, 11-14). Because of highly rarefied nature of the atmosphere at altitudes where a satellite may make one or more successful orbits, the molecular mean free path is generally much larger than any characteristic body dimension and free-molecular

flow exists. Aerodynamic forces and moments on vehicles in this flow regime are due solely to the molecular bombardment and subsequent reflection from the surface and are most conveniently predicted within the framework of the kinetic theory of gases. The "exact" theory has been developed extensively by numerous authors but the expressions for the free-molecular pressure and shearing stress coefficients on an arbitrary element of body surface are generally so complicated that the integration to obtain forces and moments has been performed for only the simplest bodies (c.f. Ref. 1, Section 1).

More recently, an approximate free molecular theory has been published (Ref. 21) which permits calculation of the conventional aerodynamic stability derivatives of arbitrary bodies of revolution. Davison, in Volume II of this series of reports (Ref. 1) presents a detailed application of this and similar methods to a wide variety of body shapes. The results of these studies are summarized briefly in Section 3.3 of this report.

2.3.2 Orientation of the Relative Wind Vector

The aerodynamic torques acting on a satellite may be determined once the relative wind vector has been oriented with respect to the vehicles. The relative wind vector is the velocity of the vehicle with respect to the local atmosphere, and due to atmospheric motion relative to inertial space, this vector may differ appreciably from the inertial velocity vector in direction as well as in magnitude. Although a number of possible alternatives suggest themselves, the conventional angle of attack, α, and the sideslip angle, β, are most convenient for orienting the relative wind with respect to the body axes. By retaining these angles, the aerodynamic moment coefficients may be carried over directly from conventional aerodynamic theory and the interpretation of the various terms which arise is considerably simplified.

Referring to Fig. 7, the components of the relative velocity vector $\vec{V}_R$ may be expressed in the body axes by the matrix equation

$$\begin{bmatrix} V_{R_x} \\ V_{R_y} \\ V_{R_z} \end{bmatrix} = V_R \begin{bmatrix} \cos\alpha \cos\beta \\ \sin\beta \\ \sin\alpha \cos\beta \end{bmatrix} . \qquad (25)$$

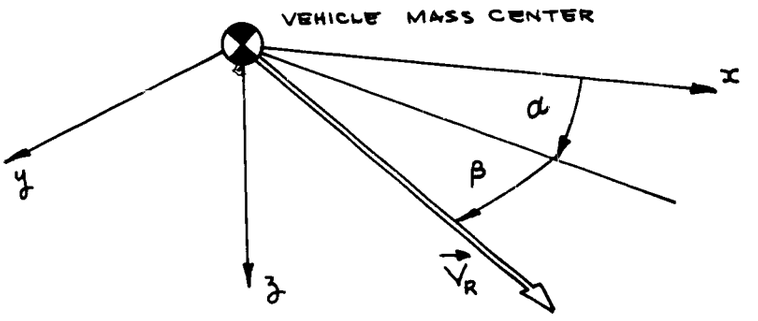

Figure 7. Orientation of the Relative Wind Vector with Respect to the Vehicle

The relative velocity components in the body axes may also be obtained through an independent transformation which involves the previously introduced orientation angles θ , ψ , ϕ . To obtain this relationship, first orient the relative wind vector with respect to the orbital coordinates by two new angles γ and Λ , as shown in Fig. 8. These angles are completely specified by the motion of the vehicle's mass center.

In this case the components of $\vec{V}_R$ in the orbital coordinates may be given in matrix form as

$$\begin{bmatrix} V_{R_{x_o}} \\ V_{R_{Y_o}} \\ V_{R_{Z_o}} \end{bmatrix} = V_R \begin{bmatrix} \cos\gamma \cos\Lambda \\ -\sin\Lambda \\ -\sin\gamma \cos\Lambda \end{bmatrix} . \qquad (26)$$

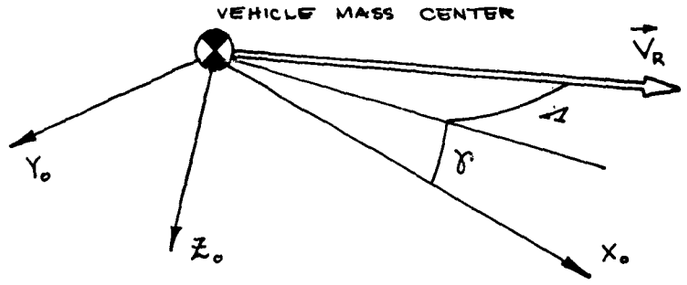

Figure 8. Orientation of the Relative Wind Vector with Respect to the Orbital Coordinates

Now, introducing the transformation from the orbital coordinates to the body-fixed axes as given by Eq. (4), there results

$$\begin{bmatrix} V_{R_x} \\ V_{R_y} \\ V_{R_z} \end{bmatrix} = V_R \begin{bmatrix} c\psi c(\theta-\gamma)c\Lambda + s\psi s\Lambda \\ s\phi s(\theta-\gamma)c\Lambda + c\phi s\psi c(\theta-\gamma)c\Lambda - c\phi c\psi s\Lambda \\ c\phi s(\theta-\gamma)c\Lambda - s\phi s\psi c(\theta-\gamma)c\Lambda + s\phi c\psi s\Lambda \end{bmatrix}. \tag{27}$$

Equating corresponding components of Eqs. (25) and (27) gives the desired relationships for α and β in terms of other known angles. Unfortunately, the complexity of these relationships for the general large angle case virtually precludes their use in analytic work. Accordingly, it is desirable to introduce the assumption of small angles consistent with what was done in Section 1.4. In order to do this, it must first be shown that γ and Λ are truly small.

The atmosphere of Earth essentially rotates as a rigid body attached to the Earth. Although it is probably true that at sufficiently great distances such motion will not occur, at altitudes where the aerodynamic influences predominate the assumption of rigid body atmospheric rotation

should be acceptable. The presence of local wind anomalies may be neglected, since they are generally fluctuating in magnitude and direction and are not sufficiently well defined at satellite altitudes to allow a satisfactory generalization to be made. Accordingly, the relative velocity vector may be related to the inertial velocity vector through the equation

$$\vec{V}_R = \vec{V} - k\,\vec{\omega}_E \times \vec{r} \tag{28}$$

where $\vec{\omega}_E$ is the angular velocity vector of the Earth, $\vec{V}$ is the inertial velocity vector and k is a coefficient which may depend upon altitude and permits deviation of the atmospheric motion from a purely rigid body rotation. The components of $\vec{\omega}_E$ in the orbital coordinates are found from Eq. (2) to be

$$\begin{bmatrix} \omega_{E_{x_o}} \\ \omega_{E_{y_o}} \\ \omega_{E_{z_o}} \end{bmatrix} = -\omega_E \begin{bmatrix} -\cos u \sin \iota \\ \cos \iota \\ \sin u \sin \iota \end{bmatrix} \tag{29}$$

while by definition of the orbital coordinates, $\vec{r}$ lies along $-\vec{z}_o$. The vector product $\vec{\omega}_E \times \vec{r}$ given in Eq. (2) then becomes, in matrix form,

$$\left[\vec{\omega}_E \times \vec{r}\right] = r\,\omega_E \begin{bmatrix} \cos \iota \\ \cos u \sin \iota \\ 0 \end{bmatrix}. \tag{30}$$

Now previous arguments have shown $\dot{\Omega}$, $\dot{\iota}$ and $\dot{\omega}$ to be negligibly small and hence the motion of the vehicle's mass center is planar. By definition of the orbital coordinates, this plane is coincident with the x_o-z_o plane, and so $\vec{V}$ has no component along y_o. Let the components of $\vec{V}$ in the orbital coordinates be given in matrix form by

$$\begin{bmatrix} V_{x_o} \\ V_{y_o} \\ V_{z_o} \end{bmatrix} = V \begin{bmatrix} \cos \gamma^* \\ 0 \\ -\sin \gamma^* \end{bmatrix} \tag{31}$$

where γ^* is the inclination angle of the inertial velocity vector (or the tangent to the orbit) with respect to the X_o axis. Clearly γ^* is also completely specified by the motion of the mass center. From Krause (Ref. 18) or Eq. (B-5), Appendix B, there is found

$$\text{Tan}\,\gamma^* = \frac{\dot{r}}{r\dot{\upsilon}} = \frac{\epsilon \sin\upsilon}{1+\epsilon\cos\upsilon}$$

where ϵ is the orbital eccentricity. For elliptical orbits of small eccentricity (say less than .06), it follows that γ^* is a small angle.

Combining Eqs. (30) and (31) with Eq. (28), the components of the relative velocity vector in the orbital coordinates are found to be[1]

$$\begin{bmatrix} V_{R_{X_o}} \\ V_{R_{Y_o}} \\ V_{R_{Z_o}} \end{bmatrix} = - \begin{bmatrix} r\omega_a \cos\iota - V\cos\gamma^* \\ r\omega_a \cos u \sin\iota \\ V\sin\gamma^* \end{bmatrix} \tag{32}$$

and the magnitude of $\vec{V}_R$ is given in terms of known quantities as

$$\left(\frac{V_R}{V}\right)^2 = 1 - 2\left(\frac{r\omega_a}{V}\right)\cos\iota\cos\gamma^* + \left(\frac{r\omega_a}{V}\right)^2\left(1-\sin^2 u \sin^2\iota\right). \tag{33}$$

Sterne (Ref. 19) has also presented this result. Comparing Eqs. (26) and (32) allows the angles γ and Λ to be evaluated:

$$\sin\Lambda = \frac{r\omega_a}{V}\left(\frac{V}{V_R}\right)\cos u \sin\iota$$

$$\sin\gamma = \frac{\sin\gamma^*}{\cos\Lambda}\left(\frac{V}{V_R}\right). \tag{34}$$

For low altitude orbits about the Earth, k is near unity and so $\omega_a \cong \omega_E \neq 0$ (2×10^3) while at altitudes for which aerodynamic effects are significant $V \cong 0$ (2×10^4) hence $r\omega_a/V$ is small compared to unity. In this case, the ratio V/V_R may be developed from Eq. (33) by a binomial expansion in the form,

---

[1] It is convenient to introduce the abbreviation $\omega_a = k\omega_E$ to denote the angular velocity of atmospheric rotation.

$$\frac{V}{V_R} = 1 + \frac{r\omega_a}{V} \cos\iota \cos\gamma^* + O\left(\frac{r\omega_a}{V}\right)^2 \qquad (35)$$

where the terms omitted produce an error of less than 1%. Note that the last term in Eq. (33) contains the only latitude-dependent contribution to V/V_R[1], and that this term is of order $(r\omega_a/V)^2$ and hence negligible in Eq. (35). Inserting this relation into the first of Eqs. (34), and again neglecting terms of order $(r\omega_a/V)^2$ there results

$$\sin\Lambda \cong \frac{r\omega_a}{V} \sin\iota \cos u . \qquad (36)$$

This expression shows that Λ is a small angle so that $\cos\Lambda \cong 1$. Hence the second of Eqs. (34) becomes, to first order terms in $r\omega_a/V$,

$$\sin\gamma \cong \sin\gamma^*\left(1 + \frac{r\omega_a}{V} \cos\iota \cos\gamma^*\right).$$

Since it has already been observed that γ^* is small, then it follows that γ is also small and is given approximately by

$$\gamma \cong \gamma^*\left(1 + \frac{r\omega_a}{V} \cos\iota\right). \qquad (37)$$

Now assuming ϕ, ψ, θ, γ and Λ are all small angles, and comparing Eqs. (25) and (27),

$$\cos\alpha \cos\beta \cong 1$$

$$\sin\beta \cong (\psi - \Lambda)$$

$$\sin\alpha \cos\beta \cong (\theta - \gamma)$$

---

[1]Spherical trigonometry yields the relation: $\sin\iota \sin u = \sin\vartheta$.

from which it follows that α and β are also small and given by the linear equations

$$\alpha \cong (\theta - \gamma)$$
$$\beta \cong (\psi - \Lambda) \,. \tag{38}$$

It is important to note that this representation fails completely in the case of large angular deviations.

2.3.3 Expansion of the Aerodynamic Torques

With the orientation of the relative wind vector completely specified for small angles by Eqs. (38), the aerodynamic moments may be determined. Following the conventional practice

$$\begin{bmatrix} L_{A_x} \\ L_{A_y} \\ L_{A_z} \end{bmatrix} = \frac{1}{2} \rho V_R^2 S_\pi \bar{c} \begin{bmatrix} C_\ell \\ C_m \\ C_n \end{bmatrix} \tag{39}$$

where ρ is the local atmospheric density, S_π is a reference area on the vehicle, $\bar{c}$ is a reference length on the vehicle and C_ℓ, C_m and C_n are respectively the dimensionless rolling, pitching and yawing moment coefficients. It is conventional to expand C_ℓ, C_m and C_n about the equilibrium position as a Taylor series in the variables α, β, $\dot{\alpha}$, $\dot{\beta}$, p, q and r. When the angular deviation of the body from equilibrium is small, only the leading terms in the series need be retained, and if the body possesses symmetry, a number of the remaining coefficients may be shown to be small or else identically zero. For a body of revolution, this "linearized" representation takes the form,

$$C_\ell = C_{\ell_\beta} \beta + \frac{\bar{c}}{2V_R} \left\{ C_{\ell_p} p + C_{\ell_r} r \right\}$$

$$C_m = C_{m_\alpha} \alpha + C_{m_\beta} \beta + \frac{\bar{c}}{2V_R} \left\{ C_{m_q} q + C_{m_{\dot{\alpha}}} \dot{\alpha} \right\}$$

$$C_n = C_{n_\beta} \beta + \frac{\bar{c}}{2V_R} \left\{ C_{n_p} p + C_{n_r} r + C_{n_{\dot{\beta}}} \dot{\beta} \right\}$$

where the second subscript on the coefficient of any term indicates differentiation and evaluation as indicated below:

$$C_{l_\beta} = \left\{\frac{\partial C_l}{\partial \beta}\right\}_{\substack{\beta \to 0 \\ \alpha, \dot{\alpha}, \dot{\beta}, p, q, r = 0}}$$

$$C_{l_p} = \left\{\frac{\partial C_l}{\partial\left(\frac{p\bar{c}}{2V_R}\right)}\right\}_{\substack{p \to 0 \\ \alpha, \dot{\alpha}, \beta, \dot{\beta}, q, r = 0}}$$

Note that the rate derivatives have been non-dimensionalized by replacing the rate ($\dot{\alpha}$, $\dot{\beta}$, p, etc.) by $\bar{c}/2V_R$ times the rate ($\dot{\alpha}\bar{c}/2V_R$, $\dot{\beta}\bar{c}/2V_R$, etc.) These equations show a strong coupling between C_l and C_n, while C_m is essentially uncoupled from them except for the term $C_{m_{\dot{\beta}}}\dot{\beta}$ which is generally small for symmetric configurations. The terms involving the angular rates p, q and r represent aerodynamic damping, which is the only "natural" damping present in the system. For the purpose of simplification, only the following dominant terms shall be retained:

$$\begin{aligned} C_l &= \frac{\bar{c}}{2V_R} C_{l_p} p \\ C_m &= C_{m_\alpha}\alpha + \frac{\bar{c}}{2V_R} C_{m_q} q \\ C_n &= -C_{m_\alpha}\beta + \frac{\bar{c}}{2V_R} C_{m_q} r \end{aligned} \tag{40}$$

Here $C_{n_\beta} = -C_{m_\alpha}$ and $C_{n_r} = C_{m_q}$ since only bodies of revolution are to be considered. The negative sign must be imposed on C_{m_α} since a stable body at positive α and β (see Fig. 7) experiences a negative pitching moment but a positive yawing moment and hence for bodies of revolution, C_{m_α} and C_{n_β} are equal in magnitude but differ in sign. Inserting Eqs. (38) and (40) into Eq. (39) and expanding p, q and r, the complete linearized expression for the aerodynamic torques becomes, for small angles and angular rates,

$$\begin{bmatrix} L_{A_x} \\ L_{A_y} \\ L_{A_z} \end{bmatrix} = \frac{1}{2}\rho V_R^2 S_\pi \bar{c} \begin{bmatrix} \frac{\bar{c}}{2V_R} C_{l_p}(\dot{\phi} + \dot{u}\psi) \\ C_{m_\alpha}(\theta - \gamma) + \frac{\bar{c}}{2V_R} C_{m_q}(\dot{\theta} - \dot{u}) \\ -C_{m_\alpha}(\psi - \Lambda) - \frac{\bar{c}}{2V_R} C_{m_q}(\dot{\psi} - \phi\dot{u}) \end{bmatrix} \quad (41)$$

where $\sin \Lambda \cong \Lambda$ is given by Eq. (36), γ is given by Eq. (37) and the magnitude of $\vec{V}_R$ is given to a first order in $r\omega_3/V$ from Eq. (35) by

$$V_R \cong V\left\{1 - \frac{r\omega_3}{V}\cos\iota\right\}. \quad (42)$$

In the following work the coefficients C_{l_p}, C_{m_α} and C_{m_q}, which are generally functions of altitude and velocity, will be regarded as constants of the motion. The error introduced in this way is small compared to the uncertainties in other quantities such as the atmospheric density.

2.4 Other Disturbing Torques

2.4.1 Solar Radiation Pressure Torques

Following the gravity gradient and aerodynamic torques, the next most significant external torque appears to be that due to the solar radiation pressure. For extremely high altitude orbits, this torque will doubtless transcend all other predictable external torques. In this connection, the work of Frye and Stearns (Ref. 4), Sohn (Ref. 15), and, more recently, Newton (Ref. 16), provide suitable documentation. Accordingly, the significant question in regard to the present study concerns the altitudes at which the solar radiation pressure will induce torques of comparable magnitude to the aerodynamic and/or gravitational torques.

Since the solar torques arise from the momentum flux imparted to the vehicle by the photon stream emanating from the Sun, they are amenable to analysis using suitably modified free molecular aerodynamic concepts. A detailed examination of these torques for several classes of elementary body shapes is presented in Appendix A of Ref. 1. Fig. 9 summarizes the results of these calculations by comparing the magnitudes of the initial

torque slopes due to aerodynamic and solar influences for three optimized body shapes[1]. It is seen that for these shapes, the solar torques do not become comparable to those due to aerodynamic effects until altitudes in excess of 400 miles are achieved. Wall (Ref. 11) in comparing directly the magnitudes of the solar radiation pressure and the dynamic pressure due to the satellite's motion through the atmosphere, also concludes that aerodynamically stable bodies will "trim" into the Sun at altitudes above about 400 miles.

Because the solar photon stream is not completely reflected by the body, one component of the solar flux appears as a shearing stress on the body surface. This, in turn, results in a residual torque arising from surface tractions alone which threaten to perturb all but spherically shaped satellites with mass center at the geometrical center of the body. Consequently, the solar torques may be expected to be a significant factor even with a gravity gradient stabilized vehicle. This point is illustrated in Fig. 10 where the maximum values of the torques due to aerodynamic, gravitational and solar influences are compared for the conical body shape. It is seen that the solar and gravitational torques are of comparable magnitude and significantly smaller than the aerodynamic torques for altitudes below about 400 miles. Above 600 miles altitude, the atmospheric density becomes so small that the gravitational and solar torques dominate the vehicle's motion. Although the absolute torque levels change with the geometry of the body, these qualitative relationships remain true for other configurations (Ref. 1). It appears, therefore, that the combined influence of solar and gravitational torques (rather than either separately) are required to properly analyze the passive angular response of a high-altitude satellite.

As a result of the foregoing, subsequent work in this study is limited to altitudes below 400 miles. The framework which is developed, however, is readily adaptable to the analysis of high altitude orbits.

---

[1]For these calculations, the incident solar radiation pressure is taken as 10^{-7} psf and the reflectivity of the body surface material is assumed to be 0.5.

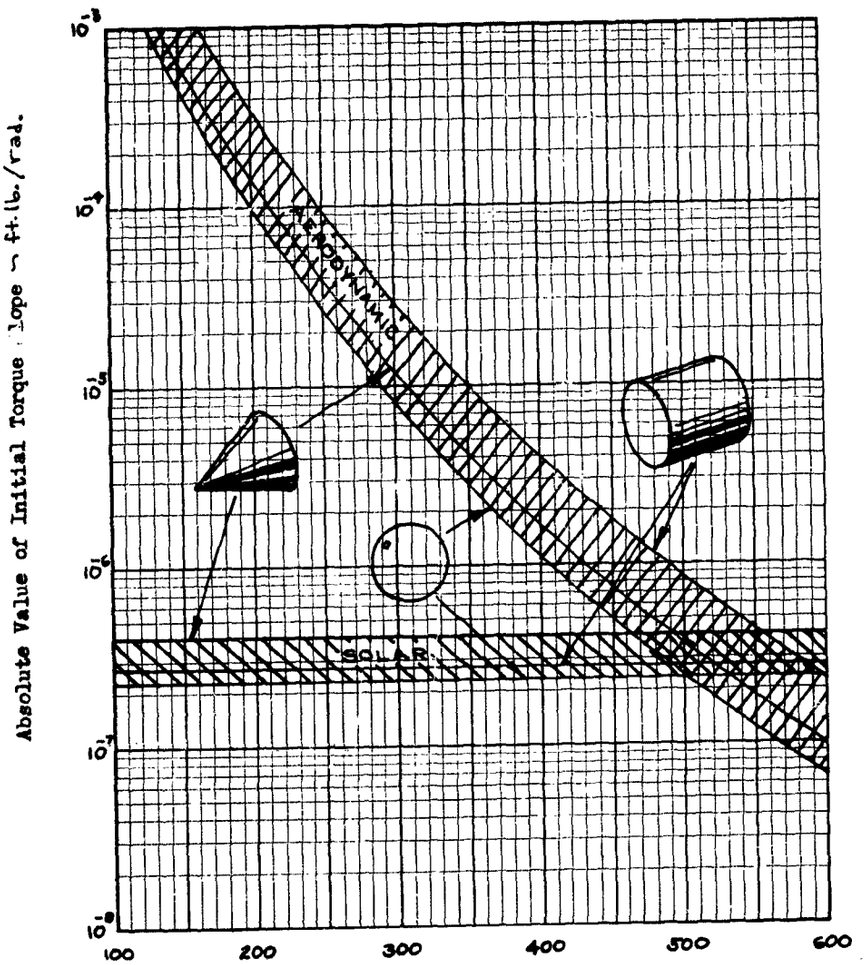

Figure 9. Comparison of Solar and Aerodynamic Initial Torque Slopes

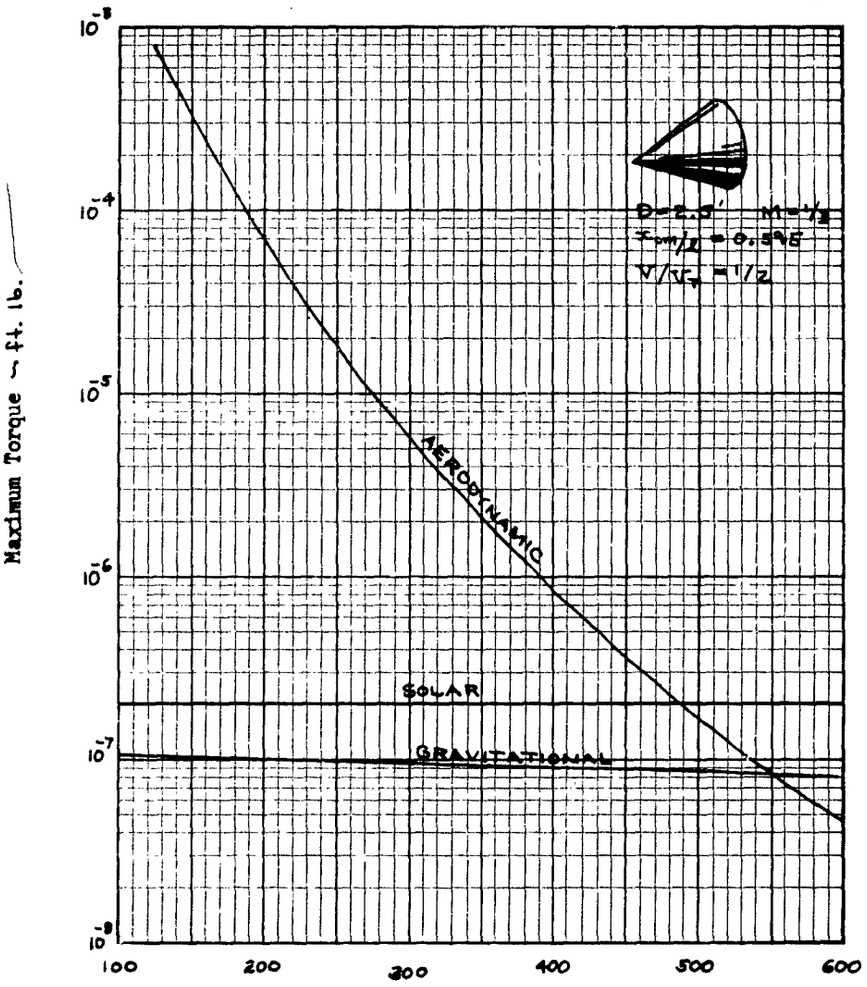

Figure 10. Maximum Values of Various Torques on a Conical Satellite

2.4.2 Additional Torques

Compared with the aerodynamic, gravitational and solar torques, the remaining torques of a "predictable" nature are generally conceded to be very small (Ref. 34). For a rapidly spinning vehicle, the most significant additional torque appears to be due to the interaction of eddy currents induced in the conducting skin of the satellite with the Earth's magnetic field. The problem has not been treated extensively (e.g., Vinti, Refs. 22, 23, and Roberson, Ref. 3) to date and appears to require further study. An estimate of the spin retardation produced by these electromagnetic effects on Sputnik III (Ref. 31) indicates this torque to be roughly comparable to the aerodynamic damping-in-roll and, as will be seen in the next section, this is an exceedingly small quantity. For the non-spinning vehicles below 400 miles altitude which are considered here, electromagnetic effects appear insignificant.

There are numerous other torques of a statistical or random nature (e.g., micrometeorites impacts, solar flares, internal moving parts, etc.) which cannot be readily predicted and which will, therefore, be neglected a priori in this study. These omissions should not significantly affect the subsequent results. It should be noted, however, that the use of internal moving parts may well be among the most efficient means of achieving long duration, precise attitude control. In this connection, the rather thorough work of Roberson (Ref. 24) is noted. The subject of active control system synthesis has not been specifically considered in this study.

3. EQUATIONS OF MOTION FOR SLIGHTLY ECCENTRIC ORBITS

3.1 Small Angle Equations for Slightly Eccentric Orbits

Since only the aerodynamic and gravitational torques are to be considered in the subsequent analysis, Eq. (41) may be substituted into Eqs. (22), for the case of a non-spinning, axisymmetric vehicle with small angular deviations, to obtain,

$$\ddot{\phi} = \rho V_R \frac{S_\pi \bar{c}^2}{4 \bar{I}_x} C_{l_p} \left[\dot{\phi} + \dot{u} \psi \right] - \dot{u} \dot{\psi}$$

$$\ddot{\theta} + 3\frac{\mu}{r^3} M\theta = \rho V_R^2 \frac{S_\pi \bar{c}}{2\bar{I}} \left[C_{m_\alpha} (\theta - \gamma) + \frac{\bar{c}}{2V_R} C_{m_q} (\dot{\theta} - \dot{u}) \right] + \ddot{u} \tag{43}$$

$$\ddot{\psi} - M\dot{u}^2 \psi = \rho V_R^2 \frac{S_\pi \bar{c}}{2\bar{I}} \left[C_{m_\alpha} (\psi - \Lambda) + \frac{\bar{c}}{2V_R} C_{m_q} (\dot{\psi} - \dot{u}\phi) \right] + \dot{u}(M+1)\dot{\phi}$$

which are the equations to be solved. Again it is to be noted that these equations are linear. As noted previously for small angles the equation for the pitching motion is uncoupled from the equations for the rolling and yawing motions and may be solved separately.

Now if the secular effects of aerodynamic drag on the argument of perigee ω are sufficiently small (see Section 1.2) so that $\dot{\omega} \cong 0$, then $\dot{u} \cong \dot{\upsilon}$ and $\ddot{u} \cong \ddot{\upsilon}$. It is, therefore, convenient to transform the independent variable from time to the true anomaly, υ. Since the motion of the vehicle's mass center is assumed to be specified and known, υ is a specified function of time alone. The necessary transformation relations are

$$\frac{d}{dt}(\,) = \dot{v}\frac{d}{dv}(\,)$$

$$\frac{d^2}{dt^2}(\,) = \ddot{v}\frac{d}{dv}(\,) + \dot{v}^2\frac{d^2}{dv^2}(\,). \tag{44}$$

In addition, it is convenient to introduce the abbreviations

$$P \equiv -C_{m_\alpha}\frac{S\pi\bar{C}}{2\bar{I}}\rho\left(\frac{V_R}{\dot{v}}\right)^2$$

$$2Q \equiv -C_{m_q}\frac{S\pi\bar{C}^2}{4\bar{I}}\rho\left(\frac{V_R}{\dot{v}}\right) + \frac{\ddot{v}}{\dot{v}^2} \tag{45}$$

$$2R \equiv -C_{\ell_p}\frac{S\pi\bar{C}^2}{4\bar{I}_x}\rho\left(\frac{V_R}{\dot{v}}\right) + \frac{\ddot{v}}{\dot{v}^2}$$

whereupon, applying Eqs. (44) and (45) to Eqs. (43), there results

$$\phi'' + 2R\phi' = -\psi' - \left[2R - \frac{\ddot{v}}{\dot{v}^2}\right]\psi$$

$$\theta'' + 2Q\theta' + \left[3\frac{\mu}{r^3\dot{v}^2}M + P\right]\theta = 2Q + \gamma P \tag{46}$$

$$\psi'' + 2Q\psi' + \left[P - M\right]\psi = \Lambda P + (M+1)\phi' + \left[2Q - \frac{\ddot{v}}{\dot{v}^2}\right]\phi$$

where primes denote differentiation with respect to v. In order to proceed, it is necessary to express the coefficients of Eqs. (46) as functions of v and other constants of the motion. Owing to the assumption that the center of mass motion is uncoupled from the angular motions about the mass center, the usual Keplerian orbit elements may be employed. The details are tedious but straightforward and may be found in Appendix B. The results are

$$P = \mathcal{P}_p \left(\frac{\rho}{\rho_p}\right)\left(\frac{V_R}{V}\right)^2 \left[\frac{(1+\epsilon)\sqrt{1+2\epsilon\cos\nu+\epsilon^2}}{(1+\epsilon\cos\nu)^2}\right]^2$$

$$2Q = 2\mathcal{Q}_p \left(\frac{\rho}{\rho_p}\right)\left(\frac{V_R}{V}\right)\left[\frac{(1+\epsilon)\sqrt{1+2\epsilon\cos\nu+\epsilon^2}}{(1+\epsilon\cos\nu)^2}\right] - \frac{2\epsilon\sin\nu}{1+\epsilon\cos\nu}$$

$$2R = 2\mathcal{R}_p \left(\frac{\rho}{\rho_p}\right)\left(\frac{V_R}{V}\right)\left[\frac{(1+\epsilon)\sqrt{1+2\epsilon\cos\nu+\epsilon^2}}{(1+\epsilon\cos\nu)^2}\right] - \frac{2\epsilon\sin\nu}{1+\epsilon\cos\nu}$$

$$\frac{\mu}{r^3\dot{\nu}^2} = \frac{1}{1+\epsilon\cos\nu} \qquad (47)$$

$$\gamma = \frac{\epsilon\sin\nu}{1+\epsilon\cos\nu} + \frac{\omega_a}{\dot{\nu}_p}\cos\iota\,\frac{\epsilon(1+\epsilon)^2\sin\nu}{(1+\epsilon\cos\nu)^3}$$

$$\Lambda = \frac{\omega_a}{\dot{\nu}_p}\sin\iota\left[\frac{1+\epsilon}{1+\epsilon\cos\nu}\right]^2\cos(\nu+\omega)$$

$$\ddot{\nu}/\dot{\nu}^2 = -\frac{2\epsilon\sin\nu}{1+\epsilon\cos\nu}$$

where the subscript p denotes that the quantity is evaluated at perigee, ϵ is the orbital eccentricity and $\mathcal{P}_p$, $\mathcal{Q}_p$ and $\mathcal{R}_p$ are constants defined by,

$$\mathcal{P}_p \equiv -C_{m_\alpha}\frac{S\pi\bar{c}}{2\bar{I}}\rho_p r_p^2$$

$$2\mathcal{Q}_p \equiv -C_{m_q}\frac{S\pi\bar{c}^2}{4\bar{I}}\rho_p r_p \qquad (48)$$

$$2\mathcal{R}_p \equiv -C_{l_p}\frac{S\pi\bar{c}^2}{4\bar{I}_x}\rho_p r_p \quad .$$

The ratio of relative to inertial velocity V_R/V may be evaluated from Eq. (42) and Eqs. (B-8) and (B-9) of Appendix B as

$$\frac{V_R}{V} = 1 - \frac{\omega_a}{\dot{v}_p}\cos\iota\left\{\frac{1+\epsilon}{1+\epsilon\cos v}\right\}^2 . \tag{49}$$

The above expressions include only the assumption that $\omega_a/\dot{v}_p$ is small compared to unity and that γ, γ^* and Λ are small angles. Unfortunately, Eqs. (47) are much too complicated for analytical work, and must be further simplified. The appropriate simplifying assumption is that the orbital eccentricity, ϵ, is sufficiently small (say $\epsilon \leq 0.1$) so that $\epsilon^2 \ll 1$. This assumption is consistent with the small angle restriction made earlier. Neglecting squares of ϵ and products of the form $\epsilon\,\omega_a/\dot{v}_p$ the above coefficients simplify to the following first order form:

$$\begin{aligned}
P &\cong \mathcal{P}_p\left(\frac{\rho}{\rho_p}\right)\left(\frac{V_R}{V}\right)^2\left[1+2\epsilon(1-\cos v)\right] \\
2Q &\cong 2\mathcal{Q}_p\left(\frac{\rho}{\rho_p}\right)\left(\frac{V_R}{V}\right)\left[1+\epsilon(1-\cos v)\right] - 2\epsilon\sin v \\
2R &\cong 2\mathcal{R}_p\left(\frac{\rho}{\rho_p}\right)\left(\frac{V_R}{V}\right)\left[1+\epsilon(1-\cos v)\right] - 2\epsilon\sin v \\
\frac{\mu}{r^3\dot{v}^2} &\cong \left[1-\epsilon\cos v\right] \\
\gamma &\cong -\frac{1}{2}\frac{\ddot{v}}{\dot{v}^2} \cong \epsilon\sin v \\
\Lambda &\cong d\cos(v+\omega)
\end{aligned} \tag{50}$$

where

$$\frac{V_R}{V} \cong 1 - d\cot\iota \tag{51}$$

and

$$d \equiv \frac{\omega a}{\dot{v}_p} \sin \iota \quad .$$

Note that to this order of approximation, V_R / V is constant and equal to its value at perigee. The variation of d as a function of perigee altitude and orbit inclination is shown in Fig. 11.

In subsequent discussions relating to the numeric integration of the "exact" equation of the pitching motion, it is the second of Eqs. (46) with coefficients given by Eqs. (50) and (51) which is solved. It has been shown in Section 1 that this equation exactly describes the small angle pitching motion of a non-spinning, axisymmetric vehicle when the rolling and yawing motions are suppressed. Moreover, the restriction to small orbital eccentricities poses no serious limitation on the results. This equation will, therefore, be regarded as "exact" in relationship to the approximate results to be obtained in the following sections.

3.2 Approximate Atmospheric Density Variation

In order to complete the evaluation of these coefficients, it is necessary to evaluate ρ / ρ_p . Since the Earth is an oblate spheroid, the Earth's atmosphere is also oblate and hence a constant density surface in the atmosphere is not a sphere. Although this latitude variation of density is partially accounted for by representing $\rho(h) = \rho(r - r_E)$ where r_E varies with latitude, two other equally significant variations, imposed by the latitude variation of surface gravity and temperature, are omitted. In order to retain the maximum simplicity, it will be assumed here that the Earth is spherical, and hence $\rho = \rho(h)$ where $h = r - a_E$.

It is now well-known that the atmospheric density variation above about 400,000 foot altitude is best approximated by a power function of the altitude (Ref. 25). However, under the assumption of small orbital eccentricity, it is also possible to approximate the density variation from perigee to apogee by an exponential relation of the form

$$\frac{\rho(h)}{\rho_p} = C_A \, e^{-\chi_A (h - h_p)} \tag{52}$$

where C_A and χ_A are constants fixed by the perigee altitude. The critical condition for Eq. (52) to be a satisfactory representation is that its error be no more than the uncertainty in the density itself

over the altitude range of interest. Based upon Minzner's 1959 model atmosphere (Ref. 26) the uncertainty due to seasonal and daily variations, as well as uncertainties due to position on the Earth is at least a factor of 2 at these altitudes. Above about 100 statute miles altitude and for orbital eccentricities less than about .05, the constants of Eq. (52) may be found such that the error is within these limits and hence the use of this representation is justified. The appropriate values of $\mathcal{K}_A$ are shown in Fig. 12.

From the equation of the elliptical orbit (Eq.(B-2) of Appendix B or Ref. 18)

$$r = \frac{r_p(1+\epsilon)}{1+\epsilon\cos\nu}$$

hence

$$h - h_p = r - r_p = \epsilon r_p \left\{ \frac{1-\cos\nu}{1+\epsilon\cos\nu} \right\}$$

which, to terms of order ϵ is

$$h - h_p \cong \epsilon r_p (1-\cos\nu) \quad . \tag{53}$$

Substituting Eq. (53) into Eq. (52), and defining $\lambda \equiv \mathcal{K}_A r_p \epsilon$,

$$\frac{\rho(h)}{\rho_p} = C_A e^{-\lambda} e^{\lambda\cos\nu} .$$

Now note that when $\nu = \pm\pi/2$, $\cos\nu = 0$ and the vehicle is at the semi-latus rectum, p, of the elliptical orbit. The altitude to this point on the orbit will be denoted here by $h_\ell \equiv p - a_E$. Then from the above equation,

$$\frac{\rho(h_\ell)}{\rho(h_p)} = C_A e^{-\lambda}$$

and with $\rho(h_\ell) \equiv \rho_\ell$,

$$\frac{\rho(h)}{\rho_p} = \frac{\rho_\ell}{\rho_p} e^{\lambda\cos\nu} . \tag{54}$$

The behavior of the dimensionless atmosphere parameter λ as a function of perigee altitude and orbital eccentricity is shown in Fig. 13.

Substituting Eqs. (50) and (54) into Eqs. (46), there results the following equations for the vehicle's rolling, pitching and yawing motion:

$$\begin{aligned}
&\phi'' + 2R\phi' = -\psi' - [2R + 2\epsilon \sin\nu]\psi \\
&\theta'' + 2Q\theta' + [3M(1-\epsilon\cos\nu) + P]\theta = 2Q + \epsilon P \sin\nu \\
&\psi'' + 2Q\psi' + [P - M]\psi = P_d \cos(\nu+\omega) + (M+1)\phi' \\
&\qquad\qquad + [2Q + 2\epsilon\sin\nu]\phi
\end{aligned} \tag{55}$$

where

$$\begin{aligned}
P &\cong \mathcal{P}_p^* e^{\lambda\cos\nu}[1 + 2\epsilon(1-\cos\nu)] \\
2Q &\cong 2\mathcal{Q}_p^* e^{\lambda\cos\nu}[1+\epsilon(1-\cos\nu)] - 2\epsilon\sin\nu \\
2R &\cong 2\mathcal{R}_p^* e^{\lambda\cos\nu}[1+\epsilon(1-\cos\nu)] - 2\epsilon\sin\nu
\end{aligned} \tag{56}$$

and, making use of the fact that V_R/V is a constant to a first order in ϵ as given by Eq. (51), the constants $\mathcal{P}_p^*$, $\mathcal{Q}_p^*$ and $\mathcal{R}_p^*$ are defined by,

$$\begin{aligned}
\mathcal{P}_p^* &\equiv \mathcal{P}_p \left(\frac{V_R}{V}\right)^2 \left(\frac{\rho_l}{\rho_p}\right) \\
\mathcal{Q}_p^* &\equiv \mathcal{Q}_p \left(\frac{V_R}{V}\right) \left(\frac{\rho_l}{\rho_p}\right) \\
\mathcal{R}_p^* &\equiv \mathcal{R}_p \left(\frac{V_R}{V}\right) \left(\frac{\rho_l}{\rho_p}\right) .
\end{aligned} \tag{57}$$

Eqs. (55) represent the fundamental small angle equations of motion for an axisymmetric satellite vehicle moving in an elliptical orbit of small eccentricity and acted upon by aerodynamic and gravitational torques. The analysis has shown that for a vehicle of this configuration, the motion is characterized by six constants: the aerodynamic parameters $\mathcal{C}_p^*$, $\mathcal{Q}_p^*$ and $\mathcal{R}_p^*$, the inertia parameter M, the orbital eccentricity ϵ and the atmosphere parameter λ. In the following work, the nature of the vehicle's angular motion will be studied in terms of these significant parameters by seeking analytical solutions to Eqs. (55). In the case of the general elliptical orbit, only the equation for the pitching motion will be solved, but before entering into this solution, it is instructive to examine the complete motion under certain simplifying assumptions.

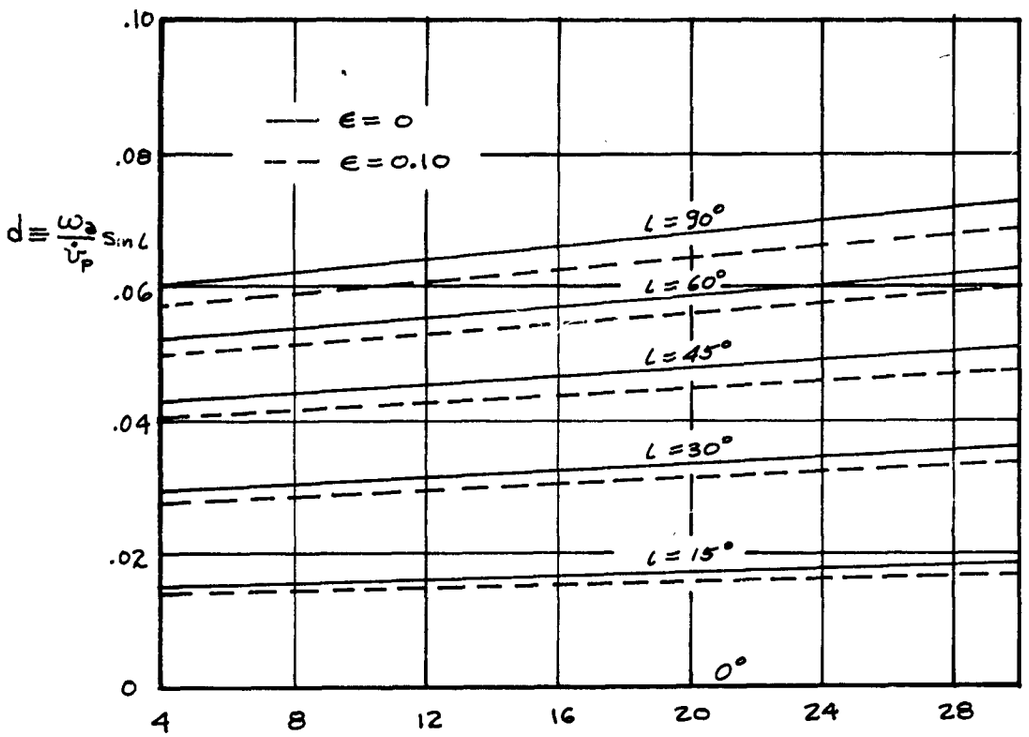

Figure 11. Atmospheric Rotation Parameter, d , as a Function of Perigee Altitude and Orbit Inclination .

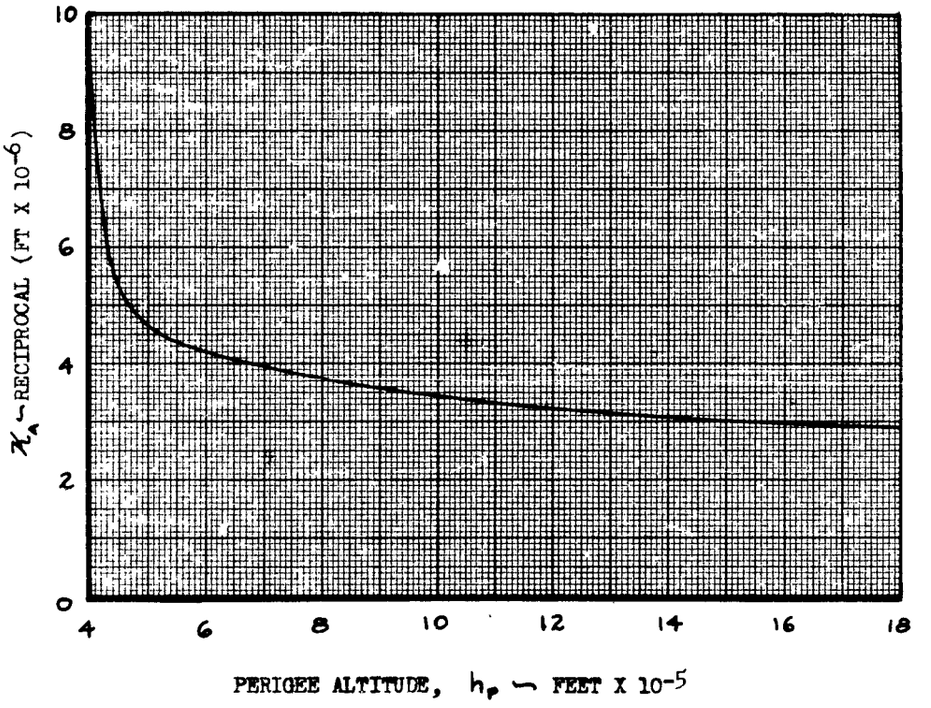

Figure 12. Variation of Exponential Factor, $\mathcal{K}_A$, with Perigee Altitude

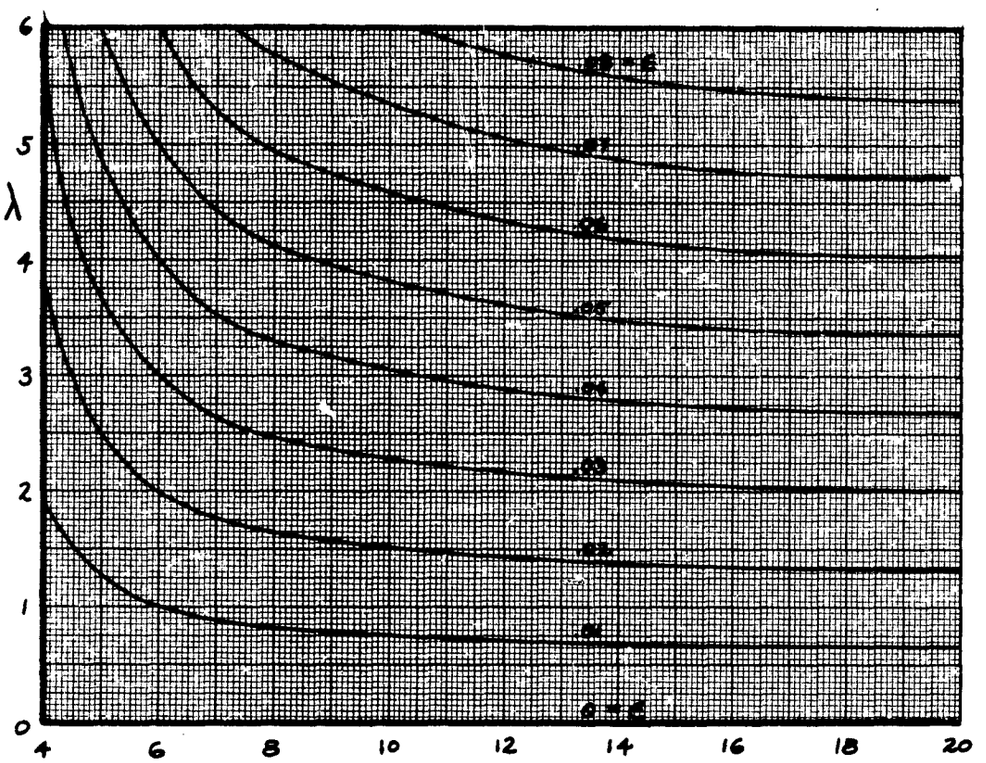

Figure 13. Atmosphere Parameter, λ, as a Function of Perigee Altitude and Orbital Eccentricity

3.3 Order of Magnitude of Aerodynamic Terms

Since Eqs. (55) will be employed for the subsequent analytical work, it is desirable to effect the maximum simplification possible. This simplification can be performed by identifying those terms remaining in Eqs. (55) which are as small or smaller than the second-order squares and products of small angles previously neglected in the analysis.

The order of magnitude of the three aerodynamic parameters P, Q and R may be estimated from Eqs. (56) as

$$\begin{aligned} P &= O(\mathcal{P}_p) \\ Q &= O(\mathcal{Q}_p - \epsilon) \\ R &= O(\mathcal{R}_p - \epsilon) \end{aligned} \tag{58}$$

where $O(\ )$ is to be read "the order of magnitude of the enclosed quantity" and where V_R/V has been taken as unity for small eccentricity orbits[1].

It is convenient to group the vehicle parameters in Eqs. (48) to form new quantities which may be more readily determined. Define:

$$\begin{aligned} \mathcal{P}_p &= \Gamma \frac{\rho_p r_p^2}{2} \quad , \quad \Gamma \equiv -C_{m_\alpha} \frac{S_\pi \bar{c}}{\bar{I}} \\ \mathcal{Q}_p &= \Gamma_q \frac{\rho_p r_p}{8} \quad , \quad \Gamma_q \equiv -C_{m_q} \frac{S_\pi \bar{c}^2}{\bar{I}} \\ \mathcal{R}_p &= \Gamma_p \frac{\rho_p r_p}{8} \quad , \quad \Gamma_p \equiv -C_{l_p} \frac{S_\pi \bar{c}^2}{\bar{I}} \quad . \end{aligned} \tag{59}$$

Davison (Ref. 1) has calculated the attainable values of the parameters Γ and Γ_q for an extensive number of satellite shapes using the approximate free molecular aerodynamic theory presented in Ref. (21). The results of these calculations may be summarized as shown in Figs. 14 through 17. It may be seen that values of Γ and Γ_q in excess of

---

[1] Note from Eqs. (54) that $(\rho_l/\rho_p)e^{\lambda \cos\nu} \leq 1$. This quantity has been set to unity here to insure a conservative estimate throughout.

10^2 are generally possible only for very small vehicles. Although values of Γ_p have not been calculated specifically, it is reasonable to assume that this parameter will not exceed the order of Γ_g. For perigee altitudes near or above 100 statute miles, ρ_p is at most 2×10^{-12} slug/ft^3 while r_p is of order 2×10^7 feet. Employing these maximum estimates of the various parameters,

$$P \cong O(\Gamma \times 10^3)$$

$$Q \cong O(\Gamma_g \times 10^{-6} - \epsilon) \qquad (60)$$

$$R \cong O(\Gamma_p \times 10^{-6} - \epsilon).$$

Clearly P is a potentially large quantity and must be retained. Q and R, however, are seen to be of order ϵ, since the aerodynamic terms in these quantities are at most of order ϵ for all reasonable satellite shapes. Inasmuch as this order of magnitude estimate has been biased to yield the largest values to be expected, it appears conservative to neglect as second order the parametric excitation terms $(2R + 2\epsilon \sin\nu)\psi$ and $(2Q + 2\epsilon \sin\nu)\phi$ in Eqs. (55). The resulting equations then become

$$\phi'' + 2R\phi' = -\psi'$$

$$\theta'' + 2Q\theta' + [3M(1 - \epsilon\cos\nu) + P]\theta = 2Q + \epsilon P \sin\nu \qquad (61)$$

$$\psi'' + 2Q\psi' + [P - M]\psi = P_d \cos(\nu + \omega) + (M+1)\phi'.$$

It should be remarked that the assumption of negligible aerodynamic damping has been made a priori in previous studies (e.g., DeBra, Ref. 12 and Wall, Ref. 11), no doubt because adequate theoretical means to predict the aerodynamic damping characteristics of arbitrary bodies were not available. It is seen in Figs. 15 and 16, however, that although this damping is always small, it need not be negligible and, consequently, its first order effects should be retained for completeness in the equations of motion.

Now introduce the exponential transformations

$$\begin{aligned} \phi &= \bar{\phi}\, e^{-\int R(\nu)\,d\nu} \\ \theta &= \bar{\theta}\, e^{-\int Q(\nu)\,d\nu} \\ \psi &= \bar{\psi}\, e^{-\int Q(\nu)\,d\nu} \end{aligned} \qquad (62)$$

The typical derivatives of these functions are illustrated by

$$\theta' = (\bar{\theta}' - Q\bar{\theta})\, e^{-\int Q(\nu)\,d\nu}$$

and

$$\theta'' = (\bar{\theta}'' - 2Q\bar{\theta}' + (Q^2 - Q')\bar{\theta})\, e^{-\int Q(\nu)\,d\nu}.$$

Inserting Eqs. (62) relations into Eqs. (61) and rearranging,

$$\bar{\phi}'' - [R^2 + R']\bar{\phi} = -[\bar{\psi}' - Q\bar{\psi}]\, e^{\int [R(\nu) - Q(\nu)]\,d\nu}$$

$$\bar{\theta}'' + [3M(1 - \epsilon\cos\nu) + P - Q^2 - Q']\bar{\theta} = [2Q + \epsilon P \sin\nu]\, e^{\int Q(\nu)\,d\nu} \qquad (63)$$

$$\bar{\psi}'' + [P - M - Q^2 - Q']\bar{\psi} = P d \cos(\nu + \omega)\, e^{\int Q(\nu)\,d\nu} + (M+1)[\bar{\phi}' - R\bar{\phi}]\, e^{\int [Q(\nu) - R(\nu)]\,d\nu}.$$

These transformed equations are particularly convenient for further order of magnitude analysis. A detailed examination of the coefficient of $\bar{\theta}$ in the pitching equation will serve to illustrate the procedure.

To terms of order ϵ , Eqs. (56) yield

$$Q' = -2_p^* \lambda e^{\lambda \cos v}\left[1 - \frac{\epsilon}{\lambda} + \epsilon(1-\cos v)\right]\sin v - \epsilon \cos v$$

and

$$Q^2 = 2_p^{*2} e^{2\lambda \cos v}\left[1 + 2\epsilon(1-\cos v)\right] + 2\, 2_p^* e^{\lambda \cos v}\, \epsilon \sin v + O(\epsilon^2)$$

so that

$$Q^2 + Q' = 2_p^{*2} e^{2\lambda \cos v}\left[1 + 2\epsilon(1-\cos v)\right] - \epsilon \cos v$$

$$- 2_p^* \lambda e^{\lambda \cos v}\left[1 - 3\frac{\epsilon}{\lambda} + \epsilon(1-\cos v)\right]\sin v .$$

In order for these terms to be retained, it is necessary that they be of comparable magnitude to P . For order of magnitude purposes, as before,

$$Q^2 + Q' = O\left(2_p^2 - \epsilon - 2_p \lambda\right)$$

while from the first of Eqs. (58),

$$P = O(\mathcal{P}_p) .$$

Now write

$$P - Q^2 - Q' = P\left\{1 - \frac{Q^2 + Q'}{P}\right\}$$

or,

$$P - Q^2 - Q' = O\left\{P\left[1 - \frac{2_p^2}{\mathcal{P}_p} + \lambda \frac{2_p}{\mathcal{P}_p} + \frac{\epsilon}{\mathcal{P}_p}\right]\right\} .$$

Introducing Eqs. (59), the following order of magnitude estimates result:

$$\frac{a_p^2}{\rho_p} = O\left(\frac{\rho_p}{16}\frac{\Gamma_g^2}{\Gamma}\right)$$

$$\lambda\frac{a_p}{\rho_p} = O\left(\frac{\lambda}{r_p}\frac{\Gamma_g}{\Gamma}\right)$$

$$\frac{\epsilon}{\rho_p} = O\left(\frac{\epsilon}{\Gamma\rho_p r_p^2}\right) .$$

Using the maximum values discussed previously, it is evident that the first two terms above are negligible in comparison to unity for all practical vehicles and orbits. Because of the appearance of Γ and ρ_p in the denominator of the last relation, however, this term need not remain small compared to unity and hence must be retained. Thus, the second of Eqs. (63) may be reduced to

$$\bar{\theta}'' + \left[3M + (1-3M)\epsilon\cos\nu + P\right]\bar{\theta} = \left[2Q + \epsilon P\sin\nu\right]e^{\int Q(\nu)d\nu} \quad (64)$$

Applying the above procedure to the first and third of Eqs. (63) and neglecting products of the form $Q\bar{\psi}$ and $R\bar{\phi}$ in comparison to $\bar{\psi}'$ and $\bar{\phi}'$ in the parametric excitation, there results

$$\bar{\phi}'' + \epsilon\cos\nu\,\bar{\phi} = -\bar{\psi}'e^{\int[R(\nu)-Q(\nu)]d\nu}$$

$$\bar{\psi}'' + \left[P + \epsilon\cos\nu - M\right]\bar{\psi} = Pd\cos(\nu+\omega)\,e^{\int Q(\nu)d\nu} + (M+1)\,\bar{\phi}'e^{\int[Q(\nu)-R(\nu)]d\nu} \quad (65)$$

It is now necessary to consider the exponential terms remaining in the right of Eqs. (64) and (65). A detailed treatment of the effect of $\exp(-\int Q(v)dv)$ in damping the satellite's pitching motion is presented in Appendix C, where it is shown that the time to damp to one-half the initial pitch amplitude is, at most, comparable to the satellite's orbital lifetime. Thus, the secular change in $\exp(-\int Q(v)dv)$ over the time interval for which $\mathcal{P}_p$, $\mathcal{Q}_p$, $\mathcal{R}_p$, ϵ etc., may be regarded as constant is insignificant and hence all exponential terms on the right of Eqs. (64) and (65) may be taken as unity without serious error. Clearly, if $\int Q(v)dv$ changes only slightly, then

$$\int [Q(v) - R(v)]dv = [\mathcal{Q}_p - \mathcal{R}_p]\int e^{\lambda \cos v}[1+\epsilon(1-\cos v)]dv$$

changes even less, since it is proportional to the difference of two small quantities of approximately equal orders of magnitude. The reduced equations of motion then become,

$$\bar{\phi}'' + \epsilon \cos v\, \bar{\phi} = -\bar{\psi}'$$

$$\bar{\theta}'' + [3M + (1-3M)\epsilon\cos v + P]\bar{\theta} = 2Q + \epsilon P \sin v \qquad (66)$$

$$\bar{\psi}'' + [P + \epsilon\cos v - M]\bar{\psi} = Pd\cos(v+\omega) + (M+1)\bar{\phi}' \ .$$

The entire effect of aerodynamic damping is now confined to the term $2Q$ appearing on the right of the pitch equation, and to the transformation equations, Eqs. (62), relating θ, ψ and ϕ to $\bar{\theta}$, $\bar{\psi}$ and $\bar{\phi}$. The apparent inconsistency of having the forced motion decay according to Eqs. (62) is removed when it is recalled that the exponentials on the right of Eqs. (64) and (65) differ from unity by terms proportional to ϵ, and these in turn give rise to terms of order ϵ^2 which are negligible as excitation. If the foregoing arguments are applied to Eqs. (62), there results

$$\frac{\theta}{\bar{\theta}} = \frac{\psi}{\bar{\psi}} \cong \frac{\phi}{\bar{\phi}} \cong e^{\epsilon\int \sin v\, dv}$$

which, for injection at perigee, becomes

$$\frac{\theta}{\bar{\theta}} = \frac{\psi}{\bar{\psi}} \cong \frac{\phi}{\bar{\phi}} \cong e^{\epsilon(1-\cos v)} \cong 1 - \epsilon(1-\cos v) + O(\epsilon^2) \quad .$$

Thus, the only significant contribution of the aerodynamic damping is to slightly alter the equilibrium pitch angle such that the damping moment (due to the inertial pitch rate of the satellite) is countered by a small static pitching moment. Subsequent numerical calculations based upon the complete equation of motion (see Section 3.1) amply confirm the negligibility of the aerodynamic damping insofar as its effect on decay of the angular oscillations is concerned, and this may be taken as a posteriori justification of the assumptions and approximation introduced above.

The reduced equations of motion, Eqs. (66), may be further simplified without additional error if the term $\bar{\phi}'$ is removed from the right of the yaw equation as follows: Integrate the first of Eqs. (66) once with respect to v, neglecting the term $\epsilon \cos v \, \bar{\phi}$. The result is

$$\bar{\phi}' \cong -\bar{\psi} + k$$

where k is a constant of integration determined by the initial conditions. Substitution of this result into the yaw equation leads to the new differential system

$$\bar{\phi}'' + \epsilon \cos v \, \bar{\phi} = -\bar{\psi}'$$

$$\bar{\theta}'' + [3M + (1-3M)\epsilon \cos v + P]\bar{\theta} = 2Q + \epsilon P \sin v \qquad (67)$$

$$\bar{\psi}'' + [1 + \epsilon \cos v + P]\bar{\psi} = Pd \cos(v+\omega) + K(M+1) \quad .$$

These equations are now uncoupled sufficiently to permit solution, since $\bar{\theta}$ and $\bar{\psi}$ may be determined from the last two equations and $\bar{\psi}'$ then substituted into the first in order to solve for $\bar{\phi}$.

Note that when the aerodynamic influences are absent, the second of Eqs. (67) becomes

$$\bar{\theta}'' + \left[3M + (1-3M)\epsilon \cos\nu\right]\bar{\theta} = -2\epsilon \sin\nu$$

which is a non-homogeneous form of Mathieu's differential equation (Refs. 32-35). That an equation of this form governs the small angle pitching motion of a rigid satellite in an elliptical orbit under the influence of the gravitational torques alone has been demonstrated by Baker (Ref. 8). This result is also implicit in the large angle equations for the pitching motion derived by Beletskiy (Ref. 27) and by Frick and Garber (Ref. 28). Inasmuch as this equation depends only on the two parameters ϵ and M, a unique solution $\bar{\theta}(M, \epsilon, \nu)$ may be obtained. The independence of altitude of this equation is due to the transformation to ν as the independent variable in place of time.

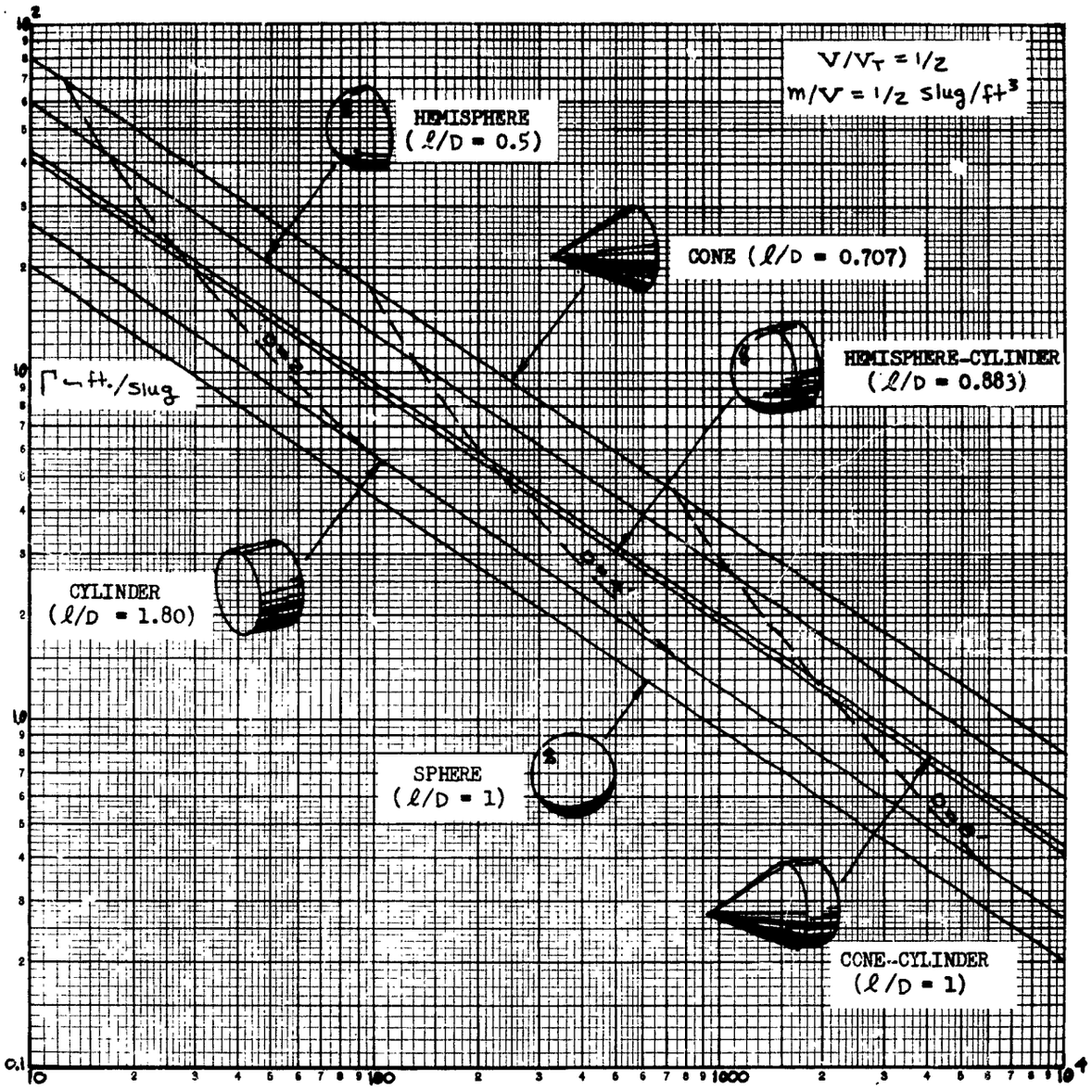

Figure 14. Aerodynamic Moment Parameter Γ for a Number of Optimum Body Shapes, $V/V_T = 1/2$.

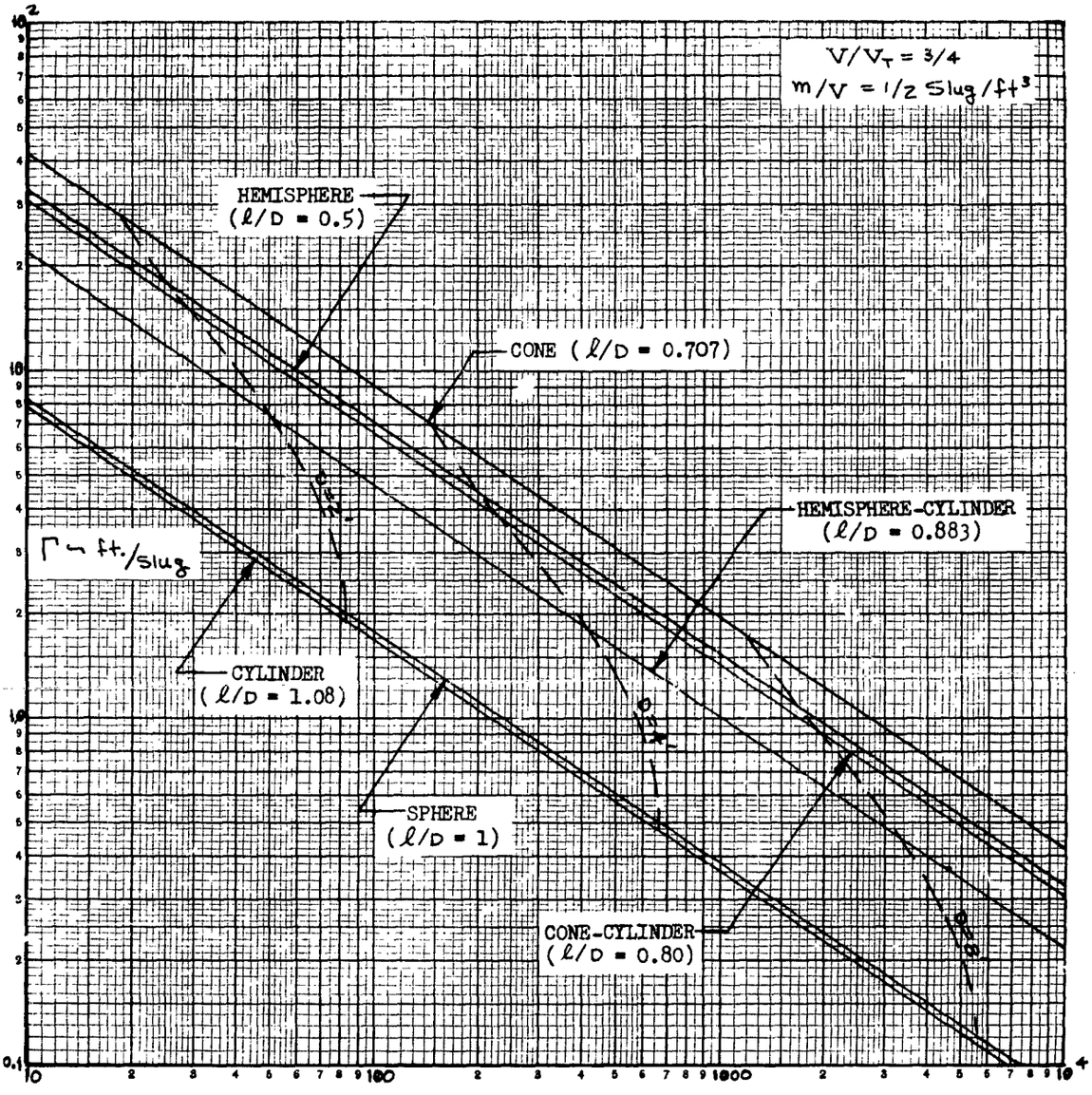

Figure 15. Aerodynamic Moment Parameter Γ for a Number of Optimum Body Shapes, $V/V_T = 3/4$

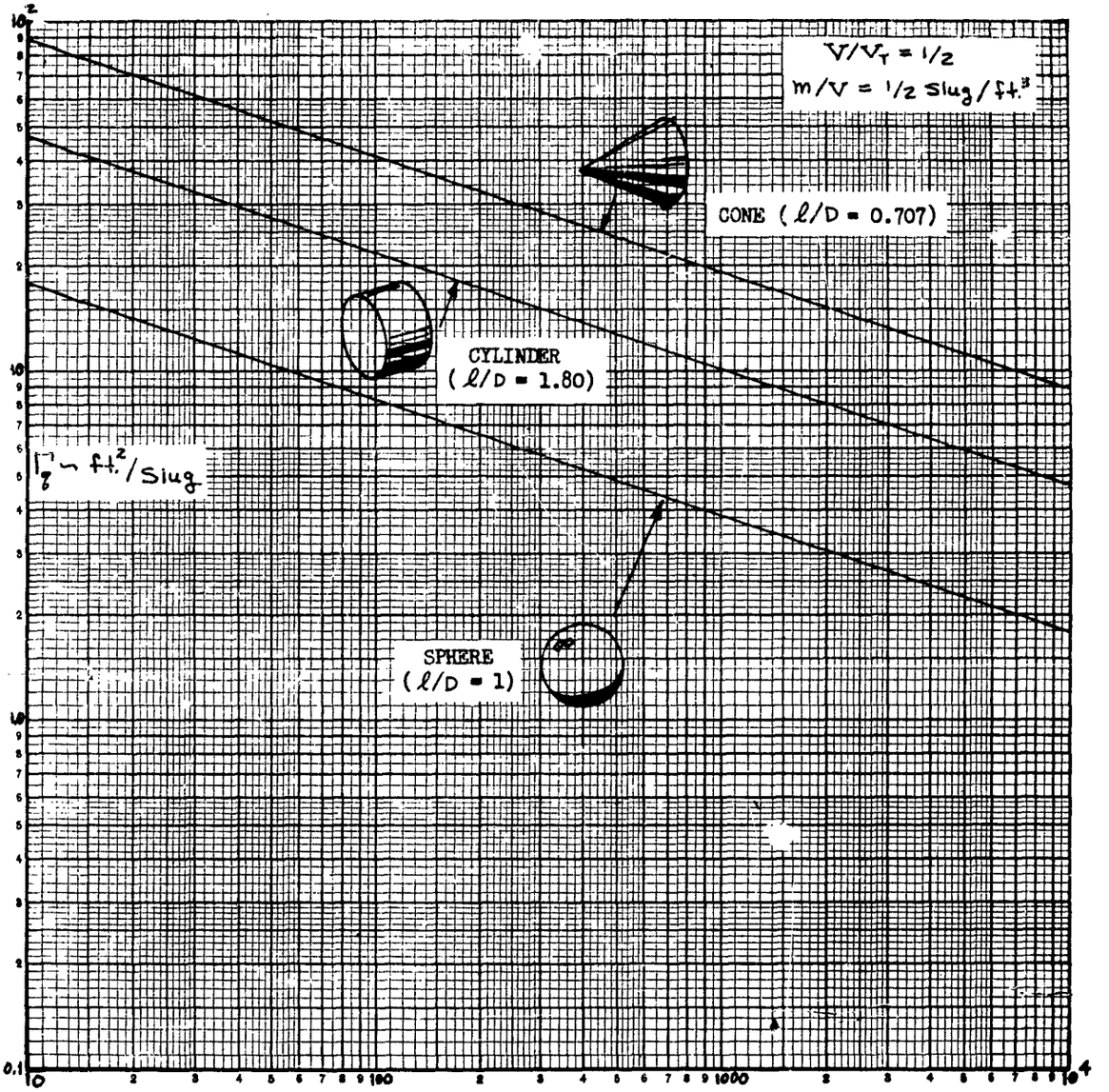

Figure 16. Aerodynamic Damping Parameter Γ_ℓ for a Number of Optimum Body Shapes, $V/V_T = 1/2$

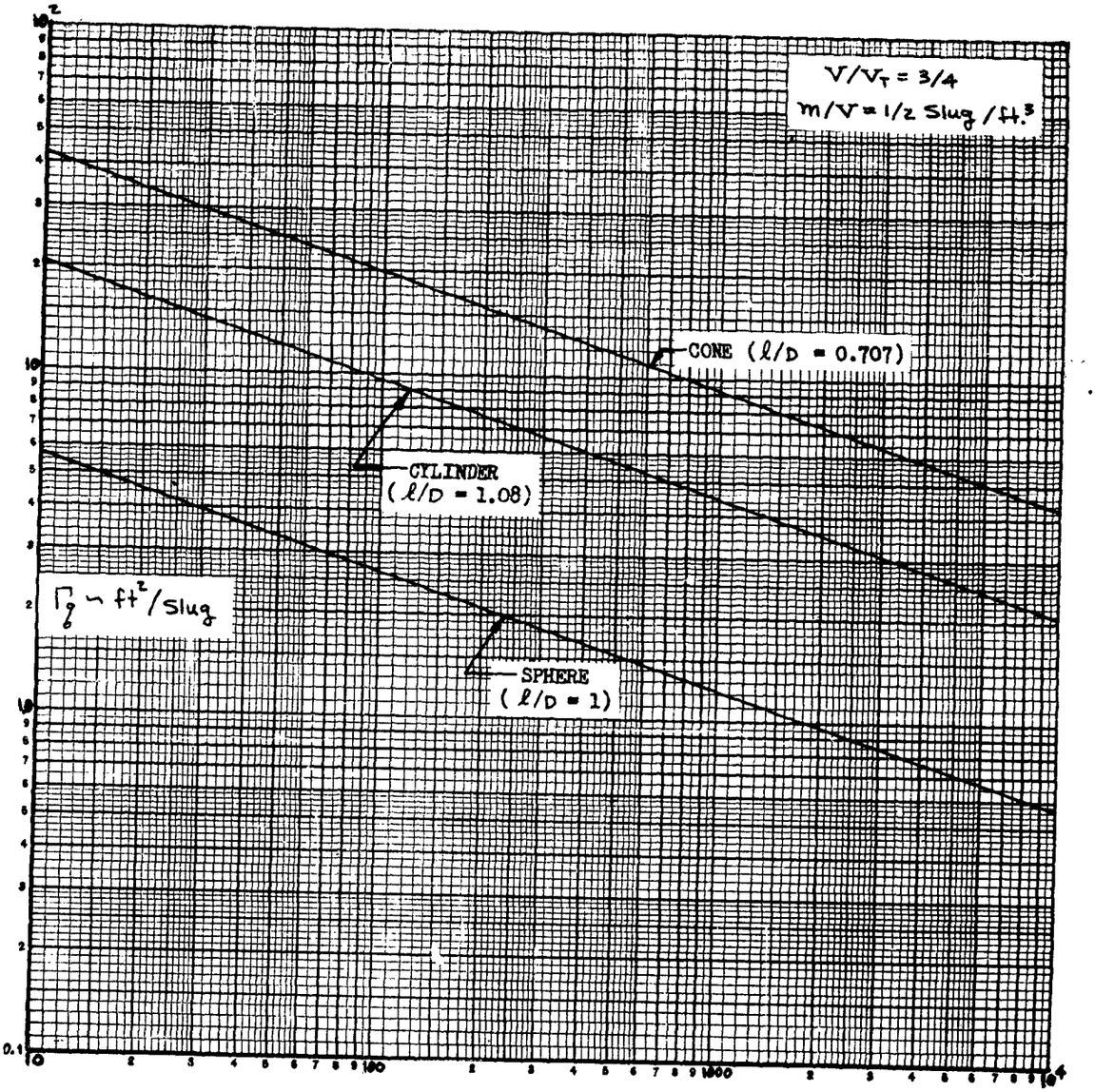

Figure 17. Aerodynamic Damping Parameter Γ_θ for a Number of Optimum Body Shapes, $V/V_T = 3/4$

3.4 Fourier Series Expansion of Periodic Coefficients

It may be noted that all of the coefficients of Eqs. (67) are periodic functions of the independent variable ν with period 2π, and hence may be expanded in Fourier series. Moreover, the coefficients of the homogeneous equations are even functions, involving $\cos\nu$ only, and thus the Fourier cosine series suffices for the expansion of these terms. In order to outline the procedure, the pitching equation is considered in detail.

Let

$$\bar{\theta}'' + \mathcal{L}(\nu)\,\bar{\theta} = \mathcal{M}(\nu) \tag{68}$$

where

$$\mathcal{L}(\nu) = 3M(1-\epsilon\cos\nu) + \epsilon\cos\nu + \rho_p^* e^{\lambda\cos\nu}\left[1 + 2\epsilon(1-\cos\nu)\right]$$

and

$$\mathcal{M}(\nu) = \left\{2Q + \epsilon P \sin\nu\right\} .$$

In order to expand the function $\mathcal{L}(\nu)$, assume

$$\mathcal{L}(\nu) = \sum_{n=0}^{\infty} A_n \cos n\nu$$

where

$$A_0 = \frac{1}{\pi}\int_0^{\pi} \mathcal{L}(t)\,dt$$

and

$$A_n = \frac{2}{\pi}\int_0^{\pi} \mathcal{L}(t)\cos nt\,dt \quad , \quad n = 1, 2, 3, \cdots \quad .$$

Evaluating the coefficients,

$$A_o = 3M + (1+2\epsilon)\frac{\mathcal{P}_p^*}{\pi}\int_o^{\pi} e^{\lambda\cos t}\,dt - 2\epsilon\frac{\mathcal{P}_p^*}{\pi}\int_o^{\pi} e^{\lambda\cos t}\cos t\,dt$$

and

$$A_n = -\frac{2\epsilon}{\pi}(3M-1)\int_o^{\pi}\cos t\cos nt\,dt + 2(1+2\epsilon)\frac{\mathcal{P}_p^*}{\pi}\int_o^{\pi} e^{\lambda\cos t}\cos nt\,dt - 4\epsilon\frac{\mathcal{P}_p^*}{\pi}\int_o^{\pi} e^{\lambda\cos t}\cos t\cos nt\,dt \quad , n=1,2,3,\cdots .$$

The integrals may be readily evaluated with the help of the integral form for the modified Bessel functions of the first kind and order n (Ref. 33, Page 151)

$$I_n(\lambda) = \frac{1}{\pi}\int_o^{\pi} e^{\lambda\cos t}\cos nt\,dt \quad , n=0,1,2,\cdots . \tag{69}$$

The results are:[1]

$$A_o = 3M + \mathcal{P}_p^*\left\{ I_o(\lambda) + 2\epsilon\left[I_o(\lambda) - I_1(\lambda)\right]\right\}$$

$$A_1 = (1-3M)\epsilon + 2\mathcal{P}_p^*\left\{ I_1(\lambda) - \epsilon\left[I_o(\lambda) - 2I_1(\lambda) + I_2(\lambda)\right]\right\} \tag{70}$$

$$A_n = 2\mathcal{P}_p^*\left\{ I_n(\lambda) - \epsilon\left[I_{n-1}(\lambda) - 2I_n(\lambda) + I_{n+1}(\lambda)\right]\right\}, \quad n=2,3,4,\cdots .$$

---

[1] The first few modified Bessel functions are shown plotted in Fig. 18, for values of the argument up to 6.0.

Eqs. (70) completely define the $\{A_n\}$ in terms of other, known quantities. When $\epsilon = 0$, $\lambda = 0$ and a circular orbit results. The coefficients $\{A_n\}$ in this case all vanish with the exception of A_0 which has the value

$$A_0 = 3M + \mathcal{P}_p^* \quad .$$

When λ is large, the $\{A_n\}$ may be evaluated with the help of the asymptotic expansion of the modified Bessel functions. From Wittaker and Watson (Ref. 34, Page 373),

$$I_n(\lambda) \cong \frac{e^\lambda}{\sqrt{2\pi\lambda}} \left\{ 1 - \frac{4n^2-1}{8\lambda} + \frac{(4n^2-9)(4n^2-1)}{128\lambda^2} + \cdots \right\} , \quad \lambda \gg 1$$

Inserting this result in Eqs. (70) and neglecting terms of order ϵ/λ, there results

$$\begin{aligned} A_0 &\cong 3M + \mathcal{P}_p^* I_0(\lambda) \\ A_1 &\cong (1-3M)\epsilon + 2\mathcal{P}_p^* I_1(\lambda) \\ A_n &\cong 2\mathcal{P}_p^* I_n(\lambda) \quad , \quad n = 2, 3, 4, \cdots \quad . \end{aligned} \tag{71}$$

One notes that as $\epsilon \to 0$, $\lambda \to 0$ also so that Eqs. (71) have the correct limiting values for circular orbits as well as for large λ. Thus, Eqs. (71) should represent reasonable approximate values for the $\{A_n\}$ over the entire range of λ considered. A numerical comparison of the exact and approximate coefficients shows the agreement to be excellent over the entire range of interest, and hence Eqs. (71) will be employed in the subsequent work.

The non-homogeneous portion of Eq. (68), $\mathcal{M}(v)$, must now be expanded in a Fourier series:

$$\mathcal{M}(v) \cong \epsilon \left\{ \mathcal{P}_p^* e^{\lambda \cos v} - 2 \right\} \sin v + 2\mathcal{Q}_p^* e^{\lambda \cos v} \quad .$$

In this case, the "forcing function" is a purely periodic function of with period 2π , and may be expanded in a Fourier series of the form,

$$m(v) = \sum_{n=0}^{\infty} \{ C_n \sin nv + D_n \cos nv \} .$$

The coefficients are evaluated in the same manner as before:

$$\begin{aligned} C_1 &= 2\epsilon \left\{ \frac{\sigma_p^*}{\lambda} I_1(\lambda) - 1 \right\} \\ C_n &= \frac{2\epsilon n}{\lambda} \sigma_p^* I_n(\lambda) \quad , n = 2,3,4,\cdots \\ D_0 &= 2\, 2_p^* I_0(\lambda) \\ D_n &= 4\, 2_p^* I_n(\lambda) \quad , n = 1,2,3,\cdots . \end{aligned} \tag{72}$$

The complete pitching equation thus assumes the form,

$$\begin{aligned} \bar{\theta}'' + \left\{ \left[3M + \sigma_p^* I_0(\lambda) \right] + \left[(1-3M)\epsilon + 2\sigma_p^* I_1(\lambda) \right] \cos v + \cdots \right\} \bar{\theta} \\ = 2\, 2_p^* I_0(\lambda) + 4\, 2_p^* I_1(\lambda) \cos v \\ + 2\epsilon \left\{ \frac{\sigma_p^*}{\lambda} I_1(\lambda) - 1 \right\} \sin v + \cdots . \end{aligned} \tag{73}$$

The yawing equation, given by the third of Eqs. (67) is amenable to a similar analysis, the result being

$$\begin{aligned} \bar{\psi}'' + \left\{ \left[1 + \sigma_p^* I_0(\lambda) \right] + \left[2\sigma_p^* I_1(\lambda) + \epsilon \right] \cos v + \cdots \right\} \bar{\psi} \\ = k(M+1) + 2\sigma_p^* d\, I_1(\lambda) \cos\omega \\ + \sigma_p^* d \left[I_0(\lambda) + I_2(\lambda) \right] \cos\omega \cos v - 2 \frac{\sigma_p^*}{\lambda} d\, I_1(\lambda) \sin\omega \sin v \\ + \cdots . \end{aligned} \tag{74}$$

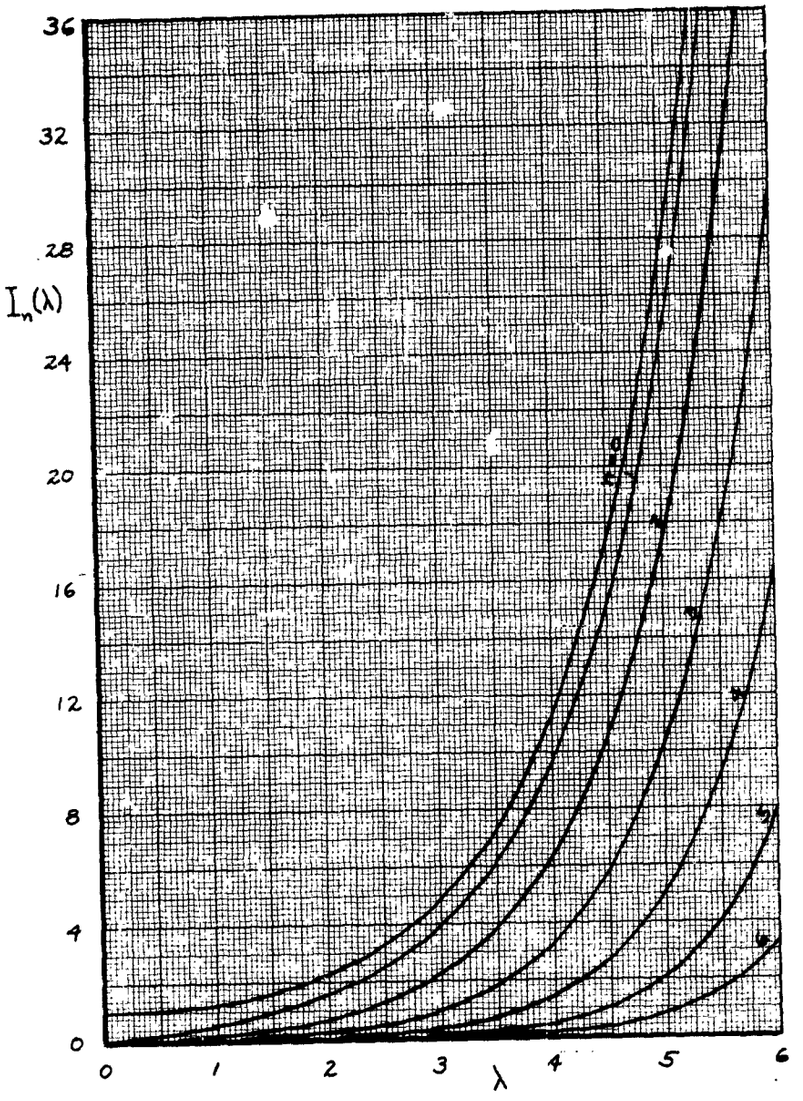

Figure 18. Modified Bessel Functions Versus λ

4. ANGULAR MOTIONS ON A CIRCULAR ORBIT

4.1 Existence and Stability of Equilibrium Positions

The general equations of motion developed in the last section apply to motion along elliptical orbits of small eccentricity and include the first order effects of aerodynamic and gravitational torques and aerodynamic damping. These equations, however, possess "simple" solutions only in exceptional circumstances and even in these cases, considerable analysis is required before the complete vehicle motion may be determined.

In order to gain some insight into the complete angular motion of an artificial satellite without such elaborate analysis, it is instructive to seek solutions of Eqs. (67) for the case of a circular orbit: $\epsilon = \lambda = 0$. The assumption of a circular orbit has a certain amount of practical significance since such orbits are desirable for numerous satellite applications (e.g., weather prediction, military reconnaissance, etc.) where stabilization of the vehicle is required. It must be noted, however, that an exactly circular orbit is impossible considering the perturbations due to planetary oblateness and atmospheric drag. As a result, this assumption must be justified primarily on the degree of mathematical simplification which it affords.

Under the assumptions of a circular orbit, Eqs. (67) simplify to read

$$\bar{\phi}' + \bar{\psi} = k$$

$$\bar{\theta}'' + (3M + \sigma_p^*)\bar{\theta} = 2 q_p^* \tag{75}$$

$$\bar{\psi}'' + (1 + \sigma_p^*)\bar{\psi} = \sigma_p^* d \cos(v+\omega) + k(M+1)$$

where the first of these results form a direct integration of $\bar{\phi}'' + \bar{\psi}' = 0$, as before. Clearly, if k is non-zero, then the rolling velocity, $\bar{\phi}'$, contains a constant (secular) term which prevents $\bar{\phi}$ from remaining small. In this sense, the first of Eqs. (69) establishes an approximate restriction upon the initial conditions which must be satisfied if the roll angle, ϕ, is to remain indefinitely bounded; namely, that $\bar{\phi}'(0) = -\bar{\psi}(0)$. Since practical accuracy requirements will probably prevent this precise condition from being met, it appears that an auxiliary roll-stabilization system will be necessary if it is required that a body of revolution orbit with one side directed toward the planet.

Two important properties of the motion may be determined directly from Eqs. (75), even before a complete solution is obtained; these are the existence and stability of equilibrium orientations of the satellite. As mentioned above, the rolling motion grows secularly if $k \neq 0$; hence any equilibrium solutions must necessarily satisfy $\bar{\phi}' + \bar{\psi} = 0$ which implies $\bar{\psi} = 0$ and, at most, $\bar{\phi} = \bar{\phi}_0$, a constant. From the third of Eqs. (75) it is seen that $\bar{\psi} = 0$ is a particular solution only when σ_p^* or d vanishes exactly. Thus, equilibrium solutions for the case of an aerodynamically responsive satellite exist only for equatorial orbits for which $d \equiv 0$.

The second of Eqs. (75) shows that an equilibrium pitch orientation is possible everywhere since $\bar{\theta} = 2\Omega_p^*/(3M + \sigma_p^*)$ represents a particular solution. The physical origin of this term is that a steady-state pitching moment must be provided to counter the damping torque produced by the fact that even in a circular orbit, the satellite is pitching at a rate equal to its angular velocity in orbit. For practical values of Ω_p^* and σ_p^* , however, this term is insignificant.[1]

Thus, for equatorial orbits, complete equilibrium is theoretically possible. In this case, the vehicle body axes remain essentially aligned with the orbital coordinates and the vehicle moves with the same side always directed toward the planet. Concerning the stability of this equilibrium, it is only necessary to examine the coefficients of the independent variables on the left-hand sides of Eqs. (75). Stability exists if the conditions

$$\sigma_p^* + 3M > 0$$
$$\sigma_p^* + 1 > 0 \qquad (76)$$

are satisfied. It follows at once that for very slender shapes (for which $M \cong -1$) pitch stability exists for $\sigma_p^* > 3$ while for dynamically spherical bodies ($M \cong 0$) , pitch stability is indicated for all positive values of σ_p^*. For disk-like bodies, for which the inertia parameter M approaches unity, the z axis becomes an axis of least inertia and the gravitational torques alone are adequate to insure a stable pitch equilibrium. The yaw equilibrium in circular, equatorial orbits is stable provided only that $\sigma_p^* > -1$.

The foregoing stability considerations are shown graphically in Fig. 19.

---

[1] In this connection, refer to Fig. 24.

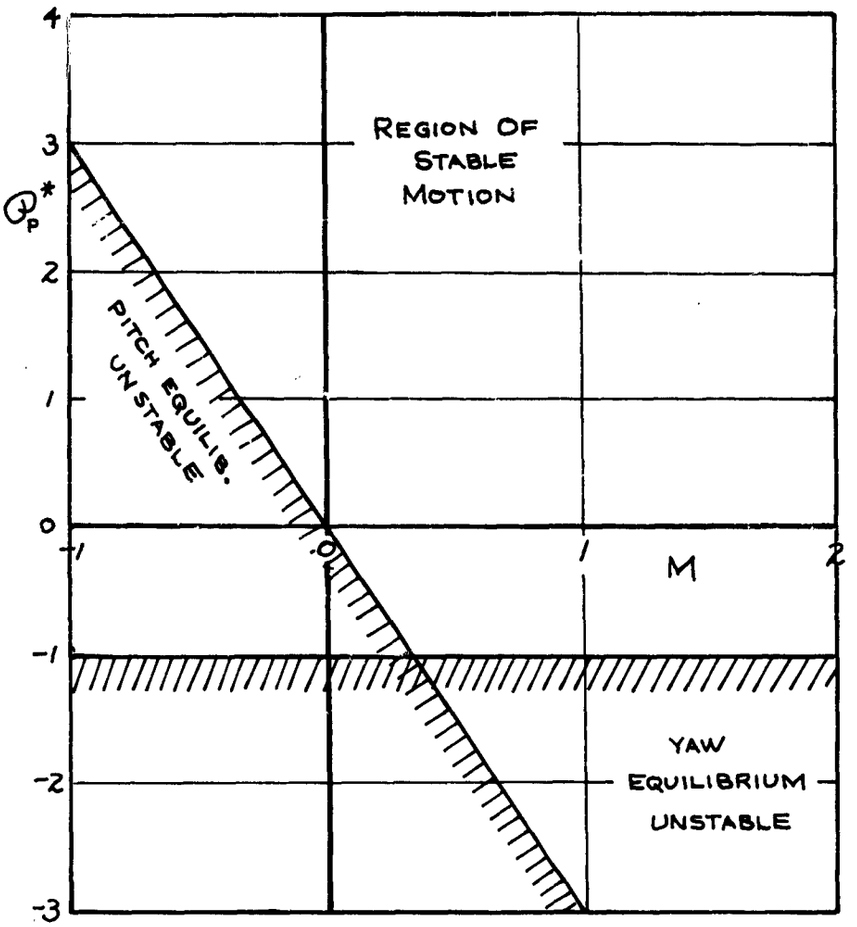

Figure 19. Stability Boundaries of the Aerodynamic Parameter Q_p^* for Circular Orbits

The general conclusions may be summarized succinctly by noting that for bodies of revolution with $M \leq 1/3$, yaw stability is insured if the pitching motion is stable, while for $M \geq 1/3$ pitch stability is insured if the yawing motion is rendered stable. In either case, the rolling motion may or may not be bounded depending upon whether the precise initial conditions required by the first of Eqs. (69) can be matched or not.

4.2 Approximate Behavior of Complete System

The complete analytical solutions to Eqs. (75) may be readily obtained, since the homogeneous equations associated with the second and third of Eqs. (75) are merely the harmonic equations. The complete results are

$$\bar{\theta} = \mathcal{A}\cos A\nu + \mathcal{B}\sin A\nu + 2\mathcal{Q}_p^*/A^2$$

$$\bar{\psi} = \mathcal{C}\cos B\nu + \mathcal{D}\sin B\nu + d\cos(\nu+\omega) + \frac{k}{B^2}(M+1) \qquad (77)$$

$$\bar{\phi} = \bar{\phi}(0) - \frac{\mathcal{C}}{B}\sin B\nu + \frac{\mathcal{D}}{B}(\cos B\nu - 1) + d(\sin\omega - \sin(\nu+\omega)) + \frac{k\nu}{B^2}(M+1-B^2)$$

where

$$A^2 \equiv A_0 = 3M + \mathcal{P}_p^*$$

$$B^2 \equiv 1 + \mathcal{P}_p^* \qquad (78)$$

$$k \equiv \bar{\phi}'(0) - \bar{\psi}(0) = \phi'(0) - \psi(0)$$

and $\mathcal{A}$, $\mathcal{B}$, $\mathcal{C}$, $\mathcal{D}$ are constants defined by the initial conditions of the motion. Since the orbit is circular, no generality is lost by taking $\nu = 0$ as the initial (or injection) point, whereupon there results (for $A>0$, $B>0$),

$$\mathcal{A} = \theta(0) + 2\mathcal{Q}_p^*/A^2 \cong \theta(0)$$

$$\mathcal{B} = \theta'(0)/A$$

$$\mathcal{C} = \psi(0) - d\cos\omega - \frac{k}{B^2}(M+1) \cong \psi(0) \qquad (79)$$

$$\mathcal{D} = \psi'(0)/B - d\sin\omega/B \cong \psi'(0)/B \quad .$$

Now in general, injection into orbit will be accomplished in such a way that the initial angular deviations will be small, as will the rolling and yawing rates $\phi'(0)$ and $\psi'(0)$. The pitch rate, $\theta'(0)$, however, will generally be of order unity, corresponding to an approximate rectilinear injection path tangent to the orbit. These considerations suggest that suitable approximations to Eqs. (77)-(79) are

$$\bar{\theta} \cong \frac{\theta'(0)}{A} \sin A\upsilon + 2\frac{\mathcal{P}_p^*}{A^2}$$

$$\bar{\psi} \cong d\cos(\upsilon+\omega) + k\left\{\frac{M+1}{\mathcal{P}_p^*+1}\right\} \qquad (80)$$

$$\bar{\phi} - \bar{\phi}(0) \cong -d\sin(\upsilon+\omega) - k\left\{\frac{\mathcal{P}_p^*-M}{\mathcal{P}_p^*+1}\right\}\upsilon \ .$$

The first of Eqs. (80) shows that although the pitching motion is stable for all $\mathcal{P}_p^*$ such that $A \geq 0$, when A becomes too small, the pitch amplitude may exceed that for small oscillations and the entire analysis will fail. Likewise, when the natural frequency of the pitching motion, A, becomes comparable to the orbital frequency (unity) the motion must be considered effectively divergent. Practically speaking, then, values of $A < 1$ will not be of great value in providing the desired degree of vehicle orientation, although an estimate of the order of these effects will be required to higher altitudes even for inertially stabilized systems.

The terms on the right of the second of Eqs. (74) represent the steady-state motion of $\bar{\psi}$. The first term represents that motion which is induced by the rotation of the atmosphere. Over the altitude range of interest, the amplitude of this forced motion never exceeds about $\pm 4^\circ$ as shown in Fig. 11. Moreover, since this forced oscillation is periodic in υ with period 2π, it may be removed by inertial devices such as inertia wheels, etc., without the device becoming saturated. The second term represents a constant displacement of the yaw equilibrium. Note that when the initial conditions are adjusted so that $k = 0$, then the yawing motion is essentially independent of the aerodynamic characteristics of the body; that is, independent of $\mathcal{P}_p^*$. The reason for this independence is that the aerodynamic damping is virtually negligible, and hence an aerodynamically stable body ($\mathcal{P}_p^* > 0$) aligns itself along the relative wind vector and moves in phase with it. When $-1 < \mathcal{P}_p^* < 0$, the forced yawing motion becomes 180° out of phase with the forcing function.

Finally, from the third of Eqs. (74), it is seen that the rolling motion is 90° out of phase with the yawing motion and is wholly oscillatory provided that the initial conditions are properly adjusted so that $k = 0$. If k is different from zero, a small secular term will appear, causing $\bar{\phi}$ to eventually become large.

Thus when the pitching motion is absent, the rolling and yawing motions may be approximately displayed on a phase diagram such as shown in Fig. 20(a) for $k = 0$ and as shown in Fig. 20(b) for $k \neq 0$.

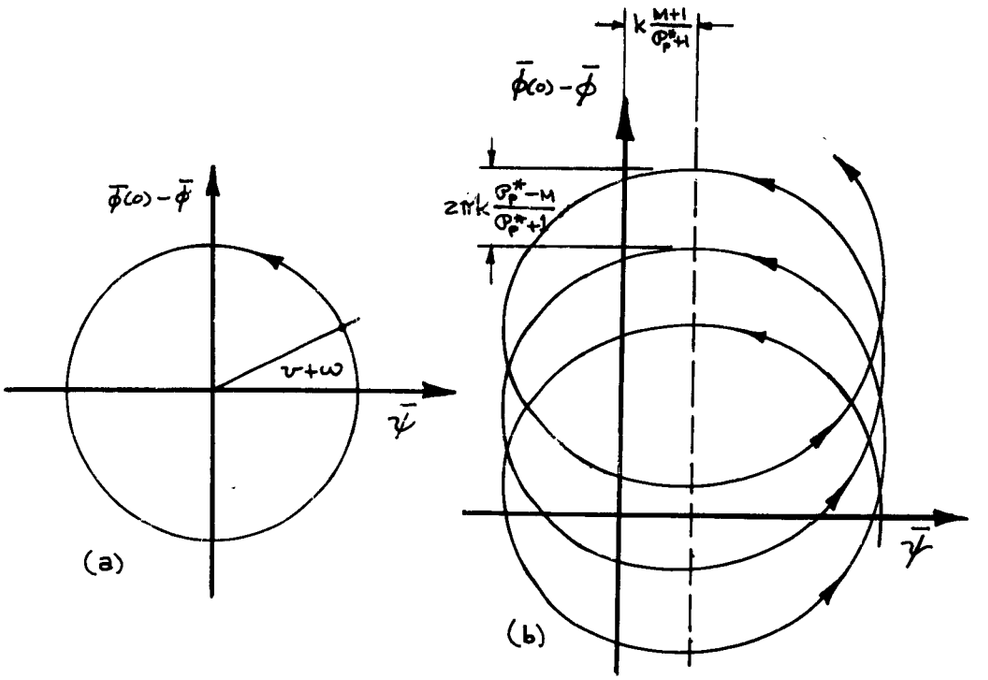

Figure 20. Approximate Behavior of the Forced Rolling and Yawing Motions. (a) $k=0$; (b) $k\neq 0$.

4.3 Exact Results for Small Angle Pitching Motion

4.3.1 General

In Section I.4, it is shown by Eq. (19) that if the rolling and yawing motions are suppressed, then the pitching motion of a non-spinning axisymmetric vehicle may be determined explicitly even for large values of θ . Since the problem of obtaining a desired satellite orientation is principally concerned with the pitching motions, it is appropriate to discuss this case in detail. Although only the small-angle equations are discussed explicitly, no fundamental change occurs for large angles. In this connection it should be noted that Beletskiy (Ref. 27) has solved this problem analytically in terms of elliptic integrals for the gravity gradient acting on the dumbbell satellite in a circular orbit.

The complete small-angle solution for the circular orbit pitching motion may be found from Eqs. (77)-(79) as

$$\bar{\theta} = \theta(0)\cos A\upsilon + \frac{\theta'(0)}{A}\sin A\upsilon + 2\frac{Q_p^*}{A^2} \qquad (81)$$

where A^2 and $2Q_p^*$ may be expanded from Eqs. (57), (59) and (78) to read

$$A^2 = 3M + \tfrac{1}{2}\Gamma\rho_p r_p^2(1-d\cot\iota)^2$$
$$2Q_p^* = \tfrac{1}{4}\Gamma_q\rho_p r_p(1-d\cot\iota) \qquad (82)$$

and where Γ and Γ_q are defined by Eqs. (59) as

$$\Gamma \equiv -C_{m_\alpha}\frac{S\pi\bar{c}}{\bar{I}} \quad , \quad \Gamma_q \equiv -C_{m_q}\frac{S\pi\bar{c}}{\bar{I}} \quad .$$

Thus, the vehicle is characterized by the three parameters Γ, M and Γ_q while the orbit is specified by the altitude h and the inclination ι. Since Eqs. (81) and (82) present the results in such a concise analytical form, the separate effects of the various parameters may be readily seen. For this reason, the following discussion and related figures are mainly for illustrative purposes.

4.3.2 Effects of Vehicle Parameters

Perhaps of greatest interest is the amplitude of the pitching motions as a function of the vehicle characteristics and the orbit altitude. Rewriting Eq. (81) in phase angle form, it is readily found that

$$\bar{\theta}_{max} = \theta_{max} = \sqrt{\theta^2(0) + \left(\theta'(0)/A\right)^2} + 2Q_p^*/A^2 \quad .$$

Figs. 21 and 22 show the results derived from this equation for several values of M and Γ, with $\Gamma_q \equiv 0$. Initial (or injection) conditions of $\theta(0)=0$ and $\theta'(0)=0.5^\circ$ are employed for definiteness but small deviations from these values will have little influence on the results. As before, atmospheric densities have been calculated from the 1959 ARDC (Minzner) atmosphere, (Ref. 26).

Fig. 21 shows clearly that even large values of Γ have relatively little effect in containing the pitch oscillations above about 400 miles altitude, even for $M > 0$. It is seen that the asymptotic (or $\Gamma = 0$) results are very rapidly reached at or near these heights. For those shapes for which the gravity torques oppose those due to aerodynamic forces (i.e., $M < 0$), the deterioration of small angle motion occurs at lower altitudes. In all cases, however, it is seen that for altitudes below about 180 miles, the effect of M is negligible, even for the relatively small values of Γ. In this sense, Figs. 21 and 22 permit the definition of regions of influence of the various external torques[1]:

Region I (below 180-200 miles) Aerodynamic torques dominate the angular motions.

Region II (180-400 miles) Aerodynamic and gravitational torques are of comparable importance.

Region III (400-600 miles) Aerodynamic, gravitational and solar torques are of comparable significance.

Region IV (above 600 miles) Solar and gravitational torques dominate the angular motions.

Fig. 23 presents the typical effect of M on the actual librations of a satellite with aerodynamic stability. As expected, the increased stability associated with increasing M both depresses the amplitude and shortens the period of the oscillations. For comparison, the corresponding curve for a gravity gradient stabilized vehicle is also shown.

The effect of Γ_ℓ, as previously mentioned, is too small to be of practical significance for all reasonable configurations. Fig. 24 presents the equilibrium angle $2\,Q_p^*/A^2$ versus altitude for several values of Γ_ℓ/Γ in order to substantiate this point. Insofar as the decay of the oscillations are concerned, Appendix C is to be consulted.

4.3.3 Effects of Orbit Parameters

The effects of orbit altitude are amply displayed in Figs. 21 and 22 and do not require further elaboration. Since the orbit is circular, the eccentricity is absent and the only remaining parameter is ι, the orbit inclination. Since ι influences Θ by slightly modifying the magnitude of the velocity of the satellite relative to the atmosphere, its effects

---

[1]Specific control torques can, of course, transcend any and all external torques if so desired. These have been omitted consistently in this work.

may be readily anticipated. Fig. 25 presents a typical numeric result for θ versus υ to illustrate the effect. Since the order of magnitude arguments indicated secondary importance for the atmospheric rotation, it is not surprising that only a small difference between the retrograde ($\iota = 180°$) and progressive ($\iota = 0°$) orbits occur. In general, it must be concluded that for a spherically symmetric atmosphere, the orbit inclination is of minor significance compared to (for example) the eccentricity or perigee altitude. In the presence of atmospheric oblateness, the "spring constant" of the system contains an additional periodic contribution which considerably complicates the analysis. Since the governing equation in this case is of the Mathieu type, the discussion of Section 5 may be used to estimate the effects of atmospheric oblateness.

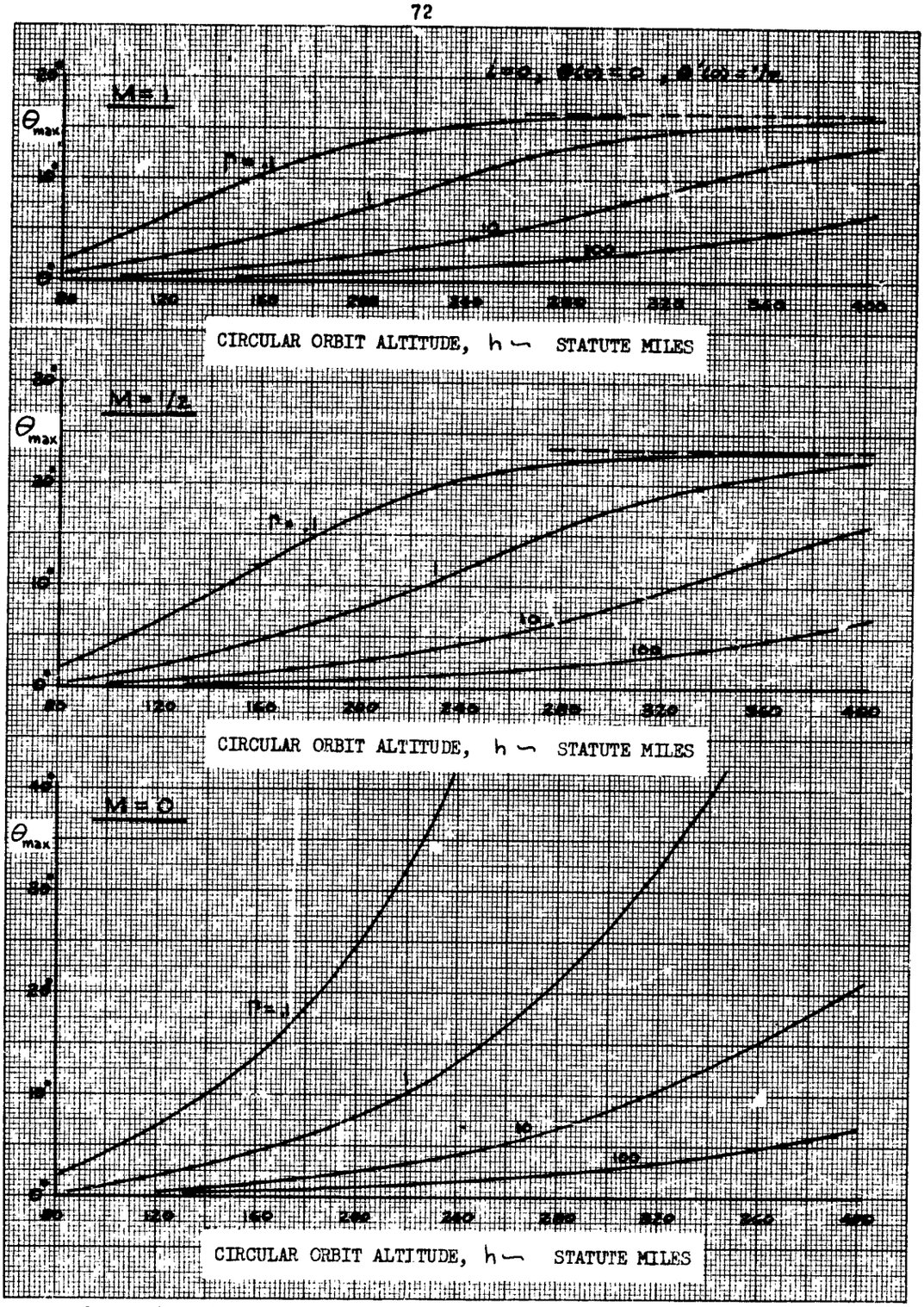

Figure 21. Combined Effects of Inertia and Static Aerodynamic Moment Parameters, M and Γ, on Circular Orbit Amplitude

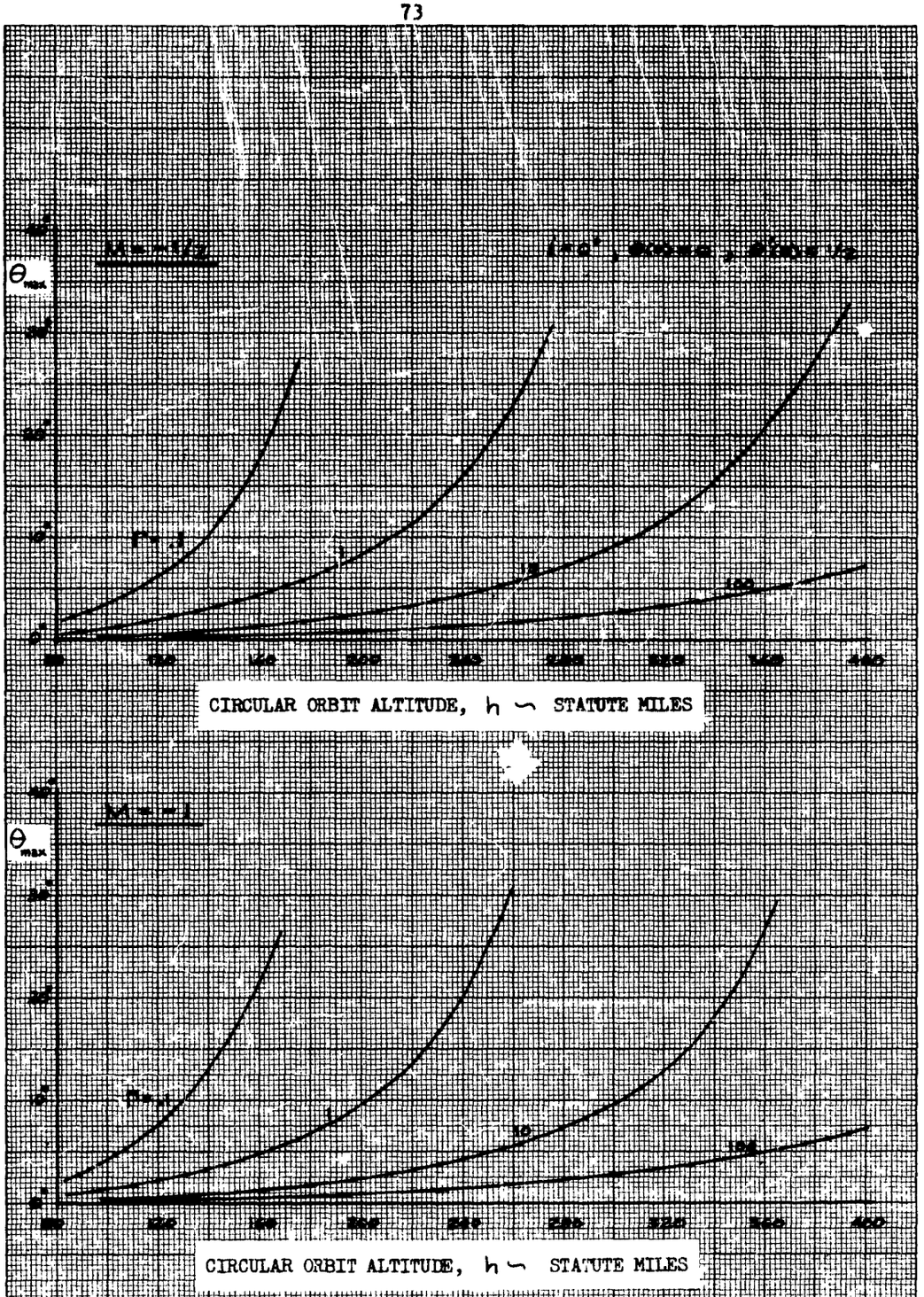

Figure 22. Combined Effects of Inertia and Static Aerodynamic Moment Parameters, M and Γ, on Circular Orbit Amplitude

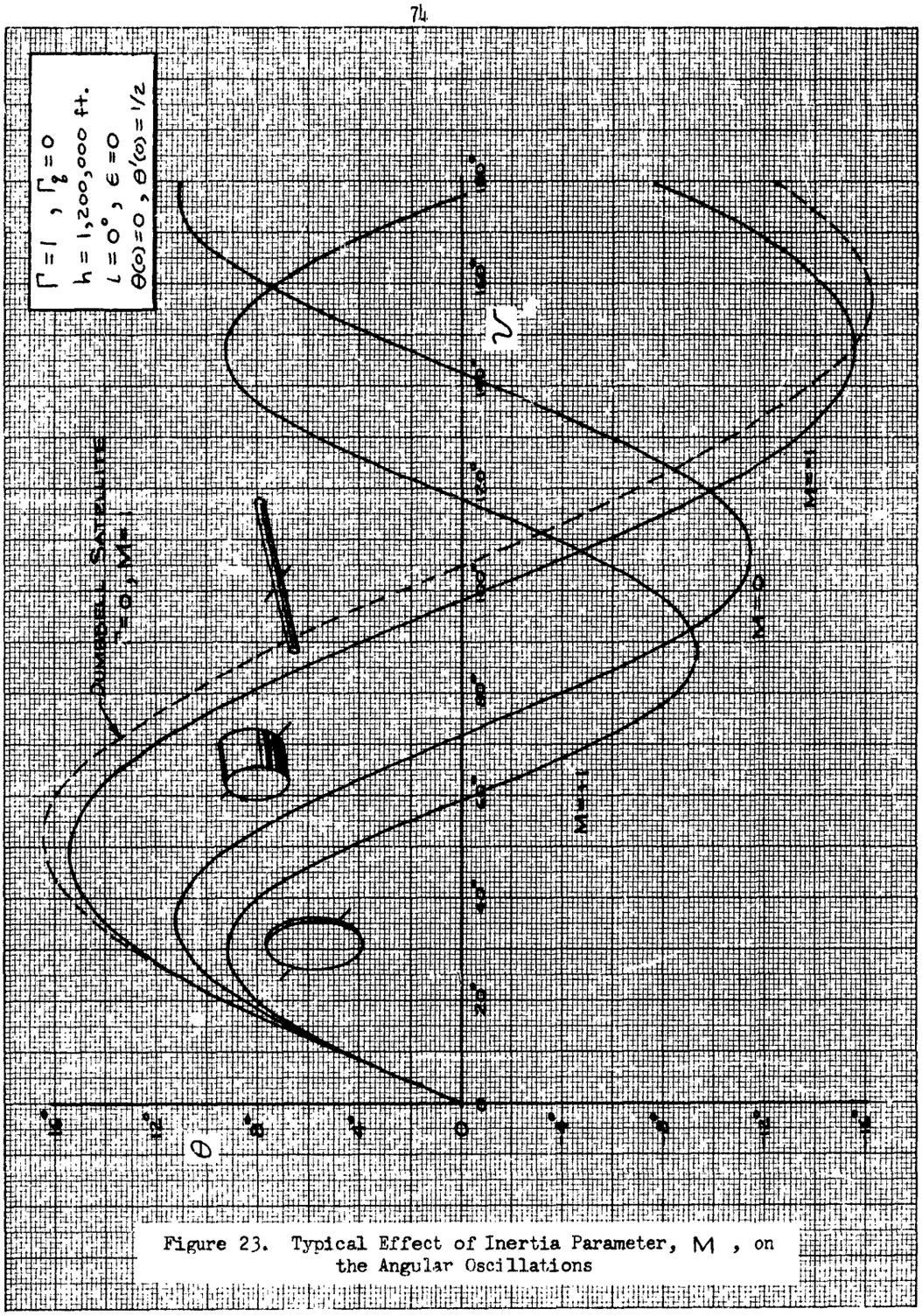

Figure 23. Typical Effect of Inertia Parameter, M , on the Angular Oscillations

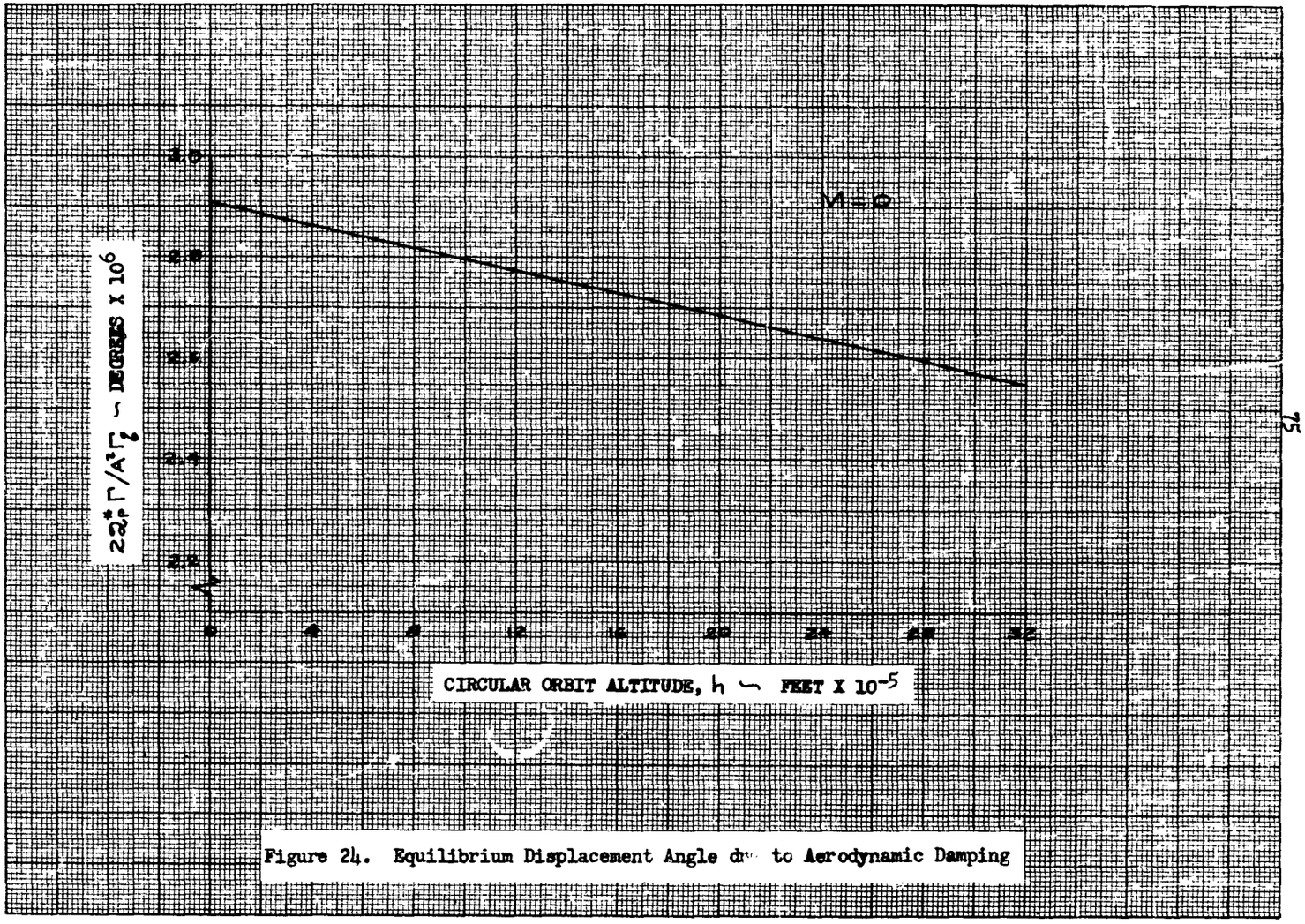

Figure 24. Equilibrium Displacement Angle due to Aerodynamic Damping

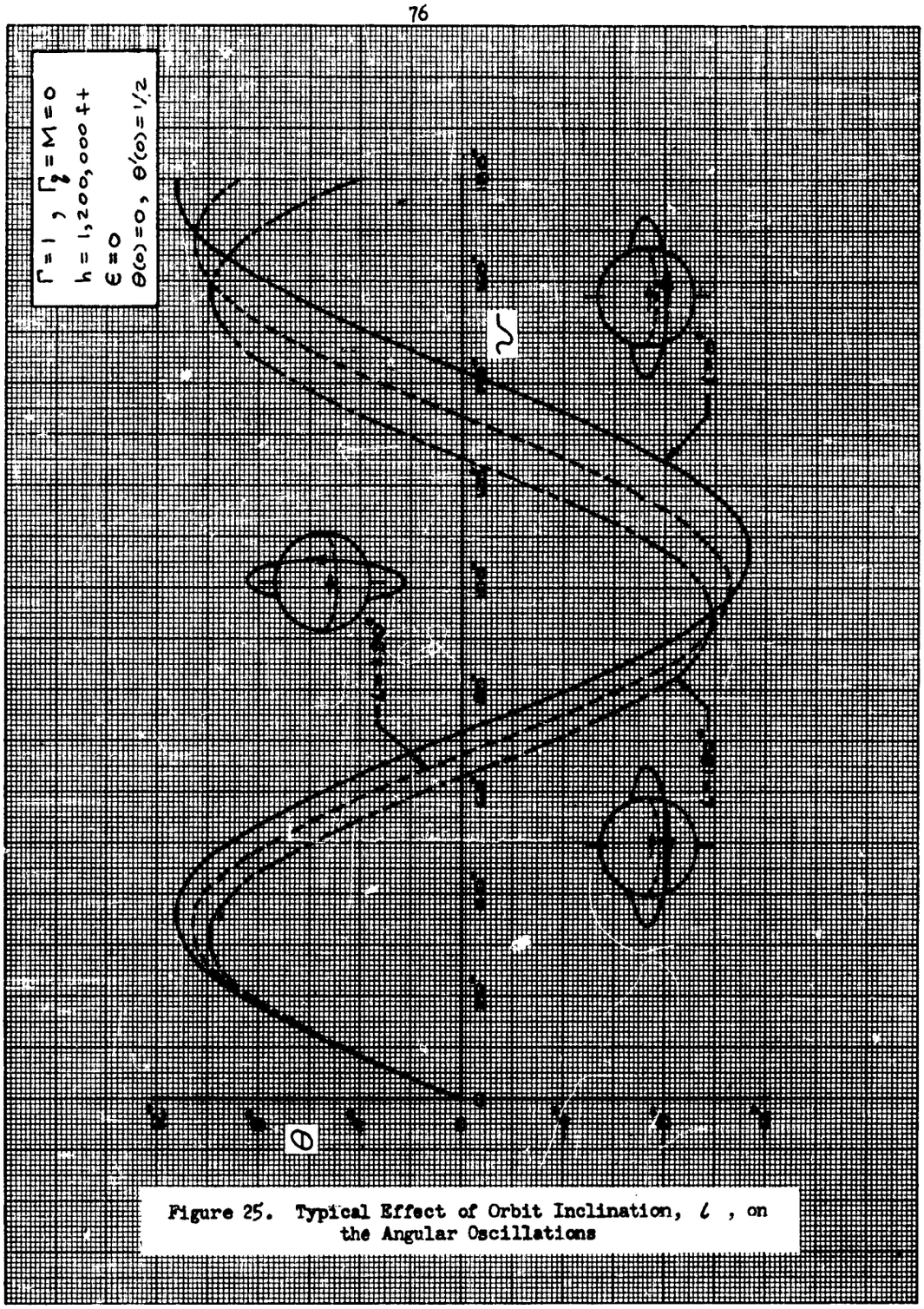

Figure 25. Typical Effect of Orbit Inclination, i , on the Angular Oscillations

5. PITCHING MOTION ON AN ECCENTRIC ORBIT

5.1 Exact Solution of the Homogeneous Pitching Equation

The equation for the pitching motion on an eccentric orbit, including the first order contributions from the aerodynamic and gravitational torques is given by Eq. (73) as:

$$\bar{\theta}'' + \left\{ \left[3M + \sigma_p^* I_0(\lambda) \right] + \left[(1-3M)\epsilon + 2\sigma_p^* I_1(\lambda) \right] \cos\nu + 2\sigma_p^* \sum_{n=2}^{\infty} I_n(\lambda) \cos n\nu \right\} \bar{\theta} = 2\Omega_p^* I_0(\lambda) - 2e \sin\nu + 4 \sum_{n=1}^{\infty} I_n(\lambda) \left[\sigma_p^* \frac{\epsilon n}{2\lambda} \sin n\nu + \Omega_p^* \cos n\nu \right] .$$

The associated homogeneous equation may be brought into the canonical form of Hill's differential equation (Wittaker and Watson, Ref. 34, Page 414) through the introduction of the transformation

$$\phi = \nu/2 ,$$

whereupon the homogeneous equation becomes

$$\bar{\theta}'' + \left\{ a_0 + 2a_1 \cos 2\phi + 2a_2 \cos 4\phi + \cdots \right\} \bar{\theta} = 0$$

where $a_0 = 4A_0$; $a_n = 2A_n$, $n = 1, 2, 3, \cdots$ and the primes now denote differentiation with respect to ϕ. With the definition $a_{-n} = a_n$, the above equation may also be written as

$$\bar{\theta}'' + \left\{ \sum_{n=-\infty}^{\infty} a_n e^{2in\phi} \right\} \bar{\theta} = 0 . \qquad (83)$$

This equation is known to have a solution of the form (c.f. Ref. 34, Page 416)

$$\bar{\theta} = \sum_{\nu=-\infty}^{\infty} b_\nu e^{(\mu + 2i\nu)\phi} \qquad (84)$$

where μ and all of the $\{b_\nu\}$ are to be determined. Differentiating Eq. (84) twice with respect to φ and substituting into Eq. (83):

$$\sum_{\nu=-\infty}^{\infty} b_\nu (\mu + 2i\nu)^2 e^{(\mu+2i\nu)\varphi} + \sum_{n=-\infty}^{\infty}\sum_{\nu=-\infty}^{\infty} a_n b_\nu e^{[\mu+2i(n+\nu)]\varphi} = 0 \quad (85)$$

The operation of rearranging the series in the second term above is justified since the series given by Eq. (84) may be shown to converge absolutely[1]. In order to obtain a recurrence relationship for the $\{b_\nu\}$, set $p = n+\nu$ in the second term of Eq. (85) and adjust the index ν so that the exponential terms may be factored out. Factoring the exponential, setting $p = \nu$ and equating the coefficients of like exponentials yields the recurrence formula for the $\{b_\nu\}$:

$$b_\nu (2i\nu + \mu)^2 + \sum_{n=-\infty}^{\infty} a_n b_{\nu-n} = 0, \quad \nu = 0, \pm 1, \pm 2, \cdots \quad (86)$$

Eqs. (86) constitute an infinite set of linear equations for the $\{b_\nu\}$ and the undetermined exponent μ. Since the $\{a_n\}$ are completely specified, the $\{b_\nu\}$ may be found once μ is known. Wittaker and Watson (Ref. 34, Page 415) show that μ is the root of the equation

$$\sin^2\left(\tfrac{1}{2}\pi i\mu\right) = \Delta(0)\sin^2\left(\tfrac{1}{2}\pi\sqrt{a_0}\right) \quad (87)$$

where $\Delta(i\mu)$ is the infinite determinant of the coefficients of $\{b_\nu\}$ in a set of equations obtained from Eqs. (86) by dividing the ν^{th} equation by $(4\nu^2 - a_0)$ to insure convergence. $\Delta(0)$ is $\Delta(i\mu)$ evaluated at $\mu = 0$, viz:

---

[1]The Fourier series representing $\mathcal{L}(v)$ is already known to satisfy this condition.

$$\Delta(0) = \begin{vmatrix} \cdots & \cdots & \cdots & \cdots & \cdots & \cdots & \cdots \\ \cdots & 1 & \frac{-a_1}{16-a_0} & \frac{-a_2}{16-a_0} & \frac{-a_3}{16-a_0} & \frac{-a_4}{16-a_0} & \cdots \\ \cdots & \frac{-a_1}{4-a_0} & 1 & \frac{-a_1}{4-a_0} & \frac{-a_2}{4-a_0} & \frac{-a_3}{4-a_0} & \cdots \\ \cdots & \frac{-a_2}{-a_0} & \frac{-a_1}{-a_0} & 1 & \frac{-a_1}{-a_0} & \frac{-a_2}{-a_0} & \cdots \\ \cdots & \frac{-a_3}{4-a_0} & \frac{-a_2}{4-a_0} & \frac{-a_1}{4-a_0} & 1 & \frac{-a_1}{4-a_0} & \cdots \\ \cdots & \frac{-a_4}{16-a_0} & \frac{-a_3}{16-a_0} & \frac{-a_2}{16-a_0} & \frac{-a_1}{16-a_0} & 1 & \cdots \\ \cdots & \cdots & \cdots & \cdots & \cdots & \cdots & \cdots \end{vmatrix} \qquad (88)$$

where a_0 cannot be zero or the square of an even integer. $\Delta(0)$ is called Hill's determinant.

The nature of the solution for $\bar{\theta}$, given by Eq. (85) is grossly dependent upon the value of μ obtained from Eq. (87). Since μ is a root of Eq. (87), $-\mu$ is also a root and in general, two linearly independent solutions to Eq. (83) correspond to these two roots. This implies that if the complex number μ contains a non-zero real part, then one of the two linearly independent solutions of the homogeneous equation contains a positive, real exponential factor, and hence this solution is unbounded for increasing Φ. Note that in the cases where the solutions corresponding to μ and $-\mu$ are not linearly independent, the second independent solution contains a logarithmic term and is again unbounded (Ref. 32, Page 556). Since the complete homogeneous solution contains a linear combination of the two independent solutions, it is, in principle, possible to find initial conditions for the motion such that the unbounded solution is absent. However, these cases are inherently unstable and the complete solution is, therefore, said to be unstable for $Re(\mu) \neq 0$. The problem thus becomes one of determining the conditions under which the solution of Eq. (83) is stable; that is, the conditions for which μ is a purely imaginary number.

In order to proceed, define,

$$\xi^2 \equiv \Delta(0) \sin^2\left(\tfrac{1}{2}\pi\sqrt{a_0}\right)$$

so that, from Eq. (87),

$$\sin^2\left(\tfrac{1}{2}\pi i\mu\right) = \xi^2 . \tag{89}$$

Now the $\{a_n\}$ are all real so it follows that $\Delta(o)$ is real and hence three cases are possible for ξ^2, viz: (i) $\xi^2 \le 0$, (ii) $0 < \xi^2 < 1$ (iii) $\xi^2 \ge 1$. Eq. (89) may be readily solved for these three cases to yield:

$$\mu = \pm \frac{2}{\pi} \sinh^{-1}(i\xi) \quad , \quad \xi^2 \le 0$$

$$\mu = \pm \frac{2i}{\pi} \sin^{-1}(\xi) \quad , \quad 0 < \xi^2 < 1$$

$$\mu = i \pm \frac{2}{\pi} \cosh^{-1}(\xi) \, , \quad \xi^2 \ge 1 \, .$$

These results may be displayed on the complex plane as shown in Fig. 26.

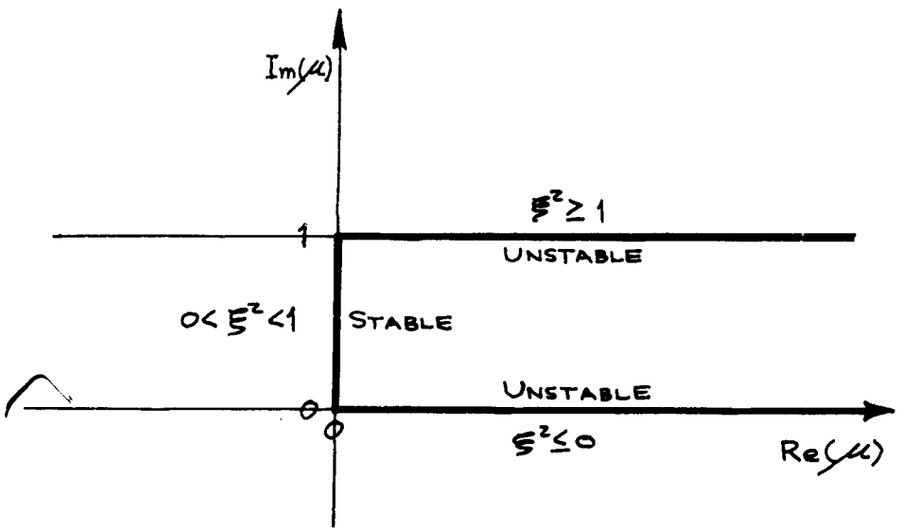

Figure 26. Behavior of the Characteristic Exponent μ as a Function of ξ^2

Thus, stable solutions occur only for ξ^2 between zero and unity. The stability of the motion may, therefore, be partially analyzed without obtaining an explicit solution, merely by determining the conditions under which $0 < \xi^2 < 1$. Unfortunately, this determination requires extensive numerical calculations since ξ^2 depends upon $\Delta(0)$ and hence upon all of the Fourier coefficients $\{a_n\}$.

Before discussing these numerical calculations, however, it is instructive to obtain explicit solutions to Eqs. (83), for it is noted that once μ is known, the solutions for $\bar{\theta}$ may be found from Eq. (84). Confining attention to the stable case wherein μ is purely imaginary (call it $i\mu_s$), two linearly independent solutions of Eq. (83) are the complex functions

$$\begin{aligned} U_1 &= \sum_{\nu=-\infty}^{\infty} b_\nu^+ \, e^{i(2\nu+\mu_s)\phi} \\ U_2 &= \sum_{\nu=-\infty}^{\infty} b_\nu^- \, e^{i(2\nu-\mu_s)\phi} \end{aligned} \tag{90}$$

Now b_ν^+ and b_ν^- must separately satisfy the recurrence formula of Eq. (86) so that,

$$\begin{aligned} -b_\nu^+(2\nu+\mu_s)^2 + \sum_{n=-\infty}^{\infty} a_n b_{\nu-n}^+ &= 0 \\ -b_\nu^-(2\nu-\mu_s)^2 + \sum_{n=-\infty}^{\infty} a_n b_{\nu-n}^- &= 0 \end{aligned} \tag{91}$$

The second of Eqs. (91) may also be written as

$$-b_{-\nu}^-(2\nu+\mu_s)^2 + \sum_{n=-\infty}^{\infty} a_n b_{-(\nu-n)}^- = 0 \tag{92}$$

whereupon, comparing Eq. (92) and the first of Eqs. (91), one concludes that b_ν^+ and $b_{-\nu}^-$ satisfy the same recurrence formula and hence,

$$b_\nu^+ = b_{-\nu}^- \equiv b_\nu \ .$$

The two solutions given by Eqs. (90) then become

$$U_1(\varphi) = \sum_{\nu=-\infty}^{\infty} b_\nu \, e^{i(2\nu+\kappa_2)\varphi}$$

$$U_2(\varphi) = \sum_{\nu=-\infty}^{\infty} b_\nu \, e^{-i(2\nu+\kappa_2)\varphi} \ . \tag{93}$$

The unknown $\{b_\nu\}$ may be found from the first of Eqs. (91). Since this recurrence formula is real, it follows that the $\{b_\nu\}$ are also real. Constant multiples of the sum and difference of the two solutions given by Eqs. (93) yield respectively the two linearly independent real solutions

$$\bar\theta_1^*(\varphi) \equiv \tfrac{1}{2}(U_1+U_2) = \sum_{\nu=-\infty}^{\infty} b_\nu \cos(2\nu+\kappa_2)\varphi$$

and (94)

$$\bar\theta_2^*(\varphi) \equiv \tfrac{1}{2i}(U_1-U_2) = \sum_{\nu=-\infty}^{\infty} b_\nu \sin(2\nu+\kappa_2)\varphi \ .$$

Finally, the complete homogeneous solution for $\bar\theta$ is given by

$$\bar\theta(\varphi) = \alpha\,\bar\theta_1^*(\varphi) + \beta\,\bar\theta_2^*(\varphi)$$

where α and β are constants (which must be real if $\bar\theta$ is to be a real function of the real variable φ) determined by the initial conditions of the motion.

Eqs. (94) show that the solution for $\bar\theta$ is wholly periodic of period π or 2π only when κ_2 is an integer, which means that these periodic solutions occur only at the respective corners $\kappa = 0$ or $\kappa = i$ of Fig. 26. Thus, the unstable regions of the solution are bounded by purely periodic solutions. In the case of Mathieu's equation (where only a_0

and a_1 differ from zero), these periodic solutions have been named Mathieu functions and are designated as even or odd according to whether they reduce to the cosine or sine function as $a_1 \to 0$ (Refs. 32-34). In the general Hill problem, the corresponding functions do not appear to have been tabulated.

In principle, the foregoing analysis yields the complete homogeneous solution for $\bar{\theta}$, provided that the exponent μ may be determined from Eq. (87). The evaluation of $\Delta(0)$ which is required for the calculation of μ, however, poses certain practical problems of convergence for moderate to large values of a_0; that is, for large values of σ_p^*. The convergence of $\Delta(0)$ may be studied by the analysis which follows.

Consider Eq. (88) for Mathieu's differential equation wherein only a_0 and a_1 differ from zero. Then the typical term in the ν^{th} row of $\Delta(0)$ adjacent to the main diagonal (of which every term is unity) reads

$$\frac{-a_1}{2\nu^2 - a_0}$$

all other terms being zero.

Now for numerical purposes the infinite Hill determinant is replaced by a large but finite determinant, say $(2m+1)$ by $(2m+1)$. Let $a_0 >> (2m)^2$. Near the center, the determinant then appears as

$$D_n = \begin{vmatrix} 1 & \epsilon & 0 & 0 & \cdots & \cdots & \cdots \\ \epsilon & 1 & \epsilon & 0 & \cdots & \cdots & \cdots \\ 0 & \epsilon & 1 & \epsilon & \cdots & \cdots & \cdots \\ \cdots & \cdots & \cdots & \cdots & \cdots & \cdots & \cdots \\ \cdots & \cdots & \cdots & \cdots & \epsilon & 1 & \epsilon \\ \cdots & \cdots & \cdots & \cdots & 0 & \epsilon & 1 \end{vmatrix}$$

since $(2\nu)^2$ is negligible compared to a_0 for $\nu \leq m$.

A determinant with such symmetry may be expanded by considering the following 4 x 4 example:

$$D_4 = \begin{vmatrix} 1 & \varepsilon & 0 & 0 \\ \varepsilon & 1 & \varepsilon & 0 \\ 0 & \varepsilon & 1 & \varepsilon \\ 0 & 0 & \varepsilon & 1 \end{vmatrix} .$$

Multiplying the first row by ε and subtracting from the second,

$$D_4 = \begin{vmatrix} 1 & \varepsilon & 0 & 0 \\ 0 & 1-\varepsilon^2 & \varepsilon & 0 \\ 0 & \varepsilon & 1 & \varepsilon \\ 0 & 0 & \varepsilon & 1 \end{vmatrix} = \begin{vmatrix} 1 & \varepsilon & 0 \\ \varepsilon & 1 & \varepsilon \\ 0 & \varepsilon & 1 \end{vmatrix} + \begin{vmatrix} -\varepsilon^2 & \varepsilon & 0 \\ 0 & 1 & \varepsilon \\ 0 & \varepsilon & 1 \end{vmatrix}$$

or

$$D_4 = D_3 - \varepsilon^2 D_2 .$$

This relation may be readily generalized to any size determinant, viz:

$$D_n = D_{n-1} - \varepsilon^2 D_{n-2} .$$

Thus,

$$D_1 = 1$$

$$D_2 = 1 - \varepsilon^2$$

$$D_3 = 1 - 2\varepsilon^2$$

$$D_4 = 1 - 3\varepsilon^2 + \varepsilon^4$$

$$D_5 = 1 - 4\varepsilon^2 + 3\varepsilon^4 - \varepsilon^6 , \text{ etc.}$$

which may be further generalized to read (to terms of order ε^4)

$$D_n = 1 + (1-n)\varepsilon^2 + \left(\frac{n^2-5n+6}{2}\right)\varepsilon^4 + \cdots$$

This expression shows clearly that as long as $a_0 \gg (2\nu)^2$, examining successively larger sizes of determinants will now show convergence regardless of the size of $\epsilon > 0$. Convergence does not begin to be seen until the determinant is sufficiently large so that $(2\nu)^2$ transcends a_0, after which the convergence should be fairly rapid. The result also generalizes to the Hill problem where all $\{a_n\}$ may be present.

Thus, the evaluation of Hill's determinant, which is troublesome even with the aid of a high speed computer, prevents the wholly analytical solution of even the homogeneous problem from being achieved. For small values of a_0, the procedure outlined above may be carried out manually. The solution of the non-homogeneous equation may then be obtained by the method of variation of parameters (Ref. 37, Page 122). The technique should yield meaningful results if applied to the librations of the dumbbell-shaped satellite moving on an eccentric orbit, but for the case where aerodynamic influences are of interest, the method is too cumbersome to be of direct value.

5.2 Stability of the Natural (Unforced) Motion

The foregoing analytic solution is of considerable value, however, in providing a qualitative description of the stability of the unforced angular motion on an elliptical orbit. Since stable motion can only exist for $0 < \xi^2 < 1$, it follows that

$$0 < \Delta(0) \sin^2\left(\tfrac{1}{2}\pi\sqrt{a_0}\right) < 1$$

is the requirement for bounded motion. When a_0 is not the square of an even integer, a sufficient condition for stable (bounded) motion is $0 < \Delta(0) < 1$; however, there is no reason to expect $\Delta(0)$ to remain on this interval.

The circumstances under which the above inequality is violated may be examined by considering the integer values of $\sqrt{a_0}$. In cases where a_0 is near an odd square, $\sin^2(\pi\sqrt{a_0}/2)$ will be close to unity while $\Delta(0)$ will be determined essentially by all of the $\{a_n\}$ and will be relatively insensitive to small changes in a_0. Regarding $\Delta(0)$ as independent of a_0 for the latter near an odd square, three subcases result: (i) For $\Delta(0) < 1$, the motion remains bounded as a_0 approaches $(2n+1)^2$. (ii) For $\Delta(0) = 1$, a single unstable point occurs for each $a_0 = (2n+1)^2$. Since $\xi^2 = 1$ in this case, $\alpha = i$ and Eqs. (94) show that periodic solutions of period 2π exist. (iii) For $\Delta(0) > 1$, a region of instability may be associated with each $a_0 = (2n+1)^2$. At the boundaries of this region, $\xi^2 = 1$ and hence periodic solutions of period 2π occur on these boundaries.

The case of $a_0 = (2n)^2$ has been excluded in the construction of $\Delta(0)$ and hence this case requires special treatment. It is not difficult to show that although $\Delta(0)$ is undefined at $a_0 = (2n)^2$, ξ^2 approaches a definite limit as $a_0 \to (2n)^2$. Unfortunately, this limit is not readily calculable. In the special case where all of the $\{a_n\}$ save a_0 vanish, $\Delta(0) = 1$ and $a_0 = (2n)^2$ are the eigenvalues of the sine problem. Since $\alpha = 0$ in this case, Eqs. (94) show that periodic solutions of period π result. When the other $\{a_n\}$ are present, a similar behavior is seen, with the possibility that another region of instability may be associated with each $a_0 = (2n)^2$.

The foregoing discussion brings out the essential features of the problem of stability determination. The specific behavior may be described as follows: Let all of the $\{a_n\}$ be fixed with the exception of one, and let this one be permitted to vary. As it does, $\Delta(0)$ will, in general, exhibit an oscillatory behavior which will cause ξ^2 to leave the range of $0 < \xi^2 < 1$. Corresponding to $\xi^2 < 0$ and $\xi^2 > 1$, the motion will be completely unstable. Corresponding to $\xi^2 = 0$ and $\xi^2 = 1$, periodic (and therefore bounded) solutions of period π and 2π respectively exist, but the two solutions given by Eqs. (94) become linearly dependent in each case and the second independent solution will be found to be unbounded (Ref. 32). Thus, alternate regions of stable and unstable motion will generally be encountered, with each unstable region bounded by periodic functions of period π or 2π.

Since this behavior is evident even when only a_0 and a_1 differ from zero, it is convenient to continue this discussion for the Mathieu equation. The stable and unstable regions for this problem have been described by numerous authors (Refs. 32-35) and may be displayed on a plot of a_0 versus a_1 (c.f., Ref. 33, Fig. 166). For the present case, however, both a_0 and a_1 (and indeed all the $\{a_n\}$ in the complete problem) depend upon the four physical parameters $\mathcal{P}_p^*$, M, ϵ and λ, as seen from Eq. (73). For illustrative purposes, assume $M = 0$ and neglect ϵ in comparison to $\mathcal{P}_p^* I_1(\lambda)$. Then Eq. (83) specializes as

$$\bar{\theta}'' + \left\{ 4\mathcal{P}_p^* I_0(\lambda) + 2\left[4\mathcal{P}_p^* I_1(\lambda)\right] \cos 2\phi \right\} \bar{\theta} = 0$$

Thus, the stable and unstable regions on the $a_0 - a_1$ plane may be mapped into corresponding regions on the $\mathcal{P}_p^* - \lambda$ plane. Fig. 27 presents an approximate construction of these regions based upon Ref. 33, and is intended for qualitative examination only.

The nature of the stability boundaries, as determined from Mathieu's problem, appear as follows for a given configuration: A maximum perigee altitude exists for any given eccentricity such that the motion may be

stable everywhere[1]. Within this stable region, however, lie isolated regions of instability. In some cases these regions reduce to merely lines, particularly for large values of ρ_p^* (low altitudes) and small values of λ (low eccentricities), but in other cases the regions may be large. A typical orbit will begin at some value of h_p and ϵ and ϵ will start to decrease while h_p remains fairly constant. During this decay, λ will drop rapidly and ρ_p^* will increase (due to the increase in ρ_e), both effects tending toward greater stability of the angular motion. However, it appears quite possible that these changes will carry the motion into a small but finite region of instability, and that the vehicle may dwell there long enough to begin tumbling. It is also possible that h_p and ϵ would initially place the vehicle in an unstable region, while the subsequent orbit decay would move it out of this region.

These results correspond to intuition. When the aerodynamic stability margin is very great, the motion should be stable as it is at low altitudes. When the margin is small, the possibility of unstable motion exists, particularly since the natural frequency of the aerodynamically induced oscillation (being of order $\sqrt{a_o}$) may become comparable to the orbital frequency. Furthermore, for a given value of ρ_p^* the stability is greater for small values of λ than for λ large, as might be expected.

The catastrophic nature of the amplitude build-up possible in these small unstable regions is illustrated in the section dealing with results of the numeric integration of the equation of motion, and hence no further elaboration of this general subject appears warranted here. It is sufficient to note that the problem of passive satellite stability appears to depend primarily on the rate at which the amplitude increases when an unstable region is encountered.

5.3 Stability of the Forced Motion

The preceding section has shown the solution of the homogeneous equation to contain numerous unstable regions. The addition of periodic excitation (or forcing) will not, in general, mitigate this condition and in fact, will generally compound the difficulties by permitting resonances to occur.

An analysis of the forced motion, based upon the properties of second order differential equations with periodic coefficients has been performed by Juelich in Volume III of this series of reports (Ref. 2) and need not be repeated here. The essential result for this discussion, is that the only effect of the periodic excitation is to induce a resonance when the

---

[1]For $M \geq 0$, and $\rho_p^* > 0$, this maximum altitude lies at infinity.

period of the homogeneous solution and that of the forcing function coincide[1]. In terms of the transformed variable ϕ, this occurs whenever the homogeneous solution is periodic of period π, or whenever $\mu = 0$. Since this point is excluded from the stable range of the homogeneous solutions, no additional instabilities in the motion occur due to forcing.

The addition of periodic forcing, however, does permit periodic solutions of period π (the period of the forcing function in ϕ) to be found for all non-resonant conditions. From Ref. 2, this may be shown as follows:

Let $\bar{\theta}_0$ be that solution of the complete equation, Eq. (73), that has

$$\bar{\theta}_0(0) = 0 \quad , \quad \bar{\theta}_0'(0) = 0$$

and let $\bar{\theta}_1$ and $\bar{\theta}_2$ be those solutions of the homogeneous equation, Eq. (83) that have, respectively,

$$\begin{aligned} \bar{\theta}_1(0) &= 1 \quad , \quad \bar{\theta}_1'(0) = 0 \\ \bar{\theta}_2(0) &= 0 \quad , \quad \bar{\theta}_2'(0) = 1 \end{aligned} \tag{95}$$

Comparing these initial conditions with Eqs. (94), it is seen that

$$\begin{aligned} \bar{\theta}_1^*(\phi) &= \bar{\theta}_1(\phi) \sum_{\nu=-\infty}^{\infty} b_\nu \\ \bar{\theta}_2^*(\phi) &= \bar{\theta}_2(\phi) \sum_{\nu=-\infty}^{\infty} b_\nu (2\nu + \mu_s) \end{aligned} \tag{96}$$

In general, any arbitrary solution of Eq. (73) may be written

$$\bar{\theta}(\phi) = \alpha\, \bar{\theta}_1(\phi) + \beta\, \bar{\theta}_2(\phi) + \bar{\theta}_0(\phi)$$

---

[1] That is, when the system is "forced" at its natural frequency, (the frequency of the homogeneous solution), "resonance" is said to exist.

If it is now required that $\bar{\theta}$ be periodic or period π (in ϕ), then it may be shown (Ref. 2) that suitable constants α and β satisfy the matrix equation

$$\begin{bmatrix} \bar{\theta}_0(\pi) \\ \bar{\theta}_0'(\pi) \end{bmatrix} = (I-W) \begin{bmatrix} \alpha \\ \beta \end{bmatrix}$$

where the determinant of W is the Wronskian of the solutions $\bar{\theta}_1$, $\bar{\theta}_2$ evaluated at $\phi = \pi$, and I is the identity matrix. A unique periodic solution of period π is then seen to exist if the matrix $(I-W)$ is non-singular. With the help of Eqs. (94) and (96), it may also be seen that

$$\det(I-W) = 2 - 2\cos \pi/\mu_s$$

and so $(I-W)$ is singular only for $\mu_s = 0$, which has been identified as the resonant case.

The existence of a unique periodic particular solution for all $\mu_s \neq 0$ insures the existence of a bounded solution of the complete problem for all non-resonant conditions. In the unstable regions, however, slight deviations from this periodic solution will amplify and the solution becomes unbounded. This behavior is illustrated in Section 5.5. It is to be noted that as resonance is approached, the periodic solution may grow in amplitude so that in the neighborhood of a resonance, the motion, although bounded, may have a prohibitively large amplitude.

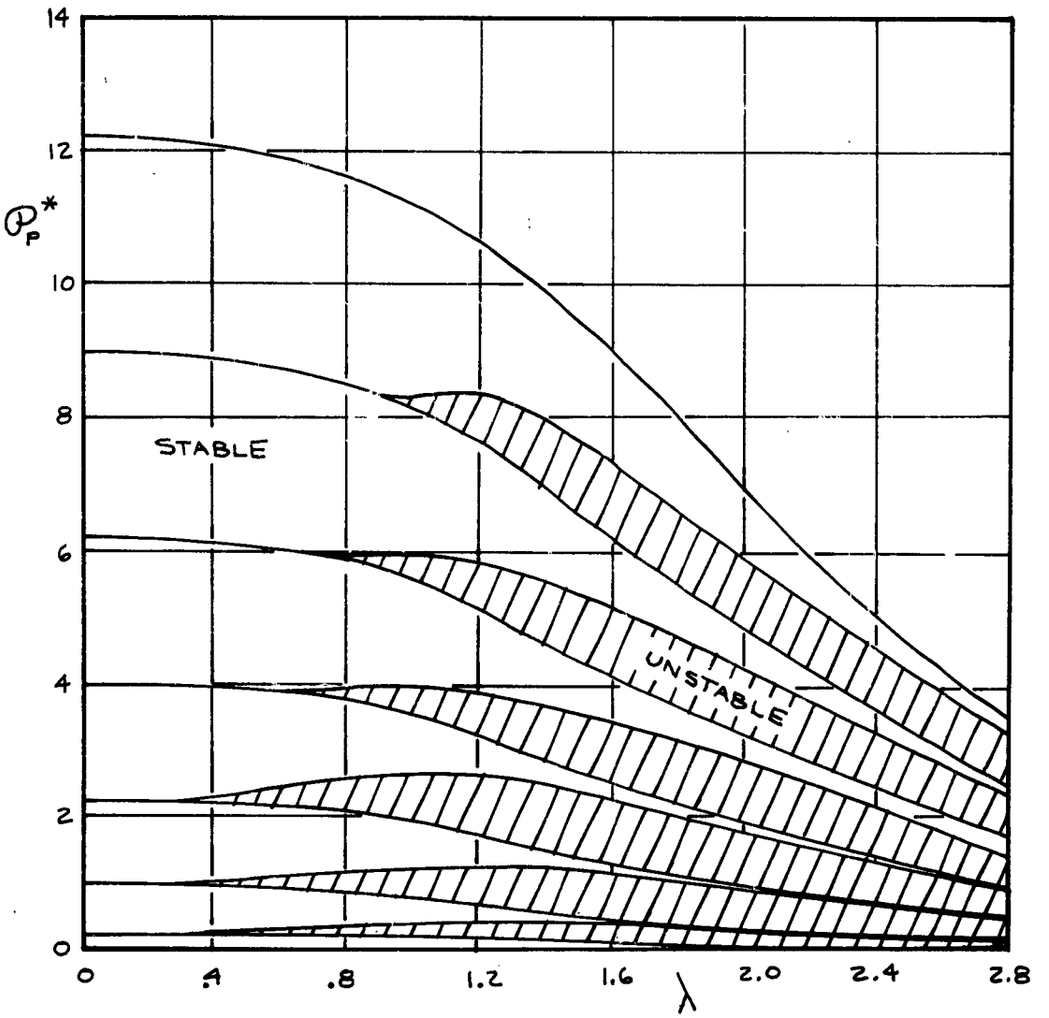

Figure 27. Stability Boundaries on the $\mathcal{P}_p^* - \lambda$ Plane Based upon Mathieu's Equation

5.4 Approximate Solution of Complete Pitching Equation

The preceding section has shown that in general, the complete solution of the equation for the pitching motion of an aerodynamically responsive satellite is quite complicated and extensive numerical computations are required. The scope of these calculations is such that a solution may be obtained with little more effort by a direct numerical integration of the equations of motion; this latter approach requiring only few simplifying assumptions.

It is of considerable value, however, to have available a completely analytical, albeit approximate, solution to the equations of motion. Such a solution has been obtained using the method of variation of parameters to solve a reduced version of Eq. (73). The reduction is accomplished by assuming the orbital eccentricity to be sufficiently small so that $I_1(\lambda) << I_0(\lambda)$ and all $I_n(\lambda)$, $n=2,3,4,\cdots$ multiplying $\bar{\theta}$ may be neglected. Thus, the homogeneous equation is reduced to Mathieu's equation. If, in addition, all terms involving $\mathcal{Q}_p^*$ except the first are neglected as excitation in Eq. (73), the equation takes the form

$$\bar{\theta}'' + \left[A^2 + q\cos\nu\right]\bar{\theta} \cong D_0 + \sum_{n=1}^{\infty} C_n \sin n\nu \qquad (97)$$

where, from Eqs. (71) and (72),

$$A^2 \equiv A_0 = 3M + \mathcal{Q}_p^* I_0(\lambda)$$

$$q \equiv (1-3M)\epsilon + 2\mathcal{Q}_p^* I_1(\lambda)$$

$$D_0 \equiv 2\mathcal{Q}_p^* I_0(\lambda)$$

$$C_1 \equiv 2\frac{\epsilon}{\lambda}\left[\mathcal{Q}_p^* I_1(\lambda) - \lambda\right]$$

$$C_n \equiv 2\frac{\epsilon n}{\lambda}\mathcal{Q}_p^* I_n(\lambda) \quad , \quad n=2,3,4,\cdots .$$

Eq. (97) is in the standard form of a non-homogeneous Mathieu equation with harmonic excitation. In order to place Eq. (97) in the customary form for a variation of parameters solution (e.g., Ref. 17), it is necessary to depress the order of the equation by writing

$$\theta_1 = \bar{\theta} \quad , \quad \theta_2 = \theta_1' = \bar{\theta}' . \qquad (98)$$

Then

$$\theta_2' + \left[A^2 + 2q\cos v\right]\theta_1 = D_0 + \sum_{n=1}^{\infty} C_n \sin nv$$

$$\theta_1' - \theta_2 = 0 \tag{99}$$

are the pair of first order equations equivalent to Eq. (97).

The zeroth order, or reference solution which will be varied is taken as the circular orbit solution of Eq. (77):

$$\bar{\theta} = a\cos Av + B\sin Av + D_0/A^2 \tag{100}$$

where the "constants" a and B will be varied such that Eqs. (99) are satisfied by an equation of the form of Eq. (100). Thus,

$$\theta_1 = a\cos Av + B\sin Av + D_0/A^2$$

$$\theta_2 = -aA\sin Av + BA\cos Av \tag{101}$$

and

$$\theta_1' = a'\cos Av + B'\sin Av + \theta_2$$

$$\theta_0' = -a'A\sin Av + B'A\cos Av - A^2\theta_1 + D_0 .$$

Substituting these results in Eqs. (99) yields, for $A \neq 0$,

$$a'\cos Av + B'\sin Av = 0$$

$$-a'\sin Av + B'\cos Av = -\frac{2q}{A}\cos v\left[a\cos Av + B\sin Av\right] + \sum_{n=1}^{\infty}\frac{C_n}{A}\sin nv .$$

These equations may be regarded as a pair of non-homogeneous, linear, algebraic equations for the derivatives a' and B' . A non-trivial solution for these derivatives is assured by Cramer's rule provided that the determinant of the coefficients does not vanish. In this case it is clear that

$$\begin{vmatrix} \cos A\nu & \sin A\nu \\ -\sin A\nu & \cos A\nu \end{vmatrix} = 1$$

and hence a solution may be found. The solutions which result after suitable algebraic and trigonometric substitutions are

$$a' = \frac{aq}{4A}\left[\sin(2A+1)\nu + \sin(2A-1)\nu\right] - \frac{\mathcal{B}q}{4A}\left[\cos(2A+1)\nu + \cos(2A-1)\nu - 2\cos\nu\right] + \sum_{n=1}^{\infty}\frac{C_n}{2A}\left[\cos(A+n)\nu - \cos(A-n)\nu\right]$$

$$\mathcal{B}' = -\frac{aq}{4A}\left[\cos(2A+1)\nu + \cos(2A-1)\nu + 2\cos\nu\right] - \frac{\mathcal{B}q}{4A}\left[\sin(2A+1)\nu + \sin(2A-1)\nu\right] + \sum_{n=1}^{\infty}\frac{C_n}{2A}\left[\sin(A+n)\nu - \sin(A-n)\nu\right]. \tag{102}$$

Eqs. (102) are exact at this point, but in order to proceed, it is necessary to perform the integrations to obtain $a(\nu)$ and $\mathcal{B}(\nu)$. Since the quantities a and $\mathcal{B}$ appear on the right-hand sides of these expressions, the integration must involve iteration. If a and $\mathcal{B}$ do not vary rapidly, however, an acceptable first-order approximation may be obtained by integrating Eqs. (102) regarding a and $\mathcal{B}$ as constant and equal to their mean values on the right of these equations. Thus, for $A \neq 0, 1/2$:

$$a - a_0 = -\frac{\bar{a}q}{2A(4A^2-1)}\left[2A(\cos\nu\cos 2A\nu - 1) + \sin\nu\sin 2A\nu\right] + \frac{\bar{\mathcal{B}}q}{2A(4A^2-1)}\left[2A\cos\nu\sin 2A\nu + \sin\nu(4A^2-1 + \cos 2A\nu)\right] + \sum_{n=1}^{\infty}\frac{C_n}{A(A^2-n^2)}\left[A\sin n\nu\cos A\nu - n\cos n\nu\sin A\nu\right] \tag{103}$$

$$\mathcal{B}-\mathcal{B}_0 = -\frac{\bar{a}\,g}{2A(4A^2-1)}\left[2A\cos v\sin 2Av + \sin v\,(4A^2-1-\cos 2Av)\right]$$

$$+\frac{\bar{\mathcal{B}}\,g}{2A(4A^2-1)}\left[2A(\cos v\cos 2Av-1) + \sin v\sin 2Av\right] \qquad (104)$$

$$+\sum_{n=1}^{\infty}\frac{C_n}{A(A^2-n^2)}\left[A\sin nv\sin Av + n\cos nv\cos Av - 1\right]$$

where a_0 and $\mathcal{B}_0$ are the values of these quantities at $v=0$ and where $\bar{a}$ and $\bar{\mathcal{B}}$ denote mean values. Inserting the above results into Eq. (100) and collecting terms, the following first-order approximation results:

$$\bar{\theta} = \left[a_0 - \frac{\bar{a}\,g}{4A^2-1}(\cos v-1) + \frac{2Ag\bar{\mathcal{B}}}{4A^2-1}\sin v\right]\cos Av$$

$$+\left[\mathcal{B}_0 - \frac{\bar{\mathcal{B}}\,g}{4A^2-1}(\cos v+1) - \frac{2Ag\bar{a}}{4A^2-1}\sin v\right]\sin Av \qquad (105)$$

$$+\frac{D_0}{A^2} + \sum_{n=1}^{\infty}\frac{C_n}{A(A^2-n^2)}\left[A\sin nv - n\sin Av\right] .$$

This solution is completed once $\bar{a}$ and $\bar{\mathcal{B}}$ have been determined. Applying the mean value theorem,

$$\bar{a} = \frac{1}{v}\int_0^v a(t)\,dt \quad , \text{ etc.}$$

to Eqs. (103) and (104) with $v = 2N\pi$, $N = 0, 1, 2, \cdots$,

$$\bar{a}\left[1-\frac{g}{4A^2-1}+\frac{g}{4\pi NA}\frac{4A^2+1}{(4A^2-1)^2}\sin 4AN\pi\right]$$

$$=a_0-\frac{\bar{\mathcal{B}}g}{4\pi NA}\frac{4A^2+1}{(4A^2-1)^2}\left[1-\cos 2AN\pi\right]$$

$$-\sum_{n=1}^{\infty}\frac{nC_n}{N\pi(A^2-n^2)^2}\left[1-\cos 2AN\pi\right]$$

$$\bar{\mathcal{B}}\left[1+\frac{g}{4A^2-1}-\frac{g}{4\pi NA}\frac{4A^2+1}{(4A^2-1)^2}\sin 4AN\pi\right]$$

$$=\mathcal{B}_0-\frac{\bar{a}g}{4\pi NA}\frac{4A^2+1}{(4A^2-1)^2}\left[1-\cos 2AN\pi\right]$$

$$-\sum_{n=1}^{\infty}\frac{nC_n}{N\pi(A^2-n^2)^2}\left[\frac{N\pi}{A}(A^2-n^2)-\sin 2AN\pi\right].$$

When $N>>1$, these expressions may be approximated by

$$\bar{a}\left[1-\frac{g}{4A^2-1}\right]\cong a_0$$

$$\bar{\mathcal{B}}\left[1+\frac{g}{4A^2-1}\right]\cong\mathcal{B}_0+\sum_{n=1}^{\infty}\frac{nC_n}{A(n^2-A^2)}\quad . \tag{106}$$

Introducing Eqs. (106) into Eqs. (105), and defining

$$\delta\equiv\frac{g}{4A^2-1}$$

$$a^*\equiv\frac{\bar{\theta}(0)-D_0/A^2}{1-\delta} \tag{107}$$

$$\mathcal{B}^*\equiv\frac{\bar{\theta}'(0)}{A(1+\delta)}$$

there results,

$$\bar{\theta}(v) = \left[a^*(1-\delta\cos v) + 2A\mathcal{B}^*\delta\sin v\right]\cos Av$$

$$+\left[\mathcal{B}^*(1-\delta\cos v) - 2Aa^*\delta\sin v\right]\sin Av$$

$$+\frac{D_0}{A^2} + \sum_{n=1}^{\infty}\frac{C_n}{A(A^2-n^2)}\left[A\sin nv - \frac{n}{1+\delta}\sin Av\right] \tag{108}$$

$$-\sum_{n=1}^{\infty}\frac{n\delta C_n}{A(A^2-n^2)(1+\delta)}\left[2A\sin v\cos Av - \cos v\sin Av\right].$$

For the range of eccentricities for which Eq. (108) is expected to reasonably approximate the actual solution, the last summation should be negligible compared to the first summation. Moreover, since products of the form δC_n should be negligible compared to C_n, Eq. (108) may be approximated by

$$\bar{\theta}(v) \cong \left[a^*(1-\delta\cos v) + 2A\mathcal{B}^*\delta\sin v\right]\cos Av$$

$$+\left[\mathcal{B}^*(1-\delta\cos v) - 2Aa^*\delta\sin v\right]\sin Av \tag{109}$$

$$+\frac{D_0}{A^2} + \sum_{n=1}^{\infty}\frac{C_n}{A(A^2-n^2)}\left[A\sin nv - \frac{n}{1+\delta}\sin Av\right].$$

In the notation of Section 5.3, the solutions $\bar{\theta}_0$, $\bar{\theta}_1$ and $\bar{\theta}_2$ are found to be:

$$\bar{\theta}_1(v) = \left[\frac{1-\delta\cos v}{1-\delta}\right]\cos Av - \left[\frac{2A\delta}{1-\delta}\right]\sin v\sin Av \tag{110}$$

$$\bar{\theta}_2(v) = \left[\frac{2\delta}{1+\delta}\right]\sin v\cos Av + \left[\frac{1-\delta\cos v}{A(1+\delta)}\right]\sin Av$$

$$\bar{\theta}_0(\nu) = \frac{D_0}{A^2}(1 - \cos A\nu) + \sum_{n=1}^{\infty} \frac{C_n}{A(A^2-n^2)}\left[A \sin n\nu - n \sin A\nu\right] \quad \begin{matrix}(110)\\(\text{cont.})\end{matrix}$$

where second order terms have been neglected in composing $\bar{\theta}_0$. The homogeneous solutions obtained in Eq. (110) correspond to the first order solution to the Mathieu equation obtained by Struble and Fletcher (Ref. 35) using a modified variation of parameters approach. In addition, for the dumbbell satellite, the solution $\bar{\theta}_0(\nu)$ becomes

$$\bar{\theta}_0(\nu) = \epsilon\left[\frac{1}{\sqrt{3}} \sin\sqrt{3}\nu - \sin\nu\right] \qquad (111)$$

which has also been obtained by Frick and Garber (Ref. 28).

Eqs. (110) have been compared with the corresponding solutions determined by direct numeric integration of the "exact" equation of the pitching motion. Two cases are examined: the gravity gradient stabilized dumbbell satellite and a body with $\Gamma = 0.1$, $M = 1$ and $\Gamma_2 = 0$ orbiting at 200 mile perigee altitude. The results are presented in Figs. 28 and 29 respectively, for small eccentricity orbits.

Fig. 28 shows that the approximate analytical results accurately reproduce the numeric computations for the dumbbell satellite. As shown by Frick and Garber (Ref. 28), the solution $\bar{\theta}_0(\nu)$ given by Eq. (111) for the dumbbell satellite is a good approximation for eccentricities as high as one-tenth, and hence the results presented here merely confirm this earlier work. When aerodynamic torques are present, however, the situation is complicated by the appearance of an infinite series in $\bar{\theta}_0$. For the particular conditions used for Fig. 29, satisfactory convergence was obtained by using only the first three terms in $\bar{\theta}_0$ and in general, five to six terms should be adequate for even the largest eccentricities of interest. Note from Fig. 29(b) that although θ_1 and θ_2 are duplicated rather well by the approximate solution, θ_0 shows a significant deviation from the exact results.

In general, the agreement between the approximate and exact results appears sufficiently good so that Eqs. (110) may be used to estimate the effects of orbital eccentricity on the vehicle's librations, at least for small values of ϵ . It must be noted, however, that the values $A = 0, 1/2, 1$ are excluded from consideration since Eqs. (110) become singular for these values. Accordingly, for an investigation of the nature of the motion near the stability boundaries, numeric integration appears required.

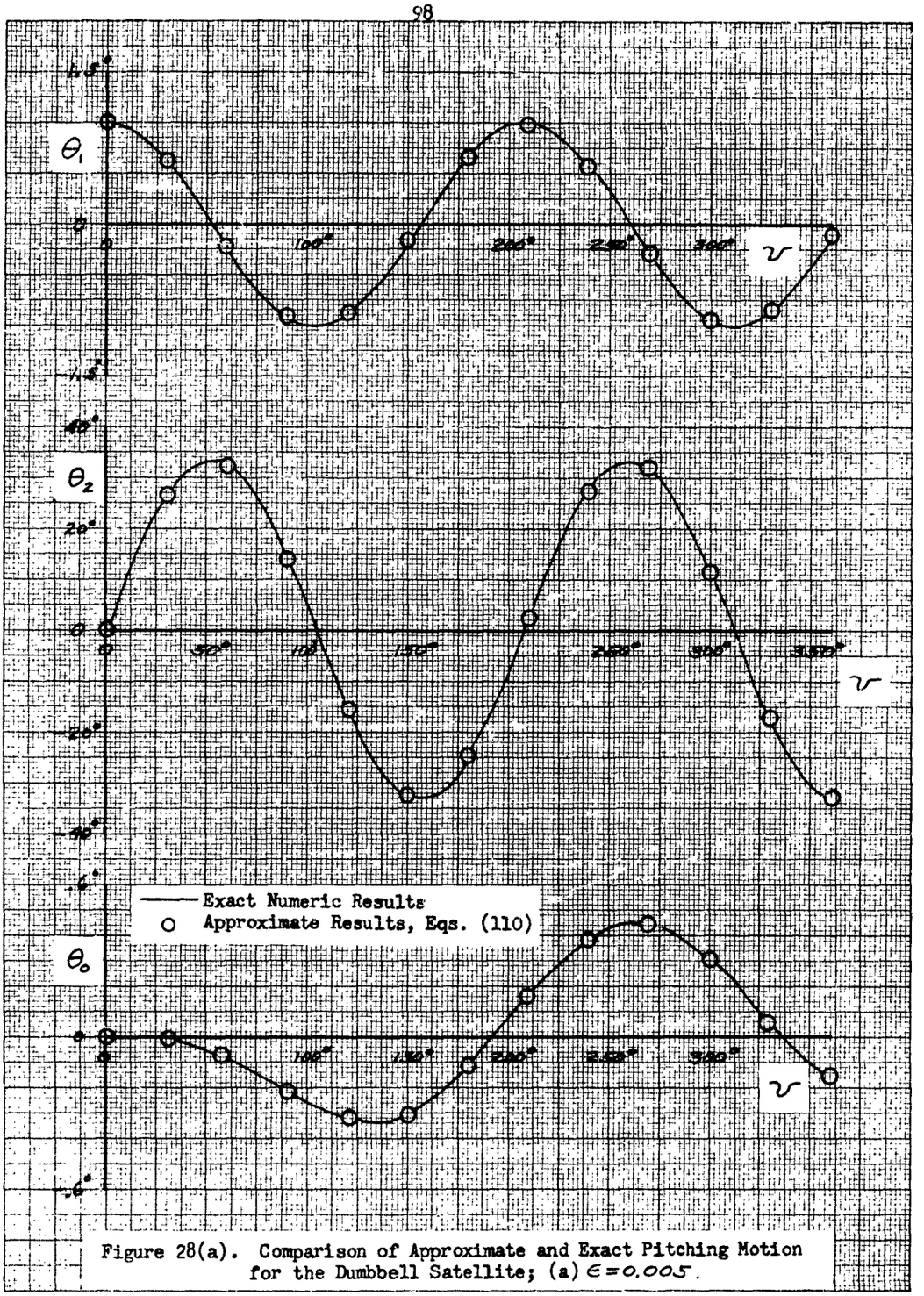

Figure 28(a). Comparison of Approximate and Exact Pitching Motion for the Dumbbell Satellite; (a) $\epsilon = 0.005$.

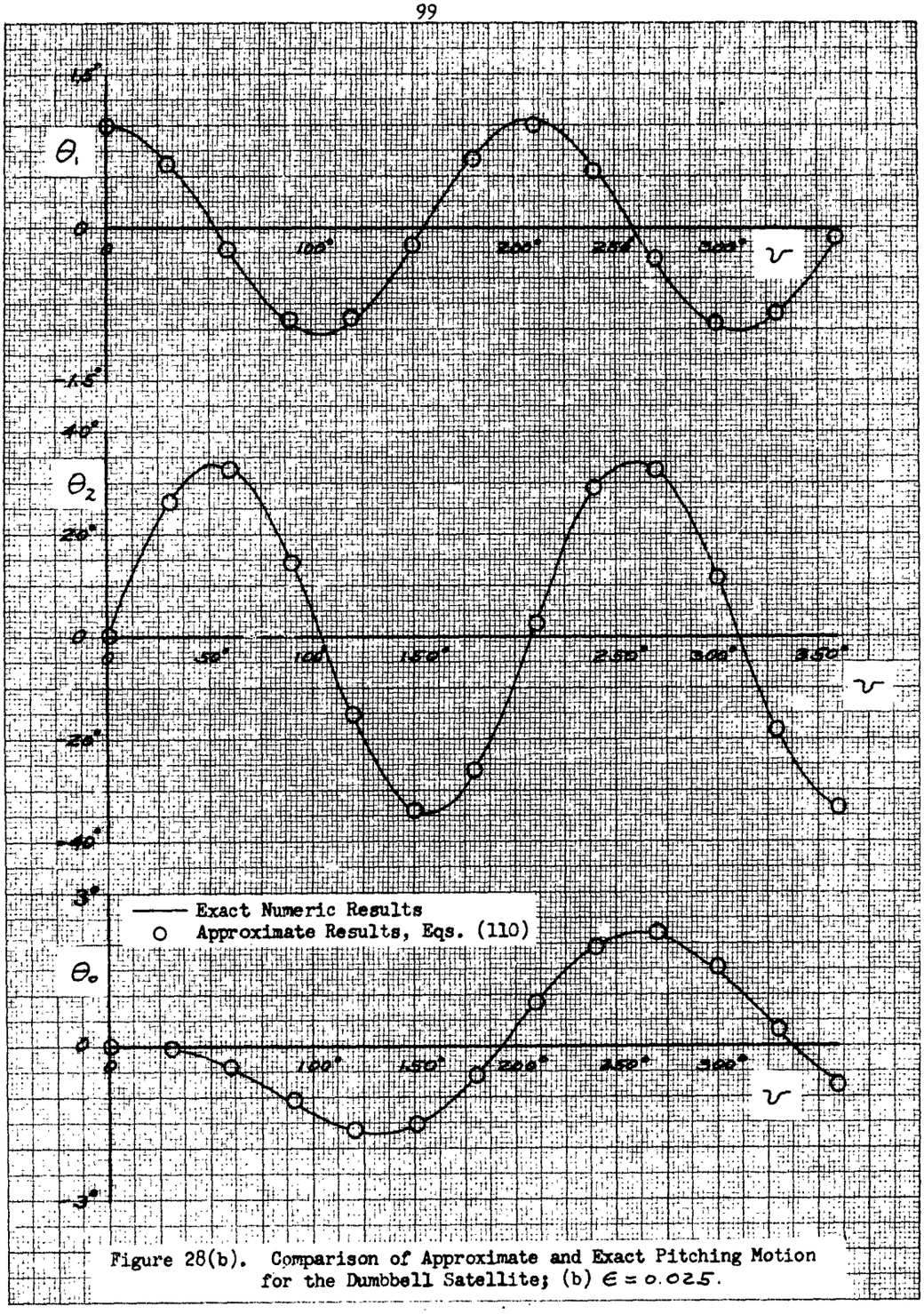

Figure 28(b). Comparison of Approximate and Exact Pitching Motion for the Dumbbell Satellite; (b) $\epsilon = 0.025$.

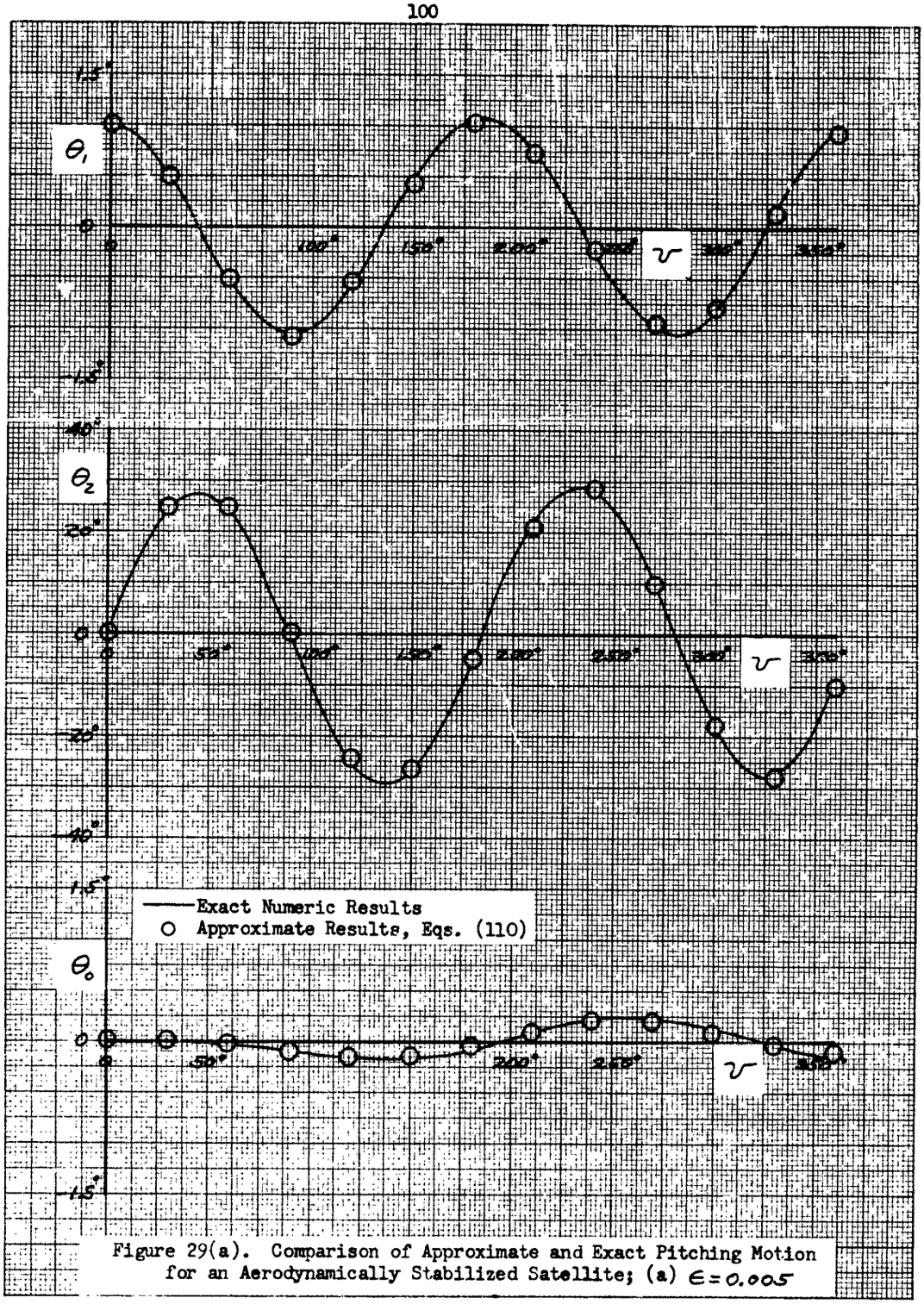

Figure 29(a). Comparison of Approximate and Exact Pitching Motion for an Aerodynamically Stabilized Satellite; (a) $\epsilon = 0.005$

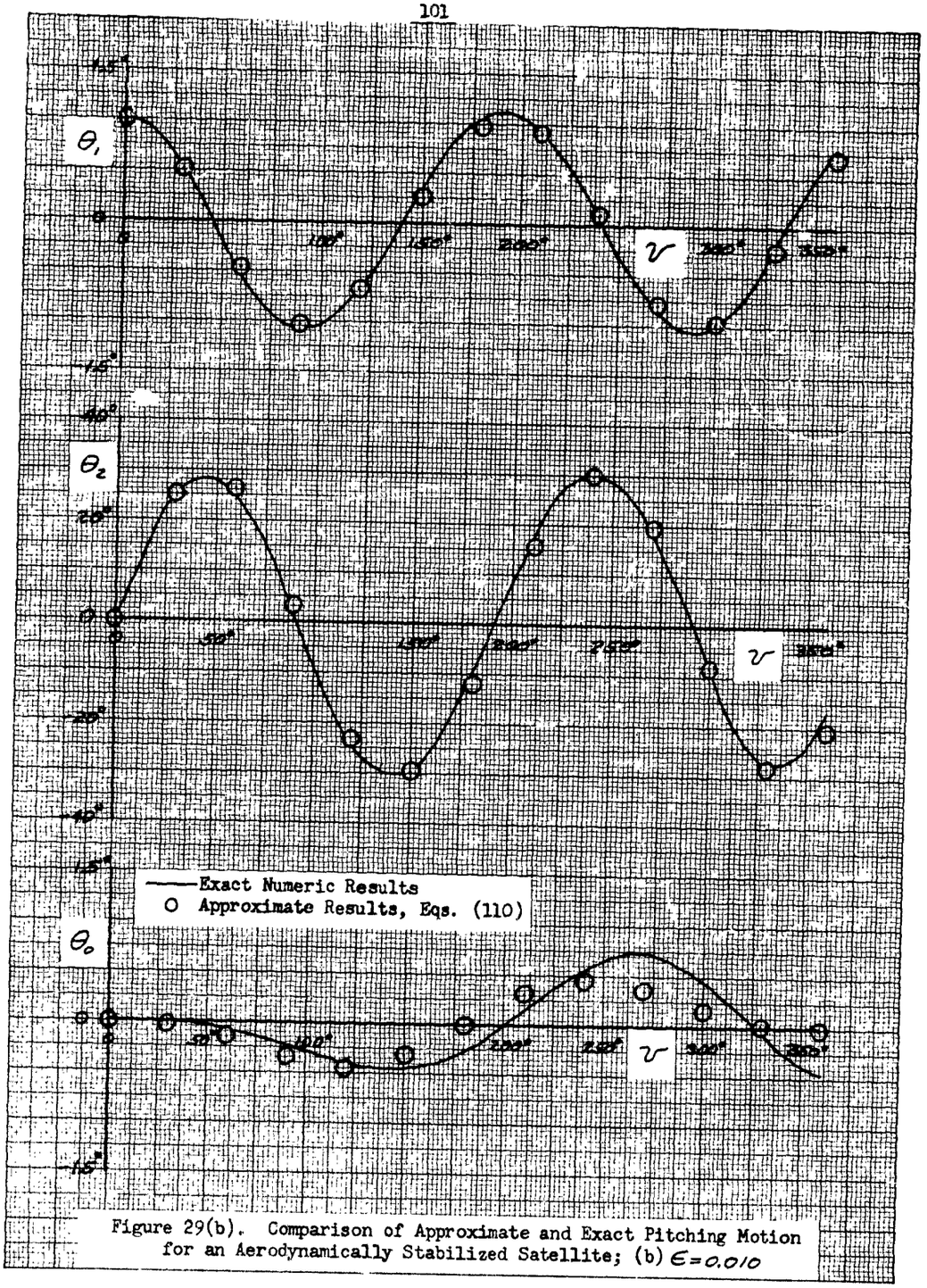

Figure 29(b). Comparison of Approximate and Exact Pitching Motion for an Aerodynamically Stabilized Satellite; (b) $\epsilon = 0.010$

5.5 Numerical Results

5.5.1 General

The purpose of this portion of the study is to determine the nature of the satellite's pitching motion on a slightly eccentric orbit when aerodynamic and gravitational torques act. The form of the governing differential equation suggests that the paramount question to be answered is whether or not the regions of instability suspected to be imbedded in the region of satellite motion do, in fact, exist and whether or not these regions actually destabilize the vehicle. In Sections 5.2 and 5.3, the analytic solution of the pitching equation is discussed and a stability diagram, Fig. 27, is presented, showing that for λ small and/or σ_p^* large, stable motion is to be expected, while for λ large and/or σ_p^* small, unstable motion will generally predominate.

Inasmuch as this analytical treatment relies on a number of assumptions about the relative magnitudes of the various factors appearing in the complete equation, one objective of the numerical analysis is to verify the existence of stability boundaries at least qualitatively similar to those presented in Fig. 27. Moreover, the numerical analysis is also intended to substantiate the assumptions and order-of-magnitude arguments made in arriving at the approximate equations of motion. Finally, the numerical analysis must give a clear picture of the satellite's angular oscillations as a function of time and/or position on the orbit, so that frequencies, amplitudes, required initial conditions, etc., may be determined.

It may be asked at the outset if it is possible to determine the boundedness of the motion for all time from a detailed integration of the differential equation over one orbit. The results of an analysis of second-order, non-homogeneous, linear differential equations with periodic coefficients (Ref. 2) indicate that such a determination is generally possible. This analysis also reveals several parameters which may be calculated specifically for this purpose.

The results presented in this section are based upon the direct numeric integration of the "exact" equation of pitching motion, determined in Section 3.1. Inasmuch as Ref. 2 contains all of the details relative to the IBM 704 computer program used for this purpose, only the essential elements are discussed here.

The basic differential equation which is solved is the second of Eqs. (46) presented in Section 3.1. This equation is

$$\frac{d^2\theta}{dv^2} + 2Q\frac{d\theta}{dv} + \left\{3M\left[1 - \epsilon\cos v\right] + P\right\}\theta = 2Q + \gamma P \qquad (112)$$

where

$$p = \rho_p \left(\frac{\rho}{\rho_p}\right)\left(\frac{V_R}{V}\right)^2 \left[1 + 2\epsilon(1-\cos\upsilon)\right]$$

$$2Q = 2\,2_p \left(\frac{\rho}{\rho_p}\right)\frac{V_R}{V}\left[1 + \epsilon(1-\cos\upsilon)\right] - 2\epsilon\sin\upsilon$$

$$\gamma = \frac{\epsilon \sin\upsilon}{1 + \epsilon\cos\upsilon} \qquad (113)$$

$$\frac{V_R}{V} \cong 1 - \frac{\omega_a}{\dot{\upsilon}_p}\cos\iota$$

$$\dot{\upsilon}_p = \frac{\sqrt{\mu(1+\epsilon)}}{r_p^{3/2}} \quad .$$

The following geophysical constants are employed:

$$\mu = 1.407{,}697{,}7 \times 10^{16} \text{ feet}^3/\text{sec}^2$$

$$a_E = r_E = 20{,}902{,}131 \text{ feet}^{(3)}$$

$$\omega_a = \omega_E = 7.292{,}115{,}1 \times 10^{-5} \text{ radians/sec.}$$

and the atmospheric density variation is taken from the 1959 ARDC (Minzner) atmosphere (Ref. 26).

The computer program generates the three solutions to the exact pitching equation θ_0, θ_1 and θ_2 (see Section 5.3) as functions of υ from $\upsilon = 0$ to $\upsilon = 2\pi$. In addition, the constants α and β associated with the unique periodic solution are computed for those cases where $(I - W)$ is non-singular. These constants, or weights, may be interpreted as the initial conditions which are required in order that the motion be precisely periodic and, therefore, bounded. An upper bound on the amplitude is also computed for each orbit.

The basic variables under study are the configuration parameters Γ, Γ_g, M and the orbit parameters (or elements) h_p, ϵ and ι. For the purposes of comparison, a wide range of these parameters are investigated in various combinations using the digital computer program described above. A small analog computer mechanization is also employed for check purposes. The results of these studies are described below.

5.5.2 Discussion of Results

5.5.2.1 Range of Variables

The six significant parameters enumerated above were studied over the following ranges:

$0 \leq \Gamma \leq 100$ ft/slug $\qquad 0 \leq \epsilon \leq 0.025$

$0 \leq \Gamma_\zeta \leq 1000$ ft^2/slug $\qquad 125 \leq h_p \leq 400$ statute miles

$-1 \leq M \leq 1$ $\qquad 0 \leq \iota \leq 90°$

The separate effects of these variables are discussed in the following sections.

5.5.2.2 Effects of Aerodynamic Damping

In Section 4.3, dealing with the circular orbit results, it is shown that the aerodynamic damping has an insignificant effect on the vehicle's angular oscillations. In the current numeric investigation, values of Γ_ζ up to 100 fail to show any effect whatever on the angular motion on the circular or eccentric orbits[1]. Analog computer results likewise reveal no appreciable effect of aerodynamic damping at altitudes as low as 100 miles and values of Γ_ζ up to 1,000.

These calculations indicate that the analytical estimates of the time-to-damp to half-amplitude (see Appendix C) and the order of magnitude arguments of Section 3.3 are substantially correct. Accordingly, it is concluded that the aerodynamic damping has essentially no direct effect on the vehicle's angular motion, at least during the time interval for which the orbit elements may be regarded as constants. The presence of even a small positive damping term, however, indicates that the motion cannot grow without bound, although the amplitude may become excessively large. For the purpose of examining the pitching motion further, the aerodynamic damping will be taken as zero. This allows the vehicle to be characterized by the two configuration parameters Γ and M.

5.5.2.3 Effects of Orbit Inclination

The effects of orbit inclination have been discussed briefly in Section 4.3. Inasmuch as the atmosphere has been assumed spherically symmetric for this work, the entire effect of ι is taken into account in

---

[1] In this case results for $\Gamma_\zeta = 0$ and $\Gamma_\zeta = 100$ agreed through the four decimal places printed.

the term V_R/V. For a given value of ζ, this term may be regarded as only slightly altering the values of Γ and Γ_g and accordingly, no numeric results are presented for this portion of the study.

While the neglected oblateness of the atmosphere produces no major direct effect on the motion, it does introduce a second harmonic in the density variation; this harmonic having period π rather than period 2π. Thus, even in a circular orbit, the governing equation for the pitching motion becomes of the Hill type, and in view of the analysis of Sections 5.2 and 5.3, unstable conditions may exist for this case. This problem appears to require further study.

5.5.2.4 Effects of Initial Conditions

The constants $\mathcal{A}$ and $\mathcal{B}$, determined from Section 5.3, may be associated directly with the initial conditions of the motion and indicate the importance of the initial conditions in composing the periodic particular solution of the equation of motion. The results of the numeric calculations show the solution corresponding to θ_1 (that solution of the homogeneous equation which has $\theta_1(0) = 1$, $\theta_1'(0) = 0$) to be given an extremely small weight; essentially zero. As shown in Ref. 2, θ_p must be an odd function whenever $\Gamma_g \equiv 0$ and so θ_p will be principally odd for small, non-zero, values of Γ_g. It is clear that if the periodic particular solution contains θ_1 with a non-vanishing weight, then it cannot be odd. Thus θ_1 should be formally absent from θ_p for $\Gamma_g \equiv 0$

5.5.2.5 Effects of Remaining Parameters

The parameters Γ and M influence the motion in essentially the same way and their effects cannot be separated. Similarly, the effects of h_p and ϵ are most conveniently treated together.

Figs. 30 and 31 illustrate the behavior of the pitching motion on the elliptical orbit ($\epsilon = 0.015$) at 400 miles perigee altitude when Γ or M or both are permitted to vary. For Fig. 30, only a very small amount of aerodynamic stability is present; $\Gamma = 0.10$. Fig. 30(a) shows the solutions for $M = 0$ and Fig. 30(b) shows the results when $M = 1$. In this case, the significant effect of M on the amplitude and frequency of the oscillations is easily seen. For Figs. 31(a) and (b), on the other hand, a large aerodynamic stability margin is present, with $\Gamma = 100$. Again Fig. 31(a) shows the results for $M = 0$ while Fig. 31(b) presents the solutions for $M = 1$. In this case the effect of M is substantially reduced. This general behavior characterizes the interplay between Γ and M throughout the altitude and eccentricity range, although at lower altitudes, the potential effect of M is greatly reduced while at higher altitudes, the effects of even large values of Γ may be readily transcended by M. These results are in general agreement with the circular orbit results of Section 4.3.

Figs. 32(a) through 32(g) illustrate the typical effect of increasing eccentricity while holding the perigee altitude and all of the vehicle parameters constant. As expected, the increased eccentricity both increases the amplitude and lengthens the period. For the particular set of parameters chosen for this example, an unstable condition is encountered between $\epsilon = 0.002$ and $\epsilon = 0.003$. Further discussion of these unstable regions is presented in the following section.

5.5.2.6 Stability of the Motion

The numeric integration has confirmed the existence of stability boundaries similar to those presented in Fig. 27. The qualitative behavior of the vehicle as it passes through these regions of stability and instability during the course of its orbit decay is described in Section 5.3 and need not be repeated here. However, it is of interest to note that the length of time the vehicle may dwell in an unstable region without catastrophic amplitude build-up depends upon the matrix W of Section 5.3 and upon the amount of deviation from the periodic particular solution associated with the orbital conditions (Ref. 2).

In order to illustrate quantitatively the behavior of the motion when an unstable region is entered, Figs. 33(a) through 33(c) have been constructed showing three complete revolutions of a satellite on its orbit for each of three orbital eccentricities, all other orbit and vehicle parameters being held constant. In each figure, the dotted curve represents the purely periodic particular solution, while the solid curve represents the motion corresponding to a 2° initial misalignment of the vehicle. The three eccentricities could well be encountered by a satellite as the orbit decays due to aerodynamic drag.

In Fig. 33(a), $\epsilon = 0.025$, the motion is stable and the solution corresponding to the initial 2° misalignment merely oscillates about the periodic particular solution. Fig. 33(b), however, is the same vehicle at an eccentricity of $\epsilon = 0.020$, which lies in one of the unstable regions. It is noted that in slightly more than two revolutions, the amplitude has built up to the point where the vehicle will certainly begin to tumble. In Fig. 33(c), however, the unstable region has been passed and the motion is again stable. Upon comparing the solutions for the first half revolution in all three cases, it is seen that they appear very similar, which might lead to the incorrect conclusion that the motion for $\epsilon = 0.020$ would be substantially the same as for $\epsilon = 0.025$ or $\epsilon = 0.015$. Moreover, the periodic particular solutions appear quite similar for the three cases.

Since the passive oscillations of any vehicle permit it to have an infinity of possible initial conditions upon entry into an unstable region, it is clear that the behavior of the motion shown in Figs. 33 must be regarded as typical. Thus, the situation resolves to the point where passive stabilization of artificial satellites depends upon the rate at

which the oscillations grow when unstable conditions are encountered during the orbit decay. These unstable regions will be encountered even by gravity gradient stabilized satellites of non-spherical shape since solar and aerodynamic effects produce a changing center of pressure which, in general, will not coincide with the vehicle's mass center. The situation can be improved by designing the vehicle for the maximum aerodynamic stability possible (see Fig. 27), but the isolated unstable regions still exist, and must be considered.

In general, the design of a passively stabilized satellite will require precise knowledge of the desired orbit, and the anticipated orbit decay. The stability boundaries for the complete problem must then be determined in a form similar to Fig. 27. The external shape ($\mathcal{P}_p^*$) and internal mass distribution (M) of the vehicle may then be decided upon such that the vehicle spends its useful lifetime in a stable region. An alternative is the use of active attitude control systems which may shorten the vehicle's useable lifetime or compromise some of its other functions.

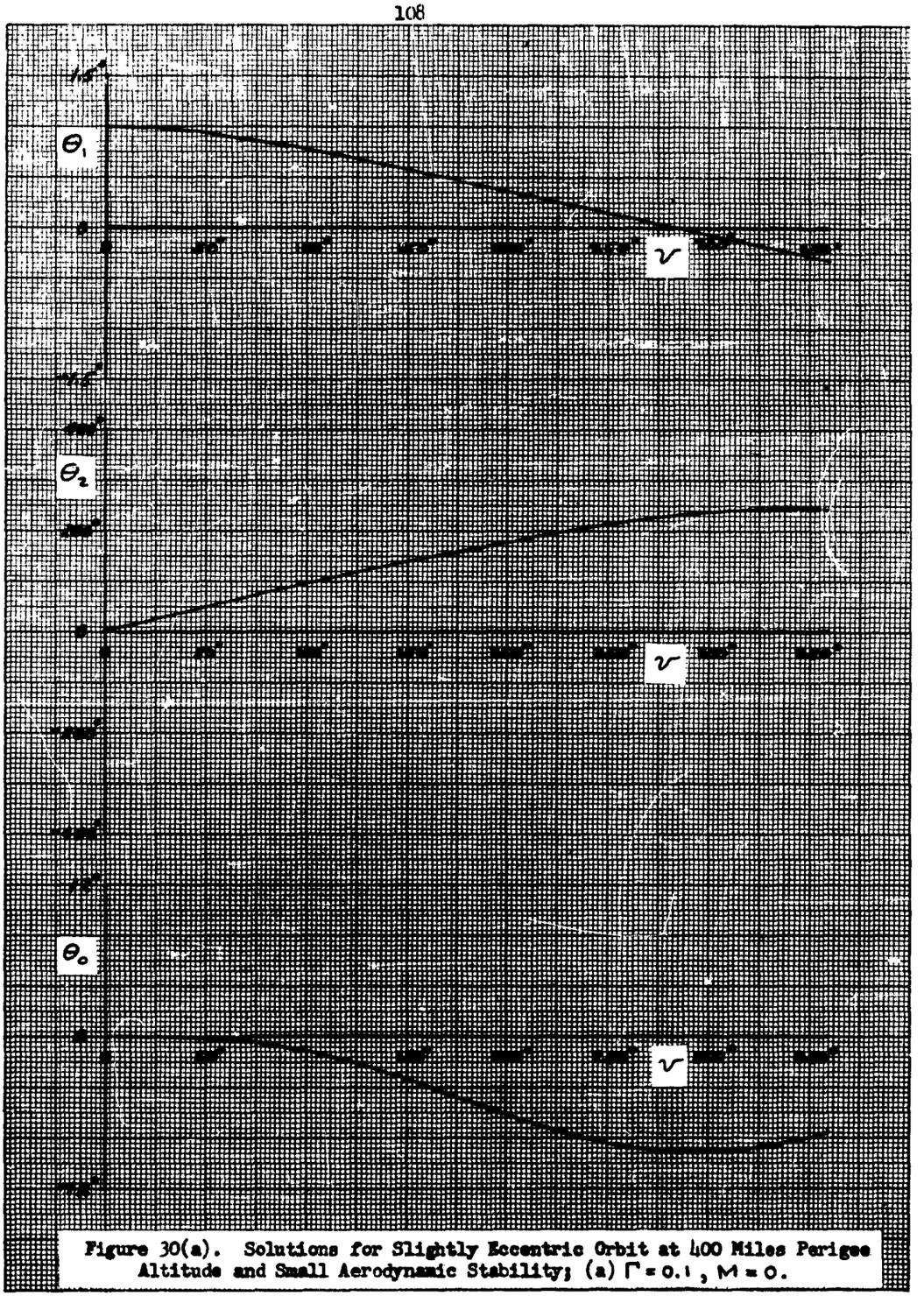

Figure 30(a). Solutions for Slightly Eccentric Orbit at 400 Miles Perigee Altitude and Small Aerodynamic Stability; (a) $\Gamma = 0.1$, $M = 0$.

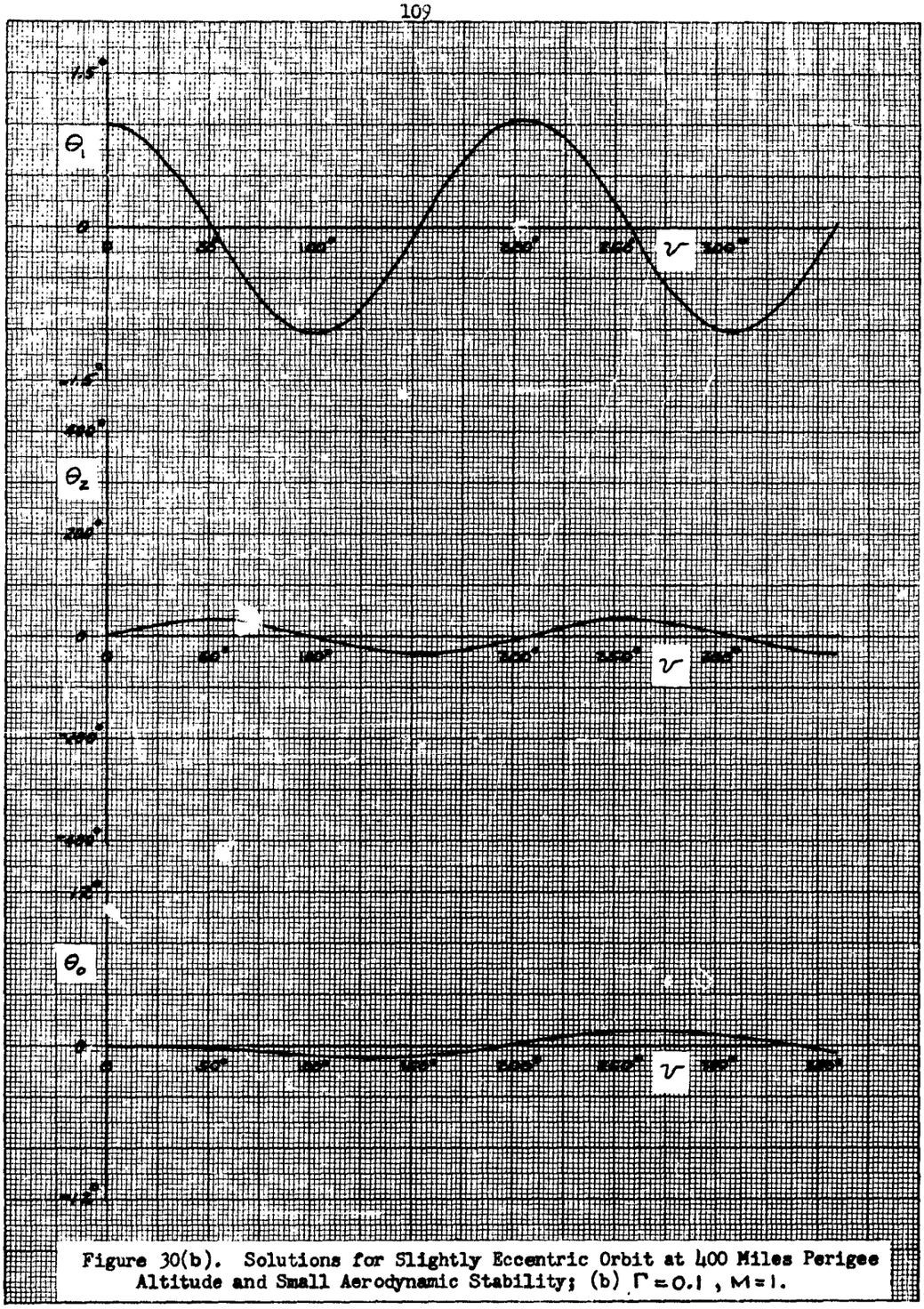

Figure 30(b). Solutions for Slightly Eccentric Orbit at 400 Miles Perigee Altitude and Small Aerodynamic Stability; (b) $\Gamma = 0.1$, $M = 1$.

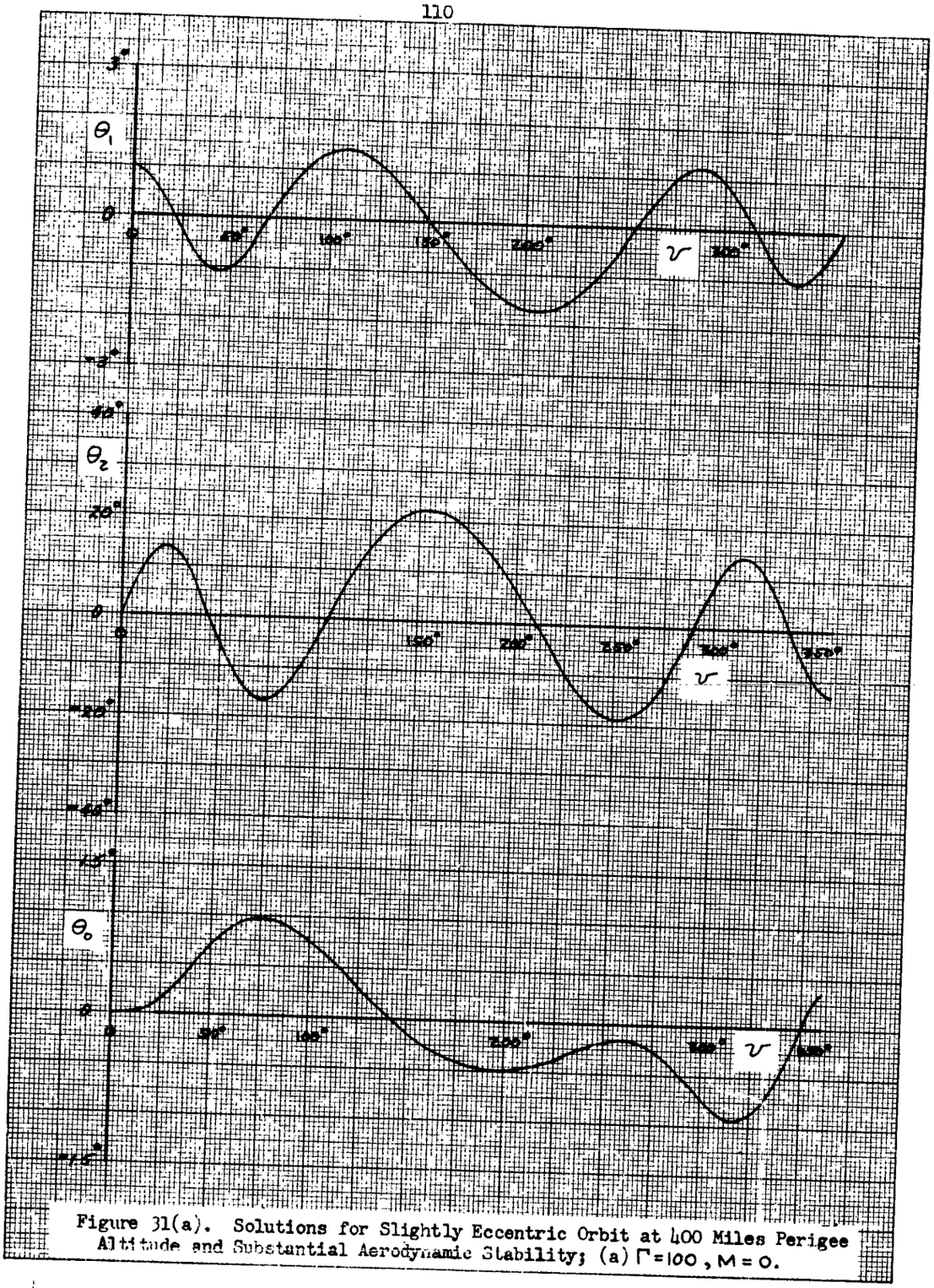

Figure 31(a). Solutions for Slightly Eccentric Orbit at 400 Miles Perigee Altitude and Substantial Aerodynamic Stability; (a) $\Gamma = 100$, $M = 0$.

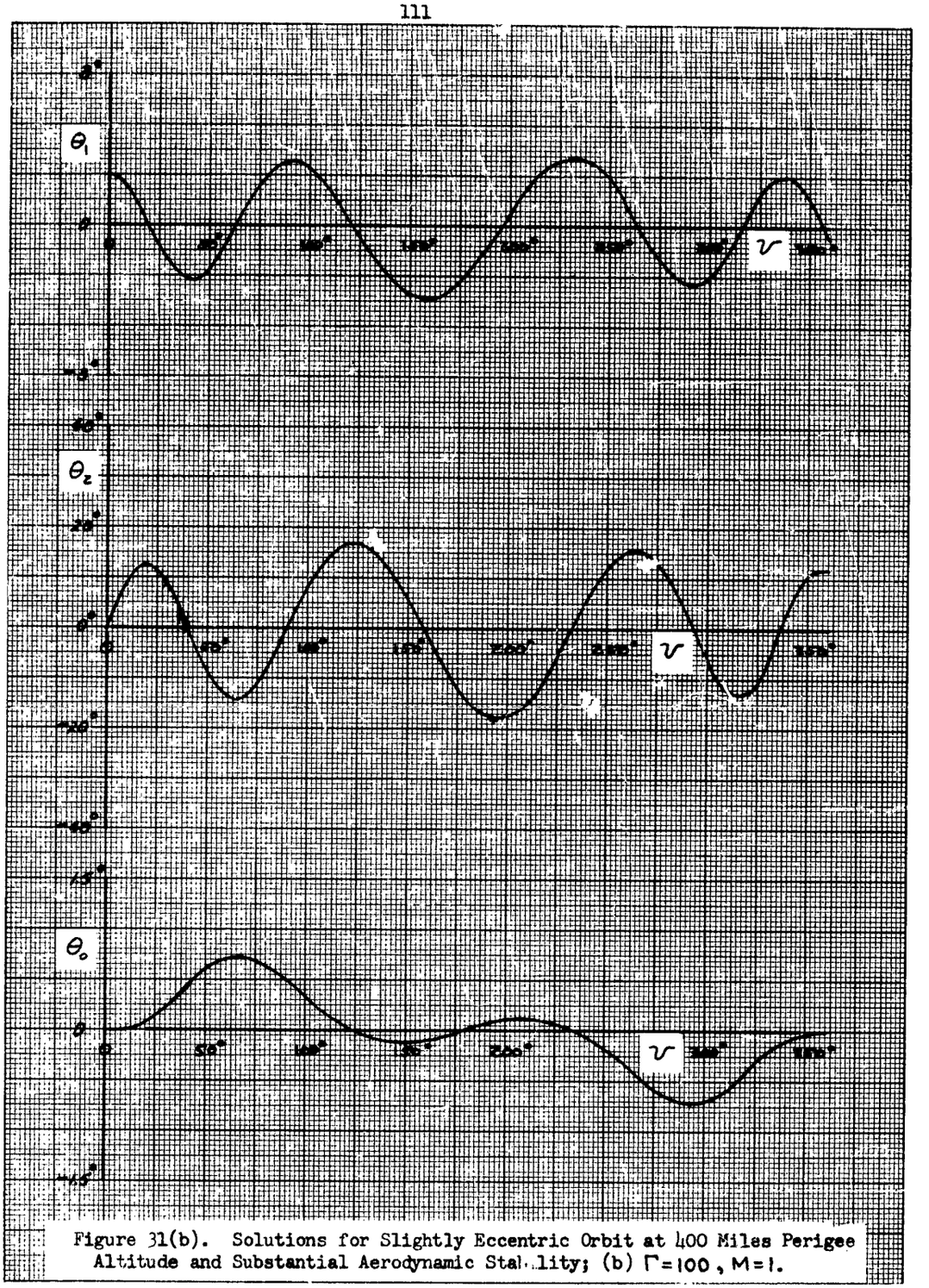

Figure 31(b). Solutions for Slightly Eccentric Orbit at 400 Miles Perigee Altitude and Substantial Aerodynamic Stability; (b) $\Gamma = 100$, $M = 1$.

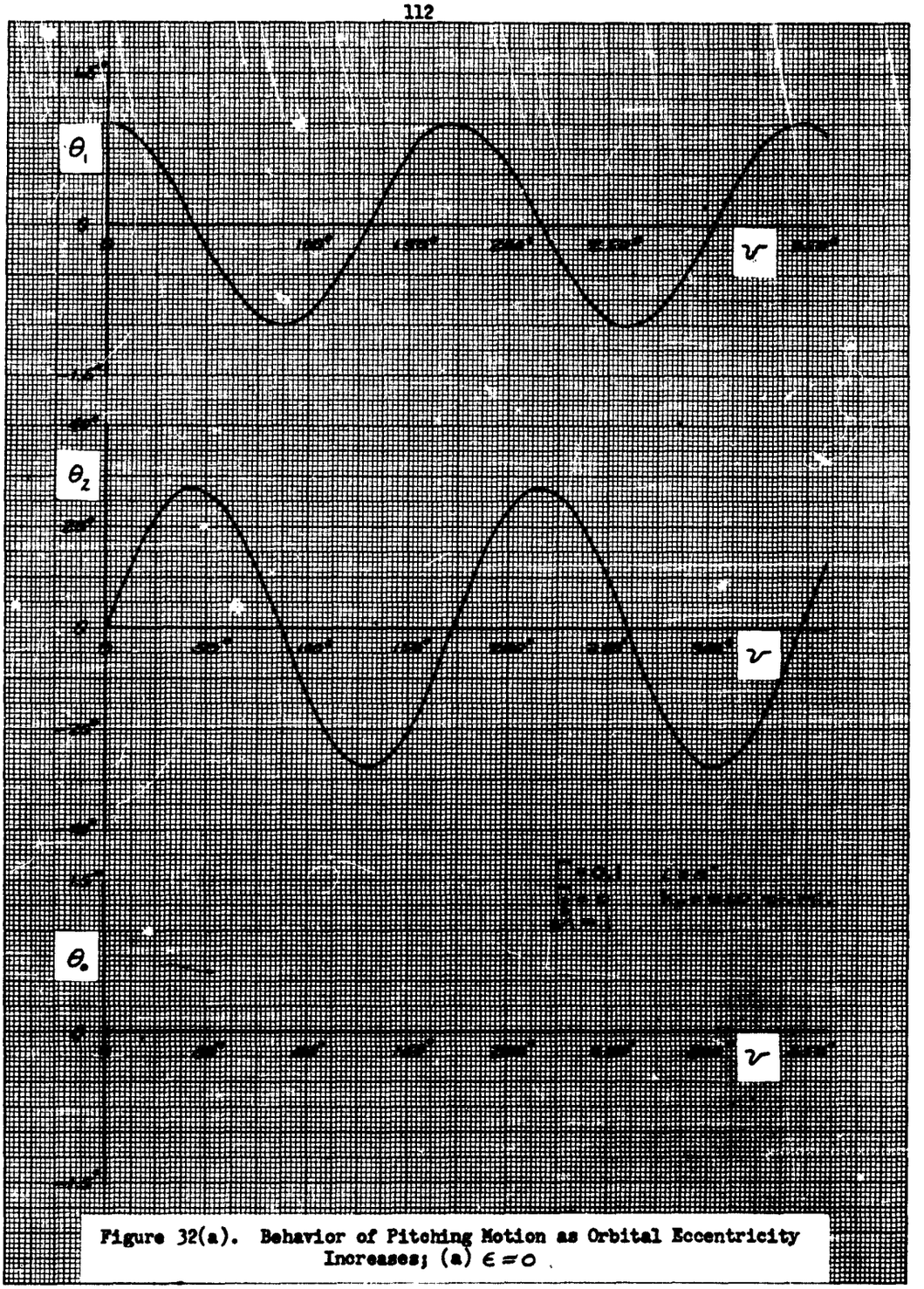

Figure 32(a). Behavior of Pitching Motion as Orbital Eccentricity Increases; (a) $\epsilon = 0$

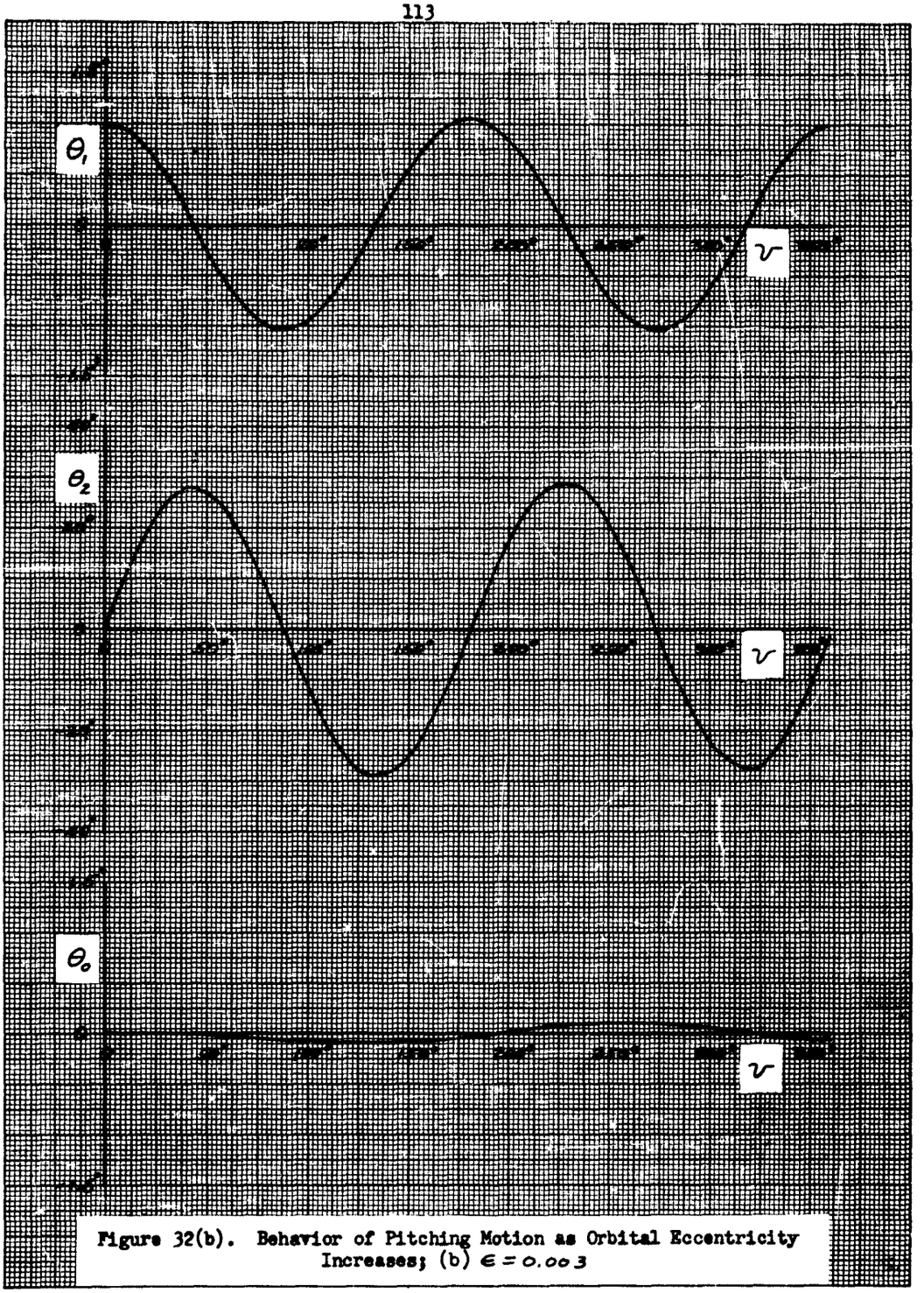

Figure 32(b). Behavior of Pitching Motion as Orbital Eccentricity Increases; (b) $\epsilon = 0.003$

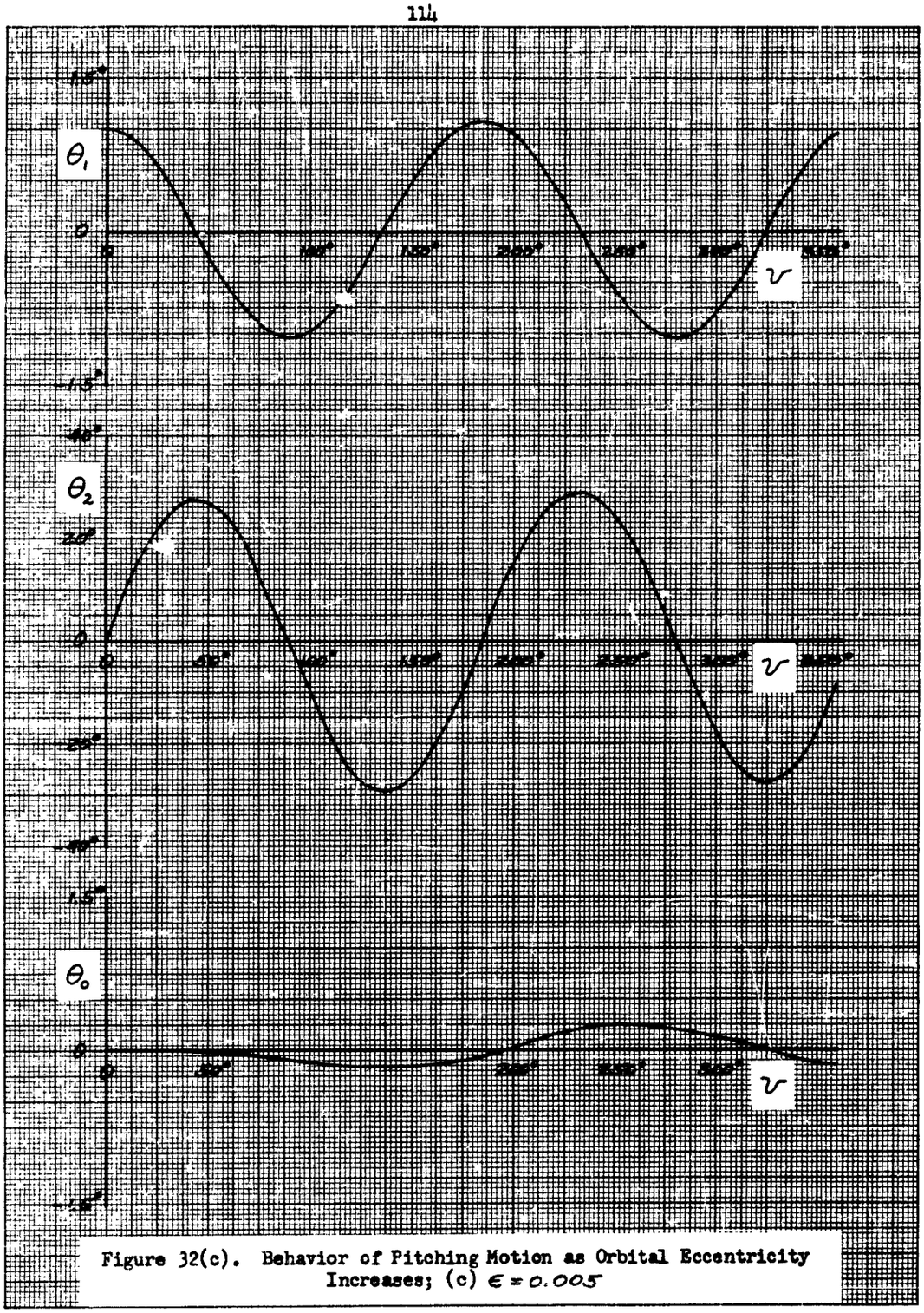

Figure 32(c). Behavior of Pitching Motion as Orbital Eccentricity Increases; (c) $\epsilon = 0.005$

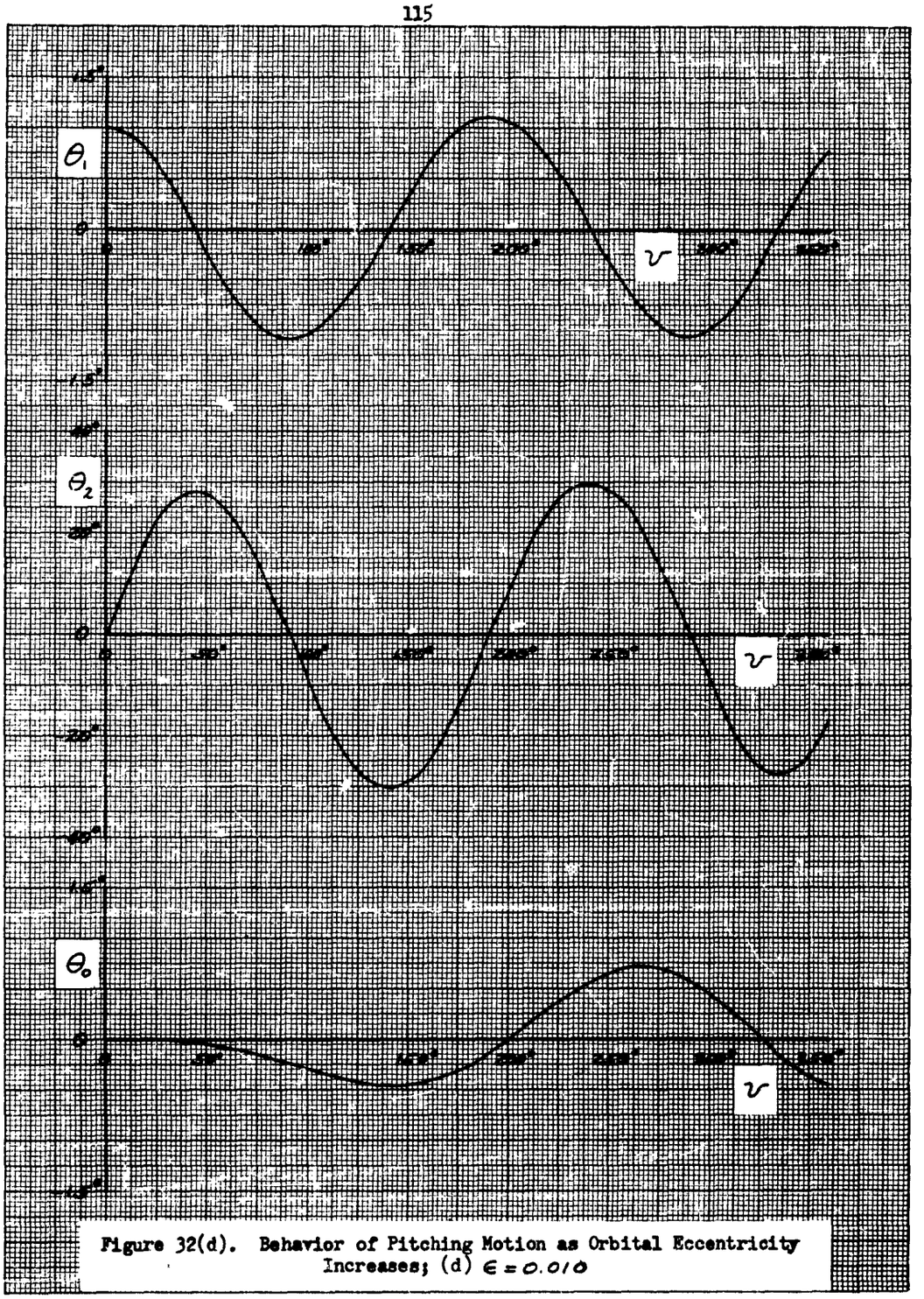

Figure 32(d). Behavior of Pitching Motion as Orbital Eccentricity Increases; (d) $\epsilon = 0.010$

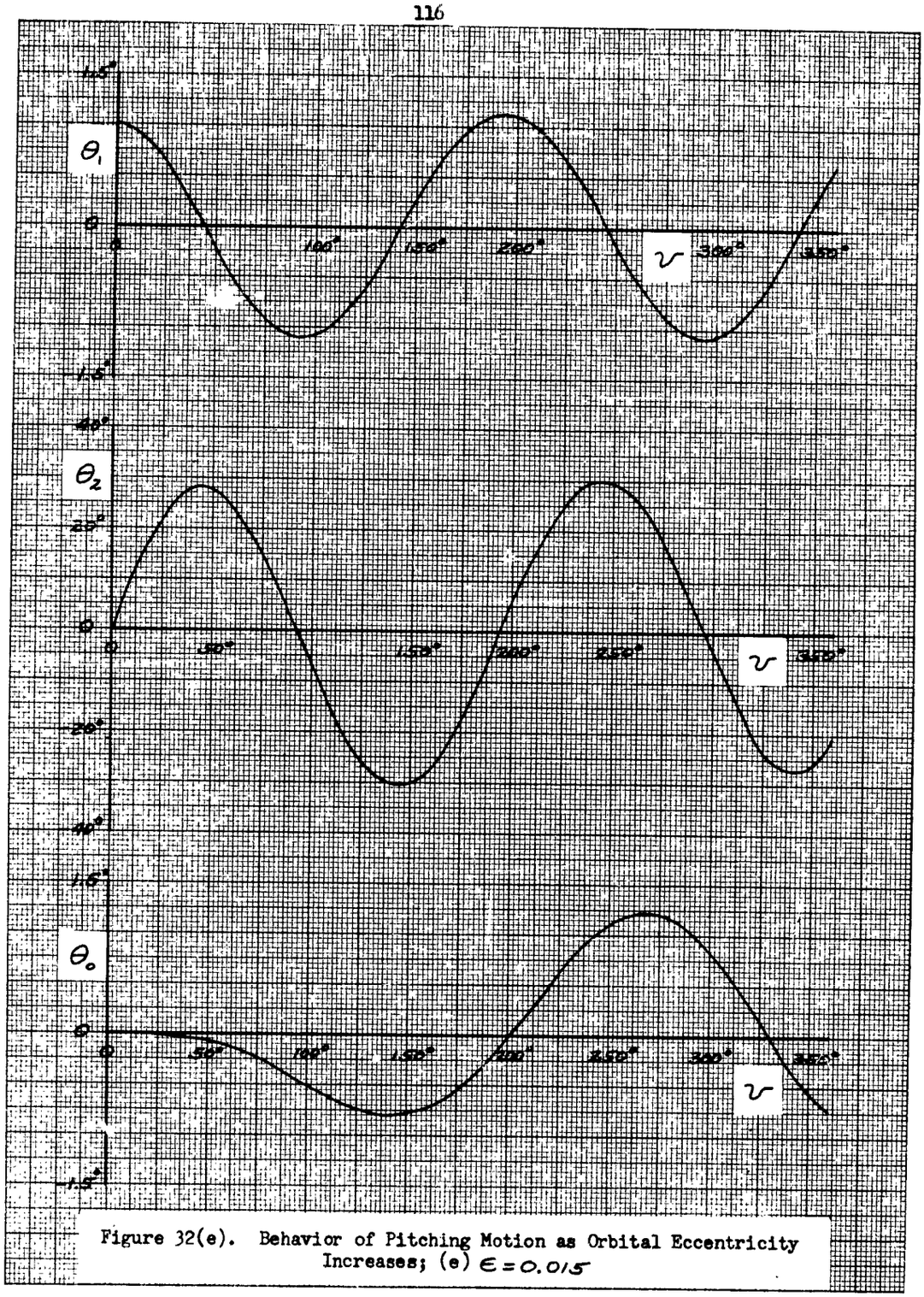

Figure 32(e). Behavior of Pitching Motion as Orbital Eccentricity Increases; (e) $\epsilon = 0.015$

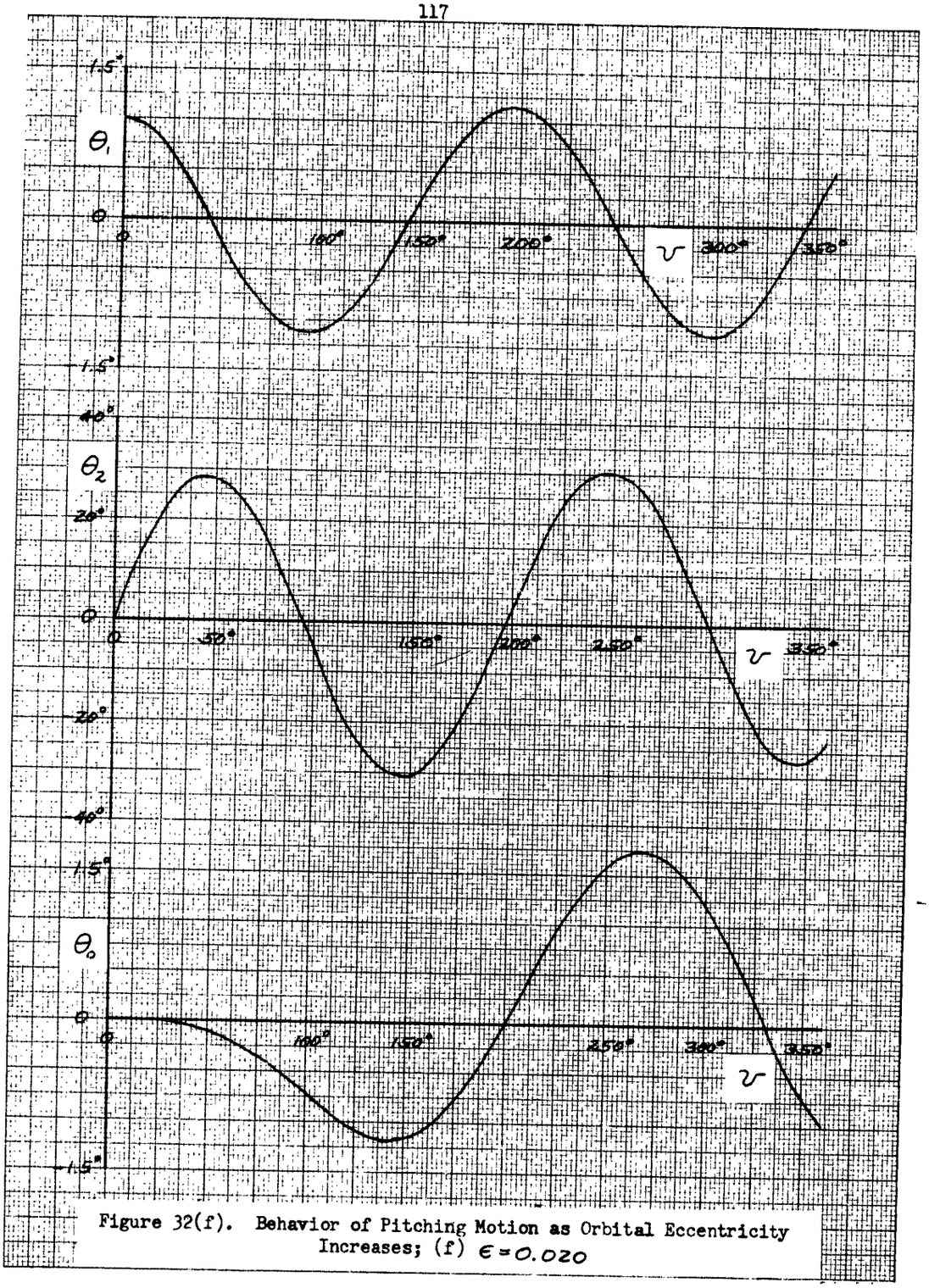

Figure 32(f). Behavior of Pitching Motion as Orbital Eccentricity Increases; (f) $\epsilon = 0.020$

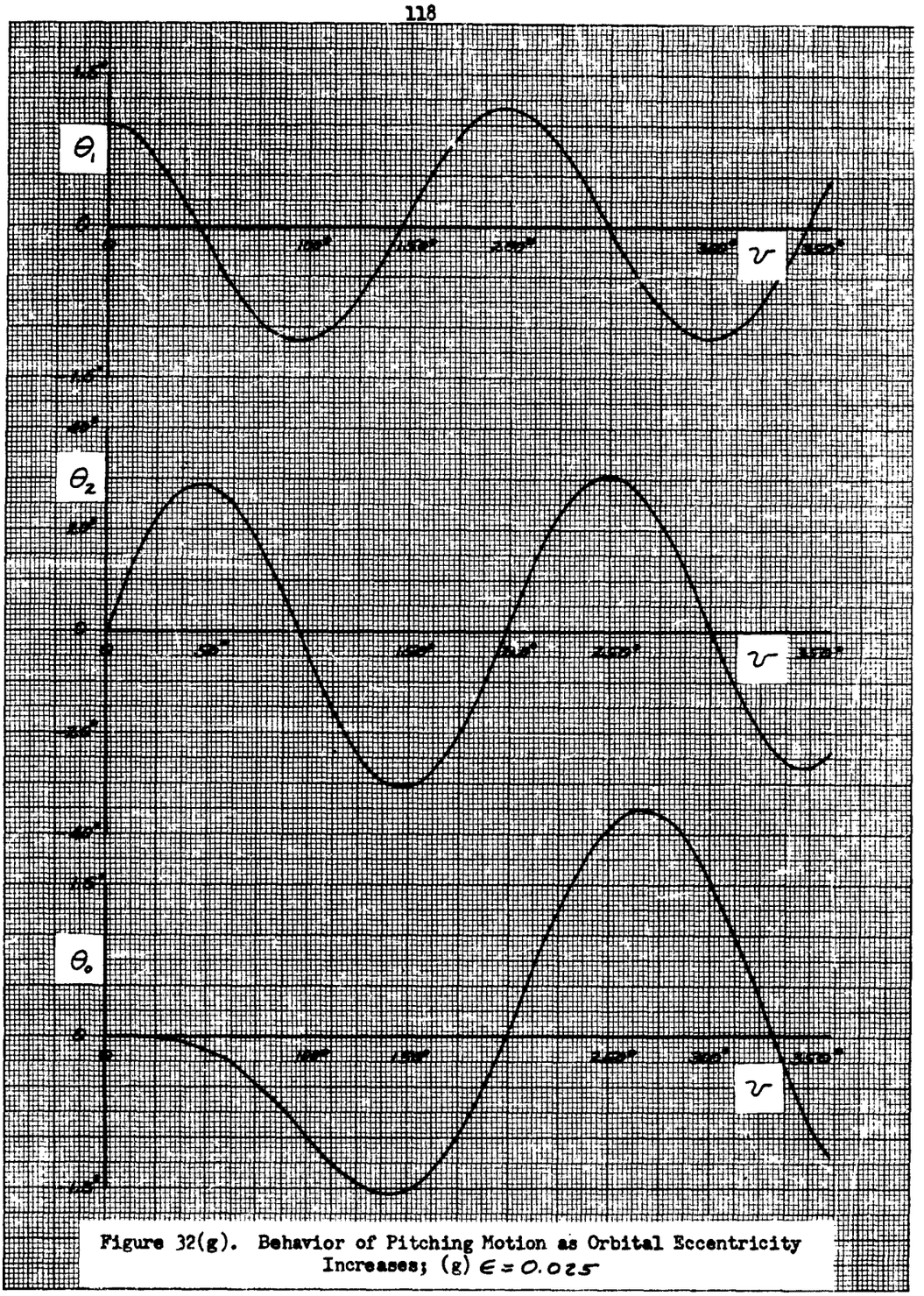

Figure 32(g). Behavior of Pitching Motion as Orbital Eccentricity Increases; (g) $\epsilon = 0.025$

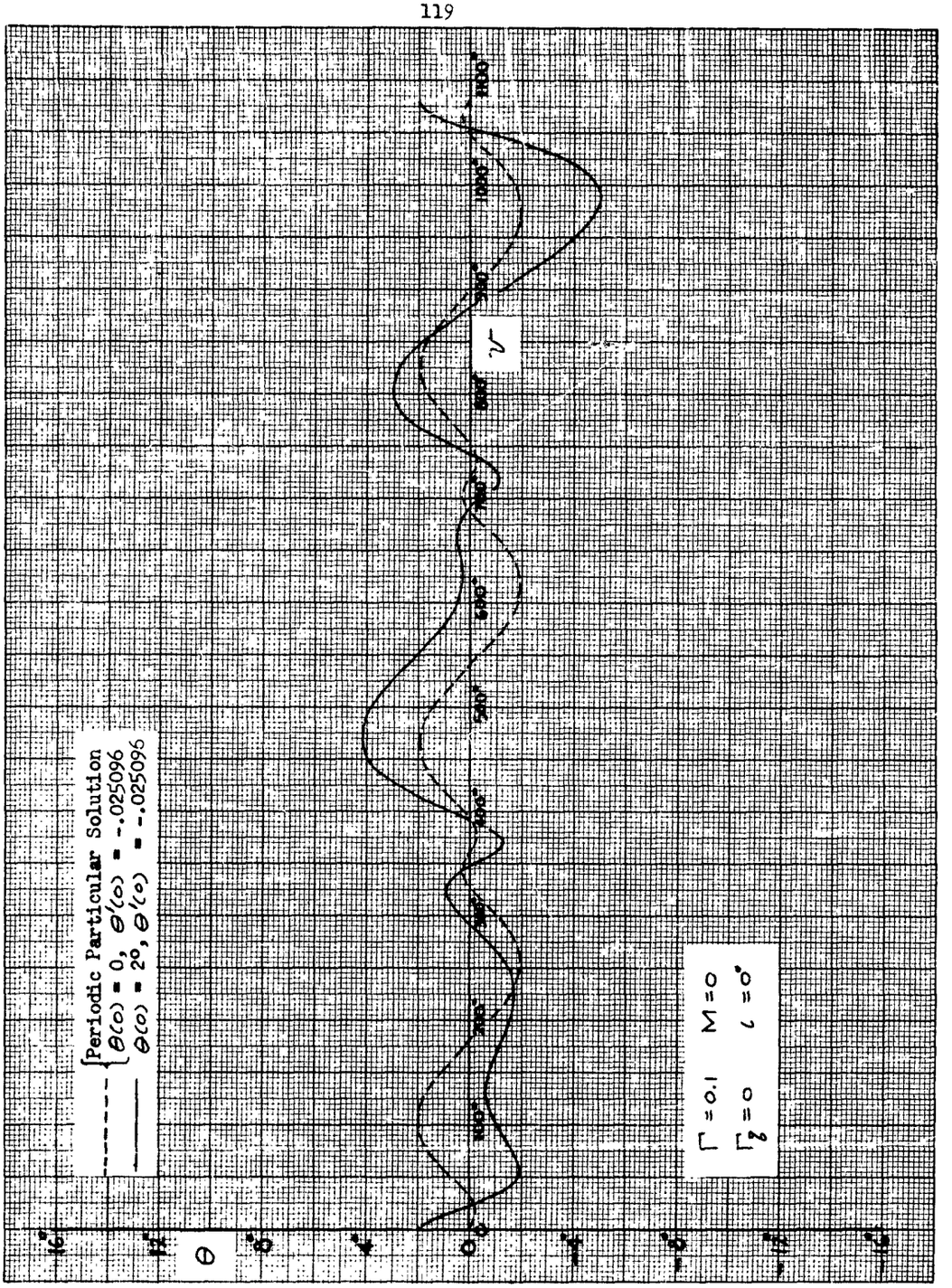

Figure 33(a). Pitching Motion on an Eccentric Orbit at 125 Miles Perigee Altitude; (a) $\epsilon = 0.025$, Stable Motion

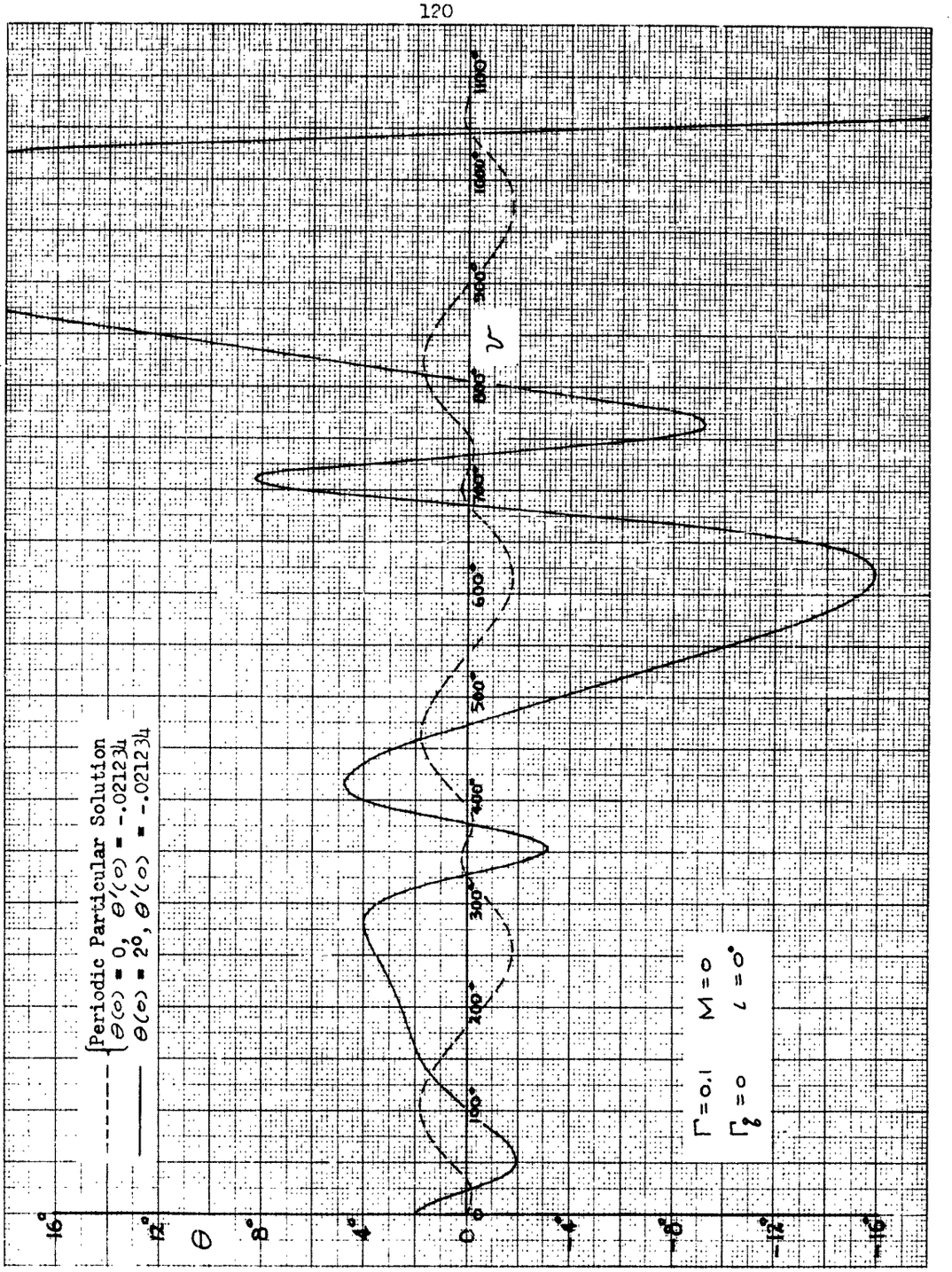

Figure 33(b). Pitching Motion on an Eccentric Orbit at 125 Miles Perigee Altitude; (b) $\epsilon = 0.020$, Unstable Motion

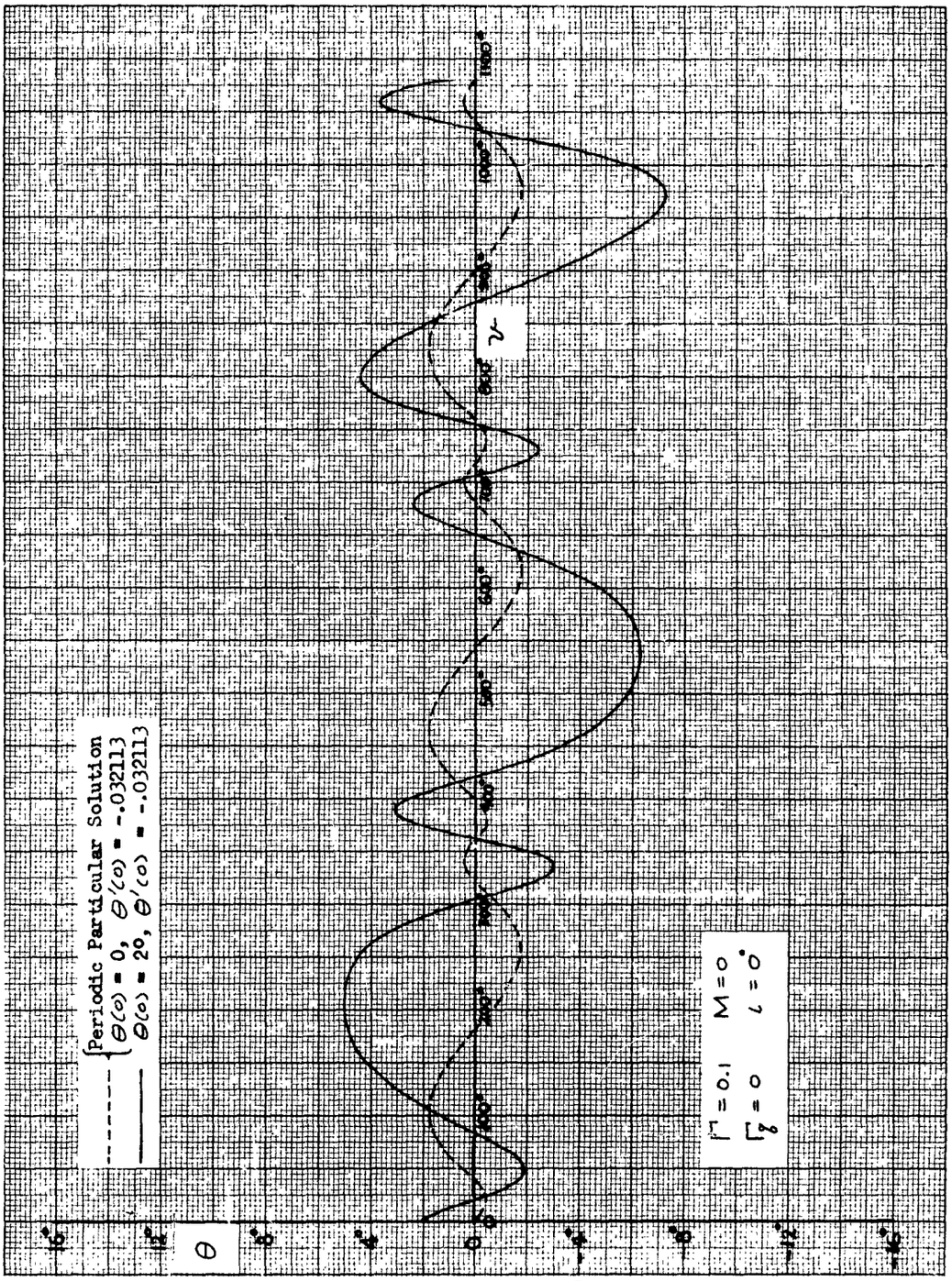

Figure 33(c). Pitching Motion on an Eccentric Orbit at 125 Miles Perigee Altitude; (c) $\epsilon = 0.015$, Stable Motion

SUMMARY AND CONCLUSIONS

The general equations governing the angular motion of a rigid satellite are derived considering the orbital motion to be independent of the angular motion and specified. Both gravitational and aerodynamic torques are included, the latter being developed in a linearized coefficient form consistent with conventional aerodynamic approximations. The atmosphere is assumed to be spherically symmetric but rotating. Aerodynamic damping is also included but other torques, such as those due to solar radiation pressure, are considered briefly and shown to be negligible at those altitudes where aerodynamic effects are significant.

By assuming the orbital eccentricity and the angular deviations from the orbital coordinates to be small, a system of linearized but coupled equations for the pitching, yawing and rolling motions of a non-spinning, axisymmetric satellite is obtained. These equations show the vehicle to be characterized by the dimensionless aerodynamic parameters $\mathcal{P}_p^*$, $\mathcal{Q}_p^*$ and $\mathcal{R}_p^*$ (which describe the static aerodynamic restoring moment and the aerodynamic damping) and the inertia ratio parameter, M (which describes the dynamic "shape" of the vehicle). The orbit is specified by the exponential atmosphere parameter λ, the orbital eccentricity ϵ, and the atmospheric rotation parameter d. The equation for the vehicle's pitching motion is shown to remain independent of those for the yawing and rolling motions when aerodynamic effects are considered. The rolling and yawing equations, however, remain coupled because of the rotating reference frame employed. The angular velocities induced by perturbations, such as those due to Earth oblateness, atmospheric drag, etc., are found to be negligible compared to the angular velocity of the satellite's motion in the orbit. In addition, it is shown that for small eccentricity orbits, the ratio of the velocity relative to the atmosphere to the inertial velocity remains constant.

The resulting equations of angular motion for the combined influence of aerodynamic and gravitational torques on an axisymmetric satellite are found to be linear. Order of magnitude arguments are presented which permit the equation for the rolling motion to be integrated directly and the equations for the pitching and yawing motions to be greatly simplified. A Fourier series expansion of the periodic coefficients of these equations, assuming an exponential density variation and small orbital eccentricities, yields approximate equations of the non-homogeneous Hill type which, for very small eccentricities, reduce to equations of the non-homogeneous Mathieu type.

The equations of motion are solved for the case of a circular orbit, and both qualitative and quantitative descriptions of the pitching, rolling and yawing motions are found. It is shown that in this case, the motion is

completely characterized by the three configuration variables, σ_p^*, $\mathcal{Q}_p^*$ and M, and by the atmospheric rotation parameter, d. It is shown that the rotation of the atmosphere with the Earth induces a steady-state yawing motion of the vehicle which prevents yaw equilibrium from being achieved for other than equatorial orbits. For equatorial orbits, a completely stable equilibrium is found to be possible for $\sigma_p^* > -1$ or $\sigma_p^* > 3M$, whichever is larger, indicating that slender bodies become unstable at lower altitudes than do blunt bodies. Although the pitching and yawing motions may be rendered stable by proper design of axisymmetric vehicles, the rolling motion will, in all but exceptional circumstances, contain a small secular term which will cause ϕ to eventually build up to large values. This effective divergence may be eliminated by relaxing the restriction to axisymmetric shapes or by providing active roll-yaw stabilization.

The effects of the various configuration and orbit variables are studied for the circular orbit case. It is found that gravity gradient effects will generally not dominate the motion until altitudes in excess of 300-400 miles are achieved, while at lower altitudes, even small amounts of aerodynamic stability will suffice to override the gravitational torques. The aerodynamic damping and the orbit inclination are shown to have only secondary effects on the pitching motion.

The general pitching motion on an eccentric orbit is investigated based upon the properties of Hill's differential equation. The exact solution is discussed and an analysis of the stability of the solution is performed. It is found that numerous unstable regions may be encountered, in which any small deviations from a purely periodic motion (of period equal to the orbital period) will amplify. Thus, stable motion exists only for certain specified combinations and values of the parameters Γ, M, h_p and ϵ. The periodic forcing or excitation, which is a natural consequence of combining aerodynamic and gravitational torques, is shown to permit a resonance phenomenon to occur on the boundaries of the previously found unstable regions.

The results of this analysis indicate that the ability to passively stabilize an artificial satellite rests on whether or not the orbit decay, produced by atmospheric drag, causes the vehicle to enter one of the unstable regions and to dwell there sufficiently long for the angular oscillations to grow excessively large. Some results of extensive numeric integrations of the equation of pitching motion are presented to illustrate the catastrophic nature of these unstable regions which may appear in a situation giving the outward appearance of stability. In this connection, the sensitivity of the motion to the initial conditions is studied. An approximate solution for the pitching motion on an elliptical orbit is also obtained using the method of variation of parameters. The results are compared with a numerical integration of the complete governing equation.

It is concluded that the aerodynamic influences play a decisive role in the angular motion of an Earth satellite, whether or not the vehicle is intended to be aerodynamically stabilized. Since it will be virtually impossible to insure that the center of pressure and the mass center exactly coincide on any given satellite, even these small residual aerodynamic torques constitute what is potentially a major disturbing influence on the satellite's orientation. Through proper vehicle design, however, these aerodynamic influences may be used to achieve partial or complete attitude stabilization and control. In particular, the design of a satellite for maximum aerodynamic stability appears to reduce the likelihood of encountering an unstable region, at least for low eccentricity orbits.

The need for additional and immediate effort in this general area is indicated by these results. Two problems of significance are: (1) the further study of the properties of the non-homogeneous Hill equation found to govern the satellite's pitching motion (in order to obtain the stability boundaries with a high degree of accuracy), and (2) the synthesis of active aerodynamic and inertial attitude control systems based upon the results presented herein.

APPENDIX A

GRAVITATIONAL TORQUES ON A RIGID BODY

Consider a collection of mass points m_i viewed from an inertial reference frame. Denote the inertial position vector to the ith particle by $\vec{Q}_i$. Then the equation of motion for this ith particle is simply

$$\vec{F}_i = m_i \ddot{\vec{Q}}_i \quad . \tag{A-1}$$

Now if the ith position vector is cross multiplied into each side of this equation, and sum taken over the N particles of the collection, the result

$$\sum_{i=1}^{N} \vec{Q}_i \times \vec{F}_i = \sum_{i=1}^{N} m_i \vec{Q}_i \times \ddot{\vec{Q}}_i = \frac{d}{dt} \sum_{i=1}^{N} m_i \vec{Q}_i \times \dot{\vec{Q}}_i \tag{A-2}$$

is obtained. Next define the mass center of the collection in the usual way (Ref. 31) such that

$$\sum_{i=1}^{N} \vec{l}_i m_i \equiv 0 \tag{A-3}$$

where $\vec{l}_i$ is the position vector of the ith particle measured in axes fixed in the mass center. Denote the inertial position vector of the mass center by $\vec{r}$. Then clearly

$$\vec{Q}_i = \vec{r} + \vec{l}_i$$

and the left-hand side of Eq. (A-2), which is the net torque on the collection, becomes

$$\sum_{i=1}^{N} \vec{Q}_i \times \vec{F}_i = \vec{r} \times \sum_{i=1}^{N} \vec{F}_i + \sum_{i=1}^{N} \vec{l}_i \times \vec{F}_i \quad .$$

Also, since $\vec{F}_i = \vec{F}_i^{(\text{INTERNAL})} + \vec{F}_i^{(\text{EXTERNAL})}$, the torque due to the internal forces cancel in pairs and the first summation is simply $\vec{r} \times \vec{F}_T^{(\text{EXTERNAL})}$ the moment of the total external force about the inertial origin. The right-hand side of the equation of motion, Eq. (A-2), expands as

$$\frac{d}{dt}\sum_{i=1}^{N} m_i(\vec{r}+\vec{l}_i)\times(\dot{\vec{r}}+\dot{\vec{l}}_i)$$

$$= \frac{d}{dt}\left\{ \sum_{i=1}^{N} m_i\, \vec{l}_i \times \dot{\vec{l}}_i + \left[\sum_{i=1}^{N} m_i\, \vec{l}_i\right]\times \dot{\vec{r}} \right. \qquad \text{(A-4)}$$

$$\left. + \vec{r}\times\sum_{i=1}^{N} \dot{\vec{l}}_i\, m_i \;+\; M\vec{r}\times\dot{\vec{r}} \right\}$$

where

$$M = \sum_{i=1}^{N} m_i \qquad \text{(A-5)}$$

and all time derivatives of $\vec{l}_i$ are relative to inertial space. By the well-known Coriolis' law (Ref. 31), these inertial time derivatives may be rewritten in terms of derivatives with respect to the rotating frame fixed in the collection with origin in the mass center, as

$$\dot{\vec{l}}_i = \dot{\vec{l}}_{i_R} + \vec{\Omega}\times\vec{l}_i$$

so that

$$\frac{d}{dt}\left\{\vec{r}\times\sum_{i=1}^{N} m_i\dot{\vec{l}}_i\right\} = \frac{d}{dt}\left\{\vec{r}\times\sum_{i=1}^{N} m_i\dot{\vec{l}}_{i_R} + \vec{r}\times\left[\vec{\Omega}\times\sum_{i=1}^{N} m_i\vec{l}_i\right]\right\} . \qquad \text{(A-6)}$$

For a rigid collection $\dot{\vec{l}}_{i_R} = o$ and by Eq. (A-3) the last term in Eq. (A-6) vanishes. For the same reason, the second term on the right of Eq. (A-4) also vanishes. Finally, the last term on the right of Eq. (A-4) is simply

$$\frac{d}{dt}\left\{M\vec{r}\times\dot{\vec{r}}\right\} = M\vec{r}\times\ddot{\vec{r}} = \vec{r}\times\left(M\ddot{\vec{r}}\right)$$

since the total mass of the collection is assumed to be constant. The complete equation of angular motion is, therefore,

$$\vec{r} \times \vec{F}_T^{(ext)} + \sum_{i=1}^{N} \vec{l}_i \times \vec{F}_i^{(ext)} = \frac{d}{dt} \sum_{i=1}^{N} m_i \vec{l}_i \times \dot{\vec{l}}_i + \vec{r} \times (M \ddot{\vec{r}}) \quad . \qquad (A\text{-}7)$$

The first and last terms in this expression cancel since together they simply represent the position vector $\vec{r}$, cross multiplied into Newton's second law written for the mass center of the collection. The only remaining term on the right of Eq. (A-7) is defined to be the true rate of change of angular momentum of the collection viewed from the moving axes:

$$\frac{d\vec{H}}{dt} \equiv \frac{d}{dt} \sum_{i=1}^{N} m_i \vec{l}_i \times \dot{\vec{l}}_i \quad .$$

Expansion of this term yields the acceleration side of the well-known Euler equations of angular motion for a rigid collection (Ref. 31) in terms of quantities expressed in axes fixed in the collection. The principal problem which remains is to expand the external torques for a rigid collection moving in an essentially inverse-square attracting force field. The external force due to gravitational attraction on any mass particle in the collection is simply

$$\vec{F}_i^{(ext)} = - m_i \, \text{grad} \, \Phi$$

where Φ is the potential function for the force field. The torques due to forces internal to the collection have already been observed to cancel in pairs and hence only the external forces are of concern. For an inverse-square attracting force field,

$$\Phi = - \frac{\mu}{Q}$$

where the origin of the inertial axes are here assumed to coincide with the force center and μ is the product of the universal gravitational constant and the mass of the primary body. Thus, the gravitational force on the ith particle is directed along the inertial position vector, $\vec{Q}_i$:

$$-m_i\{\text{grad}\,\Phi\}_i = -\frac{m_i \mu}{Q_i^2}\left(\frac{\vec{Q}_i}{Q_i}\right)$$

and hence the vector torque due to gravity about the mass center of the collection, which is denoted by $\vec{L}_g$, is

$$\vec{L}_g \equiv \sum_{i=1}^{N} \vec{l}_i \times \vec{F}_i^{(g\times r)} = -\mu \sum_{i=1}^{N} \frac{\vec{l}_i \times \vec{Q}_i}{Q_i^3} m_i$$

$$= -\mu \sum_{i=1}^{N} \frac{\vec{l}_i \times (\vec{r} + \vec{l}_i)}{Q_i^3} m_i$$

or

$$\vec{L}_g = -\mu \sum_{i=1}^{N} \frac{\vec{l}_i \times \vec{r}}{Q_i^3} m_i - \mu \sum_{i=1}^{N} \frac{\vec{l}_i \times \vec{l}_i}{Q_i^3} m_i \quad . \qquad \text{(A-8)}$$

Clearly the last term vanishes from the definition of the vector product and the remaining term on the right of Eq. (A-8) becomes

$$\vec{L}_g = -\mu \vec{r} \times \sum_{i=1}^{N} \frac{\vec{l}_i m_i}{Q_i^3} \quad . \qquad \text{(A-9)}$$

The summation does not vanish by the center of mass condition, since Q_i^3 may be interpreted as a weighting factor which, in general, does not permit cancellation of the torques due to symmetrically placed mass elements.

Now by definition,

$$Q_i^2 = \vec{Q}_i \cdot \vec{Q}_i = (\vec{r} + \vec{l}_i) \cdot (\vec{r} + \vec{l}_i)$$

$$= r^2 + l_i^2 + 2\vec{r} \cdot \vec{l}_i$$

and so

$$Q_i^3 = r^3\left\{1 + 2\frac{\vec{r}\cdot\vec{l}_i}{r^2} + \left(\frac{l_i}{r}\right)^2\right\}^{3/2}.$$

If the maximum dimension of the collection is small compared to r[1] l_i/r is small, and $1/Q_i^3$ may be expanded by the binomial theorem as,

$$\frac{1}{Q_i^3} = \frac{1}{r^3}\left\{1 - 3\frac{\vec{r}\cdot\vec{l}_i}{r^2} + \frac{1}{2}\left[-3\left(\frac{l_i}{r}\right)^2 + 15\left(\frac{\vec{r}\cdot\vec{l}_i}{r^2}\right)^2\right] + \cdots\right\}$$

and hence Eq. (A-9) becomes

$$\vec{L}_g = \frac{\mathcal{M}\vec{r}}{r^3} \times \sum_{i=1}^{N}\left\{\vec{l}_i m_i - 3\frac{\vec{r}\cdot\vec{l}_i}{r^2}\vec{l}_i m_i + O\left(\frac{l_i}{r}\right)^2\right\}.$$

Again the first summation vanishes by the center of mass condition, Eq. (A-3), while terms of order $(l_i/r)^2$ may be neglected. For "small" bodies, then, the torque due to the inverse-square gravitational attraction is simply

$$\vec{L}_g = -3\frac{\mathcal{M}\vec{r}}{r^3} \times \sum_{i=1}^{N}\frac{\vec{r}\cdot\vec{l}_i}{r^2}\vec{l}_i m_i \quad . \qquad \text{(A-10)}$$

This result has also been recently obtained by Nidey (Ref. 20).

Up to this point, nothing has been said about orientation angle and hence no small angle restrictions are inherent in this result. The detailed nature of Eq. (A-10) may be further examined by expanding $\vec{r}$ and $\vec{l}_i$ in terms of components in the moving axes. Assume rectangular axes fixed in the mass center of the body. Then let

---

[1] For a collection of maximum extent 10^2 feet at the Earth's surface, $l_i/r \cong 10^{-5}$.

$$\vec{r} = \sum_{n=1}^{3} r_n \vec{e}_n \quad \text{and} \quad \vec{l}_i = \sum_{n=1}^{3} x_{i_n} \vec{e}_n \tag{A-11}$$

so that

$$\vec{r} \cdot \vec{l}_i = \sum_{n=1}^{3} r_n x_{i_n}$$

and

$$\begin{aligned} \vec{r} \times \vec{l}_i = {} & (r_2 x_{i_3} - r_3 x_{i_2}) \vec{e}_1 \\ & + (r_3 x_{i_1} - r_1 x_{i_3}) \vec{e}_2 \\ & + (r_1 x_{i_2} - r_2 x_{i_1}) \vec{e}_3 \quad . \end{aligned} \tag{A-12}$$

Inserting Eqs. (A-11) and (A-12) into Eq. (A-10), the gravitational torque components about the body axes become

$$L_{g_1} = -3\frac{\mu}{r^5} \sum_{i=1}^{N} \left[r_1 x_{i_1} + r_2 x_{i_2} + r_3 x_{i_3} \right] (r_2 x_{i_3} - r_3 x_{i_2})\, m_i$$

$$L_{g_2} = -3\frac{\mu}{r^5} \sum_{i=1}^{N} \left[r_1 x_{i_1} + r_2 x_{i_2} + r_3 x_{i_3} \right] (r_3 x_{i_1} - r_1 x_{i_3})\, m_i$$

$$L_{g_3} = -3\frac{\mu}{r^5} \sum_{i=1}^{N} \left[r_1 x_{i_1} + r_2 x_{i_2} + r_3 x_{i_3} \right] (r_1 x_{i_2} - r_2 x_{i_3})\, m_i \quad .$$

Expanding L_{g_1} :

$$\begin{aligned} L_{g_1} = -3\frac{\mu}{r^5} \sum_{i=1}^{N} \{ & r_1 r_2 x_{i_1} x_{i_3} + r_2^2 x_{i_2} x_{i_3} + r_2 r_3 x_{i_3}^2 \\ & - r_1 r_3 x_{i_1} x_{i_2} - r_2 r_3 x_{i_2}^2 - r_3^2 x_{i_2} x_{i_3} \} \, m_i \quad . \end{aligned}$$

Defining the moments and products of inertia in the usual way by

$$\bar{I}_1 \equiv \sum_{i=1}^{N} (x_{i_2}^2 + x_{i_3}^2) m_i \quad , \quad \text{etc.}$$

and

$$\bar{J}_{mn} = \bar{J}_{nm} \equiv \sum_{i=1}^{N} x_{i_n} x_{i_m} m_i \quad , \quad \text{etc.},$$

then the gravitational torque component about the x_1-body axis is

$$L_{g_1} = -3\frac{\mu}{r^5}\left\{ r_1 r_2 \bar{J}_{13} - r_1 r_3 \bar{J}_{12} + \bar{J}_{23}(r_2^2 - r_3^2) + r_2 r_3 (\bar{I}_2 - \bar{I}_3) \right\} . \quad \text{(A-13)}$$

In a similar way the other two gravitational torque components are found to be

$$L_{g_2} = -3\frac{\mu}{r^5}\left\{ r_2 r_3 \bar{J}_{12} - r_1 r_2 \bar{J}_{23} + \bar{J}_{13}(r_3^2 - r_1^2) + r_1 r_3 (\bar{I}_3 - \bar{I}_1) \right\} \quad \text{(A-14)}$$

$$L_{g_3} = -3\frac{\mu}{r^5}\left\{ r_1 r_3 \bar{J}_{23} - r_2 r_3 \bar{J}_{13} + \bar{J}_{12}(r_1^2 - r_2^2) + r_1 r_2 (\bar{I}_1 - \bar{I}_2) \right\} .$$

It is generally most convenient to let the body-fixed axes be so chosen that the products of inertia vanish (i.e., principal axes) in which case the torques assume the simple matrix form

$$\begin{bmatrix} L_{g_1} \\ L_{g_2} \\ L_{g_3} \end{bmatrix} = -3\frac{\mu}{r^3} \begin{bmatrix} \frac{r_2 r_3}{r^2}(\bar{I}_2 - \bar{I}_3) \\ \frac{r_1 r_3}{r^2}(\bar{I}_3 - \bar{I}_1) \\ \frac{r_1 r_2}{r^2}(\bar{I}_1 - \bar{I}_2) \end{bmatrix} . \quad \text{(A-15)}$$

Note that there is no torque about any axis of symmetry. The terms r_i/r are merely the direction cosines between $\vec{r}$ and the instantaneous body axes, and may be small or large as required. Eq. (A-15) readily reduces to the results of Roberson (Refs. 9, 10) when the Euler angles used in that reference are employed.

APPENDIX B

EXPANSION OF COEFFICIENTS IN EQUATIONS OF ANGULAR MOTION

It is well-known that the unperturbed motion of a particle in an inverse-square central force field remains planar and occurs along one of the conic sections with the force center at one focus. The polar form of the equation may be written as

$$r = \frac{p}{1 + e\cos v} \tag{B-1}$$

where r is the distance from the force center to the particle, p is the semi-parameter or semi-latus rectum of the path, e is the eccentricity and v is the true anomaly. Fig. B-1 should make the geometry clear.

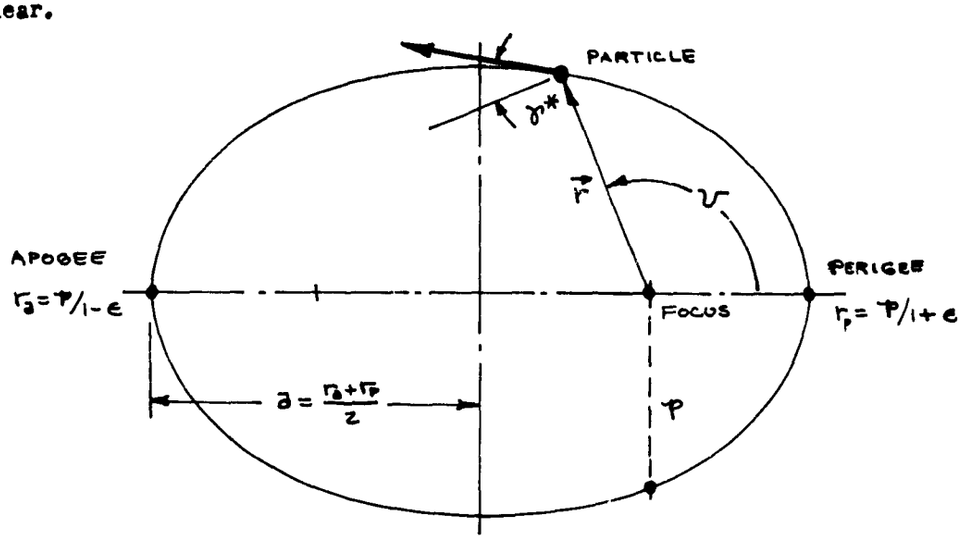

Figure B-1

The form of the path depends upon the value of e according to the following table:

$|e| > 1$, the path is a hyperbola

$|e| = 1$, the path is a parabola

$|\epsilon|<1$, the path is an ellipse

$|\epsilon|=0$, the path is a circle .

For the present purpose, only closed paths (hereafter called orbits) are of interest and so the restriction $|\epsilon|<1$ may be imposed.

From the sketch, the semi-major axis (or mean distance) of the ellipse has length

$$a = \frac{1}{2}(r_a + r_p)$$

and so it may be seen that

$$p = a(1-\epsilon^2) .$$

The eccentricity ϵ and the mean distance a are usually the fundamental constants of the orbit. In the present case, however, it is convenient to rewrite Eq. (B-1) for closed paths as

$$r = \frac{r_p(1+\epsilon)}{1+\epsilon\cos v}, \quad |\epsilon|<1 . \tag{B-2}$$

Eq. (B-2) completely defines the orbit size and shape.

The velocity vector of the particle is, by definition, always tangent to the orbit. Defining the angle between the normal to the radius vector and the velocity vector as γ^* (see sketch) then

$$r\dot{v} = V\cos\gamma^*$$

$$\dot{r} = V\sin\gamma^*$$

and

$$\tan\gamma^* = \frac{\dot{r}}{r\dot{v}} . \tag{B-3}$$

Differentiating Eq. (B-2) with respect to time,

$$\dot{r} = \frac{\epsilon r_p (1+\epsilon)}{(1+\epsilon\cos\nu)^2}\,\dot{\nu}\sin\nu$$

or

$$\dot{r} = r^2\dot{\nu}\,\frac{\epsilon}{r_p(1+\epsilon)}\sin\nu \tag{B-4}$$

and, combining Eqs. (B-3) and (B-4) leads to

$$\tan\gamma^* = \frac{\epsilon\sin\nu}{1+\epsilon\cos\nu}$$

which implies

$$\sin\gamma^* = \frac{\epsilon\sin\nu}{\sqrt{1+2\epsilon\cos\nu+\epsilon^2}}$$

$$\cos\gamma^* = \frac{1+\epsilon\cos\nu}{\sqrt{1+2\epsilon\cos\nu+\epsilon^2}} \tag{B-5}$$

and

$$V = \frac{r^2\dot{\nu}}{r_p}\sqrt{\frac{1+\epsilon^2}{(1+\epsilon)^2}+\frac{2\epsilon}{(1+\epsilon)^2}\cos\nu}\quad .$$

Making use of the fact that motion in an inverse square force field conserves angular momentum relative to the inertial coordinate origin,

$$r^2\dot{\nu} = H\ ,\ \text{a constant} \tag{B-6}$$

or,

$$r^2\dot{\nu} = rV\cos\gamma^* = r_p^2\dot{\nu}_p \tag{B-7}$$

and so

$$\frac{V}{r_p \dot{\upsilon}} = \frac{r_p}{r} \frac{\dot{\upsilon}_p}{\dot{\upsilon} \cos\gamma^*} = \frac{r}{r_p} \frac{1}{\cos\gamma^*} \quad .$$

From Eqs. (B-2) and (B-5):

$$\frac{V}{r_p \dot{\upsilon}} = \frac{(1+\epsilon)\sqrt{1+2\epsilon\cos\upsilon+\epsilon^2}}{(1+\epsilon\cos\upsilon)^2} \quad . \tag{B-8}$$

Again, using Eqs. (B-2) and (B-7)

$$\dot{\upsilon} = \left(\frac{r_p}{r}\right)^2 \dot{\upsilon}_p = \left\{\frac{1+\epsilon\cos\upsilon}{1+\epsilon}\right\}^2 \dot{\upsilon}_p \quad . \tag{B-9}$$

Differentiating with respect to time

$$\ddot{\upsilon} = 2\,\frac{1+\epsilon\cos\upsilon}{(1+\epsilon)^2}(-\epsilon\sin\upsilon)\,\dot{\upsilon}\,\dot{\upsilon}_p$$

or,

$$\frac{\ddot{\upsilon}}{\dot{\upsilon}^2} = -2\,\frac{\epsilon\sin\upsilon}{1+\epsilon\cos\upsilon} \quad . \tag{B-10}$$

The coefficients in the equations of motion developed in the text may now be expanded in terms of υ, the independent variable and r_p and ϵ, the constants of the orbit. Using the definitions of $\mathcal{P}_p$, $\mathcal{Q}_p$ and $\mathcal{R}_p$ as given by Eqs. (45) and the definition of P, Q and R as given by Eqs. (48), it is trivial to find

$$P = \mathcal{P}_p \left(\frac{\rho}{\rho_p}\right)\left(\frac{V_R}{V}\right)^2 \left\{\frac{V}{r_p \dot{\upsilon}}\right\}^2$$

$$2Q = 2\mathcal{Q}_p \left(\frac{\rho}{\rho_p}\right)\left(\frac{V_R}{V}\right) \frac{V}{r_p \dot{\upsilon}} + \frac{\ddot{\upsilon}}{\dot{\upsilon}^2} \tag{B-11}$$

$$2R = 2\mathcal{R}_p \left(\frac{\rho}{\rho_p}\right)\left(\frac{V_R}{V}\right) \frac{V}{r_p \dot{\upsilon}} + \frac{\ddot{\upsilon}}{\dot{\upsilon}^2} \quad .$$

Combining Eqs. (B-8) and (B-10) with Eqs. (B-11) yields the first three of Eqs. (47) in the text.

The small angles Λ and γ are given respectively by Eqs. (36) and (37) in the text. These may be rewritten for small values of ϵ with the help of Eq. (B-7) as

$$\Lambda \cong \frac{\omega_a}{\dot{v}_p} \sin\iota \cos u \left(\frac{\dot{v}_p}{\dot{v}}\right)$$

and

$$\gamma \cong \gamma^* \left\{ 1 + \frac{\omega_a}{\dot{v}_p} \cos\iota \left(\frac{\dot{v}_p}{\dot{v}}\right) \right\} .$$

Introducing Eqs. (B-9)

$$\Lambda \cong \frac{\omega_a}{\dot{v}_p} \sin\iota \cos u \left\{ \frac{1+\epsilon}{1+\epsilon\cos v} \right\}^2 \qquad \text{(B-12)}$$

and, with the aid of Eqs. (B-5),

$$\gamma \cong \frac{\epsilon \sin v}{1+\epsilon\cos v} \left\{ 1 + \frac{\omega_a}{\dot{v}_p} \cos\iota \left[\frac{1+\epsilon}{1+\epsilon\cos v} \right]^2 \right\} . \qquad \text{(B-13)}$$

As the final development in this Appendix, consider the term $\mu / r^3 \dot{v}^2$. From the definition of p, and Eqs. (B-1) and (B-6)

$$p = r_p(1+\epsilon) = \frac{r^4 \dot{v}^2}{\mu}$$

and hence

$$\frac{\mu}{r^3 \dot{v}^2} = \frac{1}{1+\epsilon} \frac{r}{r_p} = \frac{1}{1+\epsilon\cos v} .$$

APPENDIX C

EFFECTS OF AERODYNAMIC DRAG AND DAMPING ON THE MOTION OF NEAR-EARTH SATELLITES

1. Drag Effects

A primary problem in the study of satellite aerodynamics is the effect of perturbation forces on the size and shape of the orbit. Since atmospheric density is a dominant influence on aerodynamic stabilization, these changes in satellite altitude (and hence density) are very significant; consequently, the effect of drag perturbations on orbital eccentricity and altitude decay must be given initial consideration. The approach to this problem is to assume, as a first approximation, that only the atmospheric retardation and the attraction of a spherical, homogeneous Earth act on the satellite. Furthermore, the drag of the satellite is assumed to vary only with air density and the square of the relative velocity; i. e., the drag coefficient is constant throughout the orbit.

The perturbations which the drag force produce on the orbit elements may be determined from the classical method of variation of parameters (see, for example, Moulton, Ref. 17). Sterne (Ref. 19) has applied this theory to determine the secular variations of orbit size, shape and spatial orientation for a satellite with drag moving through a rotating atmosphere. For the present case a static atmosphere will suffice and Sterne's equations reduce to

$$\frac{da}{dt} = -2b\rho a^2 \frac{(1+\epsilon\cos E)^{3/2}}{(1-\epsilon\cos E)^{1/2}} \frac{dE}{dt}$$

$$\frac{d\epsilon}{dt} = -2b\rho(1-\epsilon^2)a \left[\frac{1+\epsilon\cos E}{1-\epsilon\cos E}\right]^{1/2} \cos E \frac{dE}{dt} \qquad \text{(C-1)}$$

where a is the mean distance, ϵ the orbital eccentricity, E the eccentric anomaly and b the ballistic coefficient. The relevant geometry is shown in Fig. C-1. In order to perform the integration of Eqs. (C-1), it is necessary to express the density in terms of a, ϵ and E. The exponential representation given in Eq. (52) of the text provides the required relation. Using the eccentric anomaly in order to rewrite the equation of motion, there results,

$$r = a(1 - \epsilon\cos E)$$

and so, Eq. (54) of Section 3.2 becomes, without further approximation,

$$\rho = \rho_b \, e^{\lambda \cos E} \tag{C-2}$$

where $\lambda \equiv \mathcal{K}_A a \epsilon$ and ρ_b is the density at $r = a$ (or $E = \pi/2$).

Since the present analysis considers only orbits of small eccentricity (say less than 0.1), Eqs. (C-1) may be simplified with little loss in accuracy. If terms of order ϵ^2 and smaller are neglected, then Eqs. (C-1) and (C-2) may be written as

$$da \cong -2ba^2 \rho_b e^{\lambda \cos E} (1 + 2\epsilon \cos E)\, dE$$

$$d\epsilon \cong -2ba(1-\epsilon^2) \rho_b e^{\lambda \cos E} (1 + \epsilon \cos E) \cos E \, dE \, . \tag{C-3}$$

The changes in a and ϵ may now be found by integrating Eqs. (C-3) over E, considering the orbit elements appearing on the right-hand sides as constants. The integrands may be expanded in Fourier series using the technique discussed at length in Section 3.4. As before, frequent use must be made of the integral form of the modified Bessel functions. Performing the integration from $E = E_o$ to any E and confining attention to the secular terms (those terms which are directly proportional to E), there is obtained,

$$a - a_o = -2b a^2 \rho_b \left[I_0(\lambda) + 2\epsilon I_1(\lambda) \right](E - E_o) + \{\text{Periodic Terms}\}$$

$$\epsilon - \epsilon_o = -2ba(1-\epsilon^2) \rho_b \left[I_1(\lambda) + \epsilon I_0(\lambda) - \frac{\epsilon}{\lambda} I_1(\lambda) \right](E - E_o) \tag{C-4}$$

$$+ \{\text{Periodic Terms}\} .$$

Since a satellite's altitude is minimum at perigee, it is usually more convenient to use the change in perigee radius rather than the change in semi-major axis. This conversion may be obtained from the geometric relation $r_p = a(1-\epsilon)$ which yields

$$\Delta r_p \cong (1-\epsilon)\Delta a - a \Delta \epsilon \, . \tag{C-5}$$

By substituting Eqs. (C-4) into Eq. (C-5) and neglecting terms of the order ϵ^2, ϵ/λ and smaller,

$$r_p - r_{p_o} \cong -2b a^2 \rho_b (1-2\epsilon)\left[I_o(\lambda) - I_1(\lambda)\right](E-E_o) \quad . \tag{C-6}$$

The second of Eqs. (C-4) and Eq. (C-6) may be written in terms of the perigee radius as,

$$r_p - r_{p_o} \cong -2b r_p^2 \rho_b \left[I_o(\lambda) - I_1(\lambda)\right](E-E_o)$$

$$\epsilon - \epsilon_o \cong -2b r_p (1+\epsilon) \rho_b \left[I_1(\lambda) + \epsilon I_o(\lambda)\right](E-E_o) \tag{C-7}$$

where $(1-2\epsilon) \cong (1-\epsilon)^2$ and where $(\epsilon/\lambda) I_1(\lambda)$ is neglected.

The only remaining problem in using Eqs. (C-7) is the determination of the modified Bessel functions I_o and I_1. Since the argument λ is a function of altitude and since I_o and I_1 vary essentially exponentially with λ, the magnitude of $(\epsilon - \epsilon_o)$ and $(r_p - r_{p_o})$ are highly sensitive to the selection of a reference altitude. Part of the problem may be alleviated by noting that the average density over N complete revolutions is

$$\bar{\rho} = \frac{1}{2N\pi} \int_0^{2N\pi} \rho_b e^{\lambda \cos t} dt = \rho_b I_o(\lambda)$$

or

$$I_o(\lambda) = \bar{\rho} / \rho_b \quad .$$

Now if the average density is assumed, as a first approximation, to be the arithmetic mean of the perigee and apogee densities, then

$$2I_o(\lambda) \cong \frac{\rho_p + \rho_a}{\rho_b} \quad . \tag{C-8}$$

The advantage of Eq. (C-8) is that $I_o(\lambda)$ may be computed without knowledge of an effective λ and since I_1 is a known function of I_o, Eqs. (C-7) may be solved (for a given ballistic coefficient) in terms of initial orbit geometry and densities. It should be noted that for eccentric orbits, the density at the average altitude, ρ_b, is always less than the arithmetic average density, i.e., $I_o(\lambda) \geq 1.0$. For initially circular orbits, $I_o(o) = 1.0$ and $I_1(o) = 0$ which leads to considerable simplification of the first of Eqs. (C-7) along with the deletion of the second of Eqs. (C-7).

This brief treatment of drag effects on satellite orbit decay shows that variations in the ballistic coefficient may alter the results considerably, since the decay of both altitude and eccentricity are directly proportional to this quantity. The problem in estimating b is not necessarily attributed to the drag coefficient alone, but to the effective drag area, S_π, upon which C_D is based. Calculations readily show that the lifetime of a high fineness ratio satellite is appreciably reduced if it tumbles rather than remaining in a streamlined, stabilized condition.

2. Effects of Damping in Pitch

In estimating the effects of pitch damping on the satellite's oscillatory motion, it is convenient to examine the time to damp an initial oscillation to one-half its initial amplitude. From Eqs. (62) this decay is simply expressed as

$$e^{-\int_{\nu_o}^{\nu_{\theta/2}} Q(t)\,dt} = 1/2 \qquad \text{(C-9)}$$

where $\nu_{\theta/2}$ denotes the value of the true anomaly for which the oscillation amplitude has been halved and where

$$Q(\nu) \cong 2_p^* e^{\lambda\cos\nu}\left\{1 + \epsilon[1 - \cos\nu]\right\} - \epsilon\sin\nu$$

$$2_p^* \equiv \Gamma_\gamma \frac{\rho_e r_p}{8}\left(\frac{V_R}{V}\right) . \qquad \text{(C-10)}$$

Substituting the first of Eqs. (C-10) and taking logarithms of both sides,

$$\int_{\nu_o}^{\nu_{\theta/2}} \left\{2_p^* e^{\lambda\cos t}\left[1 + \epsilon(1 - \cos t)\right] - \epsilon\sin t\right\} dt = 0.693 . \qquad \text{(C-11)}$$

This integration may be performed by following the procedure outlined in the preceding section. The result is

$$\mathcal{Q}_p^* \left[(1+\epsilon) I_0(\lambda) - I_1(\lambda)\right](\upsilon_{\theta/2} - \upsilon_0) \cong 0.693 \qquad \text{(C-12)}$$

where $(\upsilon_{\theta/2} - \upsilon_0)$ is proportional to the number of revolutions required to damp to one-half the initial amplitude. Initial values are assigned to ϵ, λ and $\mathcal{Q}_p^*$ as approximations since orbital decay affects these parameters between the limits of integration.

In order for the damping parameter to have a significant influence on the decay of the angular motions, the time to damp to half amplitude must be considerably less than the time required for drag to produce a significant change in the orbit elements themselves. A relative measure of these two times may be found in the ratio of $(\upsilon_{\theta/2} - \upsilon_0)$ from Eq. (C-12) and the $(E_{\Delta r_p} - E_0)$ required for a change $(r_p - r_{p_0})$ from Eq. (C-7). That is,

$$\frac{\upsilon_{\theta/2} - \upsilon_0}{E_{\Delta r_p} - E_0} \equiv \frac{N_{\theta/2}}{N_{\Delta r}} \cong \frac{1.386\, b\, r_p^2\, \rho_\ell \left[I_0(\lambda) - I_1(\lambda)\right]}{\mathcal{Q}_p^*\, \Delta r_p \left[(1+\epsilon) I_0(\lambda) - I_1(\lambda)\right]} \qquad \text{(C-13)}$$

where $N_{\Delta r}$ is the number of revolutions taken in descending Δr_p feet (a positive increment), and where, to terms of order ϵ, the density at $r = a$, ρ_b, is interchangeable with the density at the semi-latus rectum, ρ_ℓ [1]. With the definition of the ballistic coefficient and the second of Eqs. (C-10), Eq. (C-13) becomes

$$\frac{N_{\theta/2}}{N_{\Delta r}} = 11.09 \frac{b}{\Gamma_\ell} \left\{ \frac{I_0(\lambda) - I_1(\lambda)}{(1+\epsilon) I_0(\lambda) - I_1(\lambda)} \right\} \frac{r_p}{\Delta r_p}$$

or, conservatively, for small eccentricities,

$$\left(\frac{\Delta r_p}{r_p}\right) \frac{N_{\theta/2}}{N_{\Delta r}} \cong 11 \frac{b}{\Gamma_\ell} \cong -5.54 \frac{C_D}{C_{m_\ell}} \frac{\bar{I}}{m \bar{c}^2} \,. \qquad \text{(C-14)}$$

---

[1] ρ_b is used with the eccentric anomaly, E, while ρ_ℓ is used with the true anomaly, ν. After the respective integrations and after small terms are dropped, ρ_ℓ equal to ρ_b is found to be consistent with the approximations.

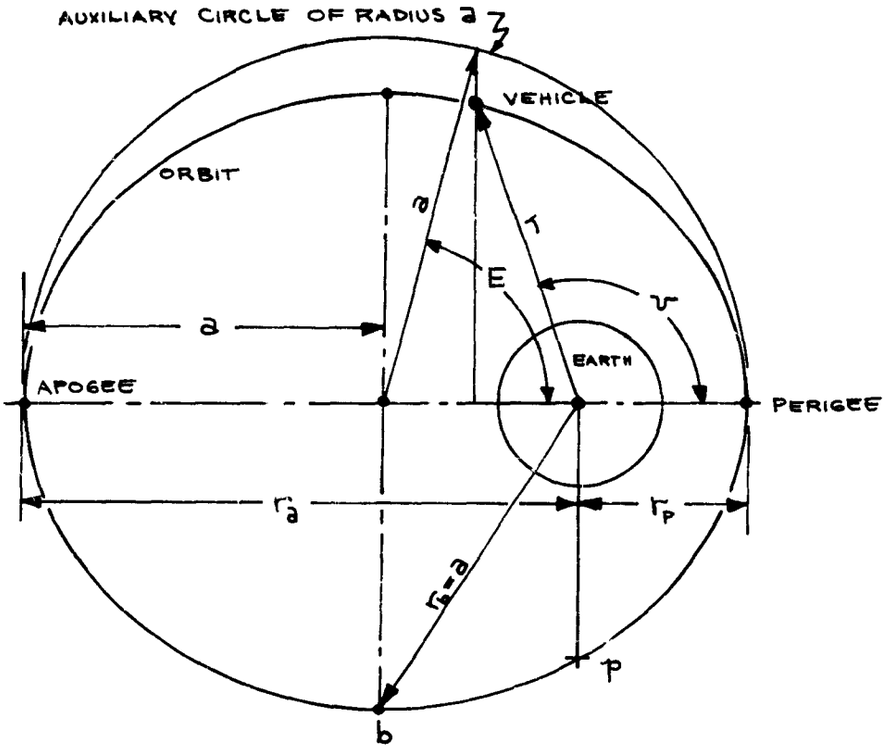

Figure C-1.

Fig. C-2 shows the results of Eq. (C-14) (see Ref. 1), as a function of the center of mass position of three elementary satellite shapes. Since $\Delta r_p / r_p$ is at most of the order 10^{-1}, it follows that the parameter $\Delta r_p N_{\theta/2} / r_p N_{\Delta r}$ must be significantly less than 10^{-1} in order for the time to damp to half-amplitude to become a small fraction of the decay time. As seen from Fig. C-2, the most forward locations of the vehicle mass center produce damping times only slightly less than the decay time, hence it must be concluded that the aerodynamic damping has little effect on the angular oscillation over the time period that the orbit elements may be regarded as constants.

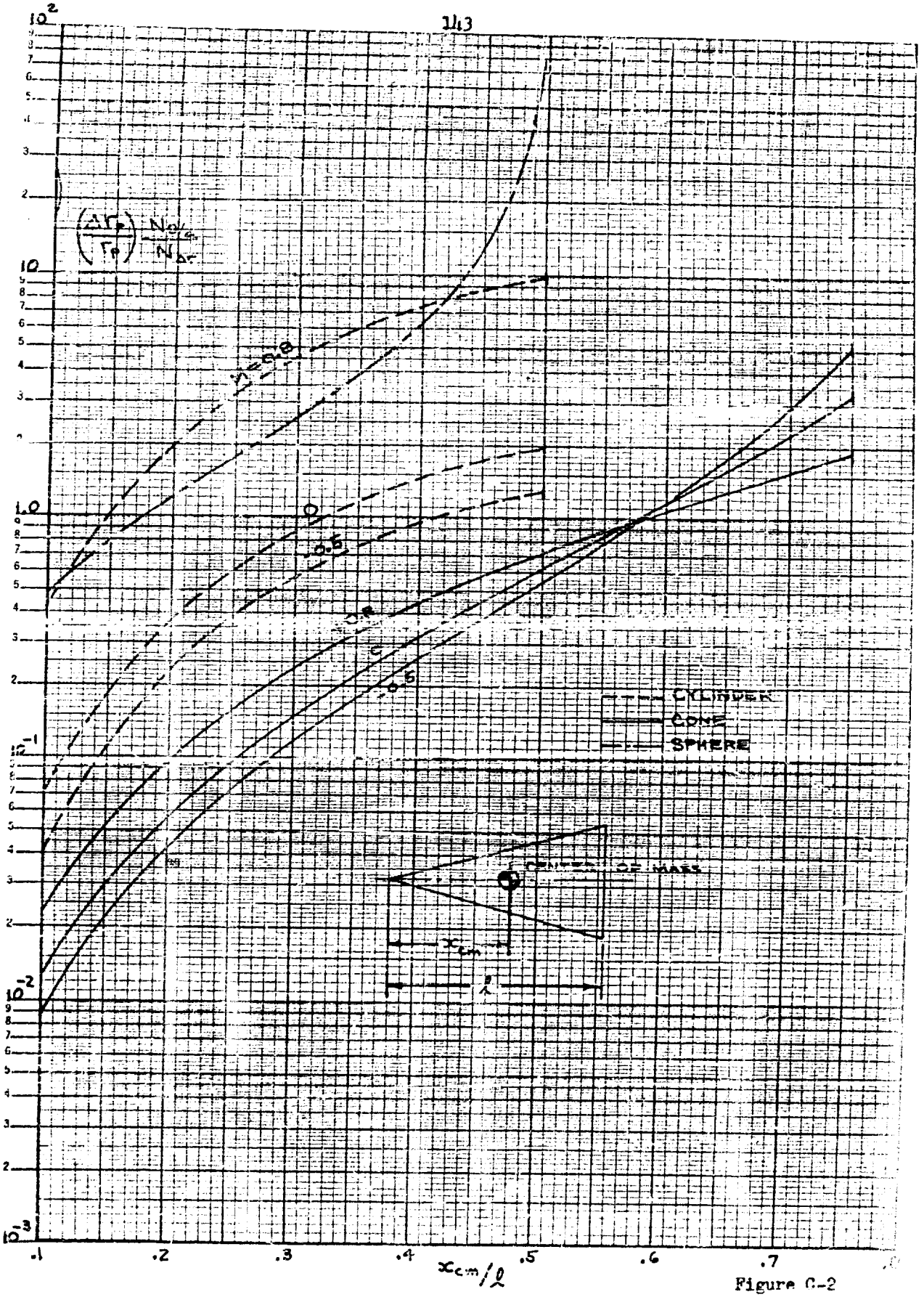

Figure C-2

BIBLIOGRAPHY

1. Davison, Paul H., "Passive Aerodynamic Attitude Stabilization of Near-Earth Satellites, Volume II - Aerodynamic Analysis," WADD Technical Report 61-133, Wright Air Development Division, Wright-Patterson Air Force Base, Ohio, March 1961

2. Juelich, O. C., "Passive Aerodynamic Attitude Stabilization of Near-Earth Satellites, Volume III - Mathematical Techniques and Computer Program," WADD Technical Report 61-133, Wright Air Development Division, Wright-Patterson Air Force Base, Ohio, March 1961

3. Roberson, R. E., "A Review of the Current Status of Satellite Attitude Control," Jour. of the Astronautical Sci., Vol. VI, no. 2, pp. 25-30, Summer 1959

4. Frye, William E. and Stearns, Edward V. B., "Stabilization and Attitude Control of Satellite Vehicles," ARS Journal, Vol. 28, no. 12, pp. 927-931, December 1959

5. Schindler, G. M., "On Satellite Librations," ARS Journal, Vol. 28, no. 5, pp. 368-370, June 1959

6. Klemperer, W. B. and Baker, R. M. L. Jr., "Satellite Librations," Astronautica Acta, Vol. 3, pp. 16-27, 1957

7. Stocker, T. A. J. and Vachino, R. G., "The Two-Dimensional Librations of a Dumbbell-Shaped Satellite in a Uniform Gravitational Field," MS Thesis, School of Engineering, Air Force Inst. of Technology Air University, WPAFB, March 1958

8. Baker, Robert M. L., Jr., "Librations on a Slightly Eccentric Orbit," ARS Journal, Vol. 30, no. 1, pp. 124-126, January 1960

9. Roberson, R. E., "Attitude Control of a Satellite Vehicle - An Outline of the Problems," ARS Preprint 485-57, Presented at the Eighth International Astronautical Congress, Barcelona, Spain, October 6-12, 1957

10. Roberson, R. E., "Gravitational Torque on a Satellite Vehicle," Jour. of the Franklin Inst., Vol. 265, no. 1, pp. 13-22, 1958

11. Wall, John K., "The Feasibility of Aerodynamic Attitude Stabilization of a Satellite Vehicle," ARS Preprint 787-59, Presented at the Controllable Satellites Conference, M.I.T., April 30 - May 1, 1959

12. DeBra, D. B., "The Effect of Aerodynamic Forces on Satellite Attitude," Jour. of the Astronautical Sci., Vol. 4, no. 3, pp. 40-45, Autumn 1959

13. DeBra, D. B. and Stearns, E. V., "Attitude Control," Elect. Eng., Vol. 77, p. 1088, 1958

14. Beletskiy, V. V., "The Motion of an Artificial Earth Satellite Relative to its Centre of Mass," Iskvsstvennye Sputniki Zemli, USSR (Moscow) 1958, pp. 25-43 (Available as Royal Aircraft Establishment Library Translation 824, June 1959)

15. Sohn, Robert L., "Attitude Stabilization by Means of Solar Radiation Pressure," ARS Journal, Vol. 28, no. 5, pp. 371-373, May 1959

16. Newton, Robert R., "Stabilizing a Spherical Satellite by Radiation Pressure," ARS Journal, Vol. 30, no. 12, pp. 1175-1177, December 1960

17. Moulton, F. R., An Introduction to Celestial Mechanics, The Macmillan Co., New York, 1914

18. Krause, H. G. L., "The Secular and Periodic Perturbations of the Orbit of an Artificial Earth Satellite," Paper presented at the 7th International Astronautic Congress, Rome, 17-22 September 1956

19. Sterne, Theo. E., "Effects of the Rotation of a Planetary Atmosphere on the Orbit of a Close Satellite," ARS Journal, Vol. 29, no. 10, pp. 777-782, October 1959

20. Nidey, Russel A., "Gravitational Torque on a Satellite of Arbitrary Shape," ARS Journal, Vol. 30, no. 2, pp. 203-204, February 1960

21. Schrello, D. M., "Approximate Free Molecule Aerodynamic Characteristics," ARS Journal, Vol. 30, no. 8, pp. 765-767, August 1960

22. Vinti, J. P., "Theory of the Spin of a Conducting Satellite in the Magnetic Field of the Earth," Aberdeen Proving Ground, BRL Report 1020, July 1957

23. Vinti, J. P., "Theory of the Spin of a Conducting Satellite in Non-Equatorial Orbits," Aberdeen Proving Ground, BRL Report 1031, October 1957

24. Roberson, R. E., "Torques on a Satellite Vehicle from Internal Moving Parts," Jour. of Applied Mech., Vol. 25, pp. 196, 287, June 1958

25. Michaelsen, H. F., "Orbit Decay and Prediction of the Motion of Artificial Satellites," Proc. of the Fifth Annual Meeting of the American Astronautical Soc., pp. 255-310, Plenim Press, Inc., 1959

26. Minzner, R. A., Champion, K. S. W., and Pond, H. L., "The ARDC Model Atmosphere, 1959," Air Force Surveys in Geophysics, no. 115, AFCRC-TR-59-267, August 1959.

27. Beletskiy, V. V., "The Librations of a Satellite," Iskusstvennyye Sputniki Zemli, No. 3, Academy of Sciences, USSR (Moscow), 1959, pp. 13-31 (Available as NASA Technical Translation F-10, May 1960)

28. Frick, R. H. and Garber, T. B., "General Equations of Motion of a Satellite in a Gravitational Gradient Field," The Rand Corporation, Report RM-2527, December 1959

29. Moran, John P., "The Effects of Plane Librations on the Orbital Motion of a Dumbbell Satellite," Therm Corporation, Report TAR-TN 603, August 1960

30. Doolin, Brian F., "Gravity Torque on an Orbiting Vehicle," NASA Technical Note D-70, September 1959

31. Notni, Peter and Oleak, Hans, "The Rotation of the Carrier Rocket of Sputnik III (1958 δ 1)," Veroeffentlichungen der Sternwarte in Babelsberg, Vol. 13, 1959 (Available as Royal Aircraft Establishment Library Translation 864, December 1959)

32. Morse, Philip M. and Feshbach, Herman, Methods of Theoretical Physics, Part I, McGraw-Hill Book Co., Inc., New York, 1953

33. Jahnke, Eugene and Emde, Fritz, Tables of Functions, with Formulae and Curves, Dover Publications, Inc., 1945

34. Wittaker, E. T. and Watson, G. N., A Course of Modern Analysis, Fourth Edition, Cambridge University Press, London, 1927

35. Struble, Raimond A. and Fletcher, John E., "General Perturbational Solutions of the Mathieu Equation," North Carolina State College, Depts. of Mathematics and Eng. Research, Tech. Memorandum No. 5, Contract No. DA-36-034 ORD-2733 RD, September 1960

36. Goldstein, Herbert, Classical Mechanics, Addison-Wesley Press, Inc. 1950

37. Ince, E. L., Ordinary Differential Equations, Dover Publications, Inc. 1956